Negative regulators of vulva development in *C. elegans* and *C. briggsae*

Genetic studies of the negative regulators of vulva development in *C. elegans* and *C. briggsae*

By Ish Jain,

A Thesis Submitted to the School of Graduate Studies in the Partial Fulfillment of the Requirements for the Master of Science

McMaster University
Master of Science (2020)
Hamilton, Ontario (Department of Biology)

TITLE: Genetic studies of the negative regulators of vulva development in *C. elegans* and *C. briggsae*
AUTHOR: Ish Jain (McMaster University)
SUPERVISOR: Dr. Bhagwati Gupta
NUMBER OF PAGES: xix, 137

Abstract

Caenorhabditis elegans and its congener, *C. briggsae* are excellent animal models for the comparative study of developmental mechanisms and gene function. Gupta lab is using the vulval tissue in these nematodes as a system to investigate conservation and divergence in signal transduction pathways. Genetic screens conducted earlier in our laboratory recovered several mutants that cause multivulva (Muv) phenotype. The Muv genes act as tumor suppressors and negatively regulate the proliferation of vulval precursors. Genetic and molecular work on these genes has revealed that *C. briggsae* vulva developmental utilizes novel genes representing a new phenotypic class termed 'Inappropriate Vulva cell Proliferation (IVP)' (Sharanya et al., 2015). This indicates that the signaling mechanism in *C. briggsae* specifies vulval cell fates differently from *C. elegans*. Interestingly, it has been found that *Cbr-ivp* mutants show higher levels of *Cbr-lin-3* (EGF) transcript, indicating that these genes act genetically upstream of *Cbr-lin-3*, similar to SynMuv family members in *C. elegans*. Moreover, RNAi knockdown of the *Cbr-lin-3* transcript resulted in the suppression of the multivulva phenotype in mutant animals. Similar suppression was also observed when a MAP kinase inhibitor was used in the previous study. In addition, the role of two other novel negative regulators of cell proliferation, *Cbr-lin(bh1)* and *Cbr-lin(bh3)* was also investigated. Preliminary findings on these regulators suggested that both *Cbr-lin(bh1)* and *Cbr-lin(bh3)* exhibiting a heritable Muv phenotype and are found to be located on Chromosome I and III respectively. Identification of novel genes and further characterization will help us understand the molecular function of genes and their involvement in the regulation of vulval cell differentiation. The findings of my research work will provide a background for future studies to understand the role of novel genes in reproductive system development. Overall, these results provide evidence that although the morphology of vulva is similar in the two nematode species, underlying mechanisms of development appear to have diverged.

Dedicated to

A big thanks to *Barb Reuter* (Lifeline of the Department of Biology)

Acknowledgements

First and foremost, I would like to express my deepest respect and gratitude to my supervisor Dr. Bhagwati Prasad Gupta for his constant support, encouragement, patience, and suggestions throughout my masters. I appreciate him for all his time and funding that helped me to complete this research.

I would like to thank my committee member, Dr. Lesley MacNeil, for her insightful comments, discussion, time, and the motivation she has provided during the completion of this thesis.

I especially thank Dr. Rosa da Silva, Dr. Jonathan Stone and Dr. Juliet Daniel for always extending their support and guidance whenever I needed them.

I am also grateful to all my present and past lab members, my partner in crime, my undergraduate student Lena So, and friends from the Department of Biology for their help and support over the years.

I express my immense gratitude and a profound sense of indebting, from the bottom of my heart to my ever-loving parents, my sisters, brother-in-law, and friends whose sacrifices and endless untiring efforts have brought me to a position to undertake and complete this work. Thank you Evansh for all the joy and enlightenment you brought to my life.

Lastly, I would like to thank the academic and administrative staff of the Department of Biology for their help and support during my stay at McMaster University.

Thank you!

Contents

List of Figures

List of Tables

Acronyms

AC	Anchor cell
APC	Adenomatous *Polyposis coli*
Cbr	Caenorhabditis briggsae
CDK	Cyclin-Dependent Kinase
Cel	Caenorhabditis elegans
CKI	Cyclin-Dependent Kinase Inhibitor
CSL	CBF1, Suppressor of Hairless, LAG-1
DE	Differentially Expressed
DIC	Differential Interference Contrast
DSL	Delta/Serrate/LAG-2
EGF	Epidermal Growth Factor
EGFR	Epidermal Growth Factor Receptor
Egl	Egg Laying Defective
EMS	Ethyl Methyl Sulfonate
GO	Gene Ontology
ERK	Extracellular Signal-Regulated Kinases
GRB-2	Growth factor Receptor-Bound protein-2
GSK-3	Glycogen synthase kinase-3
GSK3β	Glycogen Synthase Kinase 3 beta

HIF-1	Hypoxia inducible factor
Hyp	Hypodermis
ivp	Inappropriate Vulval cell Proliferation
JAK/STAT	Janus Kinase/Signal Transducer and Activator of Transcription
MAPK	Mitogen Activated Protein Kinase
MEK	Mitogen Activated Protein Kinase Kinase
Muv	MultiVulva
NHR	Nuclear Hormone Receptor
NICD	Notch Intracellular Domain
NuRD	Nucleosome Remodeling and Histone Deacetylase
Pvl	Protruding Vulva
RT-qPCR	Reverse Transcription Quantitative PCR
RB	Retinoblastoma
RTK	Receptor Tyrosine Kinase
SynMuv	Synthetic Multivulva
Utse	Uterine seam cell
VPCs	Vulva Precursor Cells
VU	Ventral Uterine
Vul	Vulvaless

Declaration of Authorship

I, Ish Jain, declare that this thesis titled, "Genetic studies of the negative regulators of vulva development in *C. elegans* and *C. briggsae*" and the work presented in it are my own. I confirm that:

- Chapter 3: Functional characterization of *Cbr-ivp* class of genes

  I have performed all the experiments mentioned in this chapter of the thesis. Sequencing and determine of the nonsense mutation and open reading frame in AF16 for all the three alleles of *Cbr-ivp-3* and *ivph-3* were done by Ramandeep Pabla and Dr. Devika Sharanya. Analysis of the RNA-Seq data was carried out separately by Dr. Ayush Ranawade. I have carried out the GO Term enrichment analysis in *Cbr-spr-4(gu163)* and *Cbr-htz-1(gu67)* to identify potential target genes and the validation of the target genes from the RNA-Seq dataset using RT-qPCR.

- Chapter 4: Genetic analysis of *Cbr-lin(bh1)* and *Cbr-lin(bh3)* mutants

  I have performed the experiments for this chapter of the thesis. The experiment "Cell fate analysis in *Cbr-lin(bh)* mutants" was also performed separately by Lena So. Her contribution is mentioned in the thesis. "Maternal effect in *Cbr-lin(bh1)* and *Cbr-lin(bh3)* mutants" experiment was solely performed by Lena So. Her data was included after getting consent from her and Dr. Bhagwati P. Gupta.

Chapter 1

Introduction

A cell is the basic structural and functional element of an organism (Mautner and Huang, 2003). Cells divide to form tissues which undergo morphological changes and results in organogenesis. A simple organism developed from a single zygote after multiple rounds of cell division (Lambie, 2002). Development is a long process and it requires tight regulation of a controlled set of events. The process of development begins when a single cell enters into the cell cycle and undergoes cell division followed by cell fate specification and differentiation (Levine, 2004). To complete a division a cell must undergo a sequence of events controlled by several genes that encode for Cyclin-Dependent Kinases, cyclins, positive and negative regulators. The process of cell proliferation is characterized by an increase in the number of cells resulting from cell division (Lambie, 2002). Cell proliferation and its regulation are crucial in tissue formation and organ development. The process of cell fate specification is a natural and vital part of development. Cell fate specification requires a cell to respond to specific factors, which causes the subsequent cells to adopt a specific fate following division (Davidson, 1990). After cell proliferation, certain cells undertake differentiation and adopt a definitive fate. These cells become differentiated cells. Differentiate cells do not undergo further division and carry out a specialized function. The progenitors of these differentiated cells continue to proliferate and produce new cells to replenish the old and damaged cells (Morrison et al., 1997). It is important to sustain a balance between cell growth, cell proliferation, and cell death. The entire system of cell proliferation and cell death is strictly regulated by sets of genes and specific factors (King and Cidlowski, 1998; Pucci et al., 2000). However, sometimes this homeostasis is disturbed and excessive cell proliferation results in uncontrollable cell growth and subsequent tumor formation. Cells accumulate mutations in their genetic material and as a result, acquire the properties of cancerous cells (Hanahan and Weinberg, 2000). These cells undergo abnormal proliferation and lose their ability for differentiation (Kim and Orkin, 2011). This phenomenon of uncontrolled, abnormal and excessive cell proliferation is characterized as Cancer. According to the Canadian

Cancer Society, cancer is the leading cause of death and is responsible for 30% of all deaths in Canada. Tumorous cancer tissues result in rapid proliferation, migration, increased blood supply to the tissues and secrete factors that enhance cancer-like properties in the neighboring cells (Seyfried and Huysentruyt, 2013). Since cancer is a disease of uncontrolled cell proliferation it is difficult to differentiate between normal cell proliferation and tumor cell growth. Thus, a study on fundamental cellular and molecular mechanism is critical to understand the regulation of cell cycle and cell division.

1.1 Cellular and molecular mechanisms of cell division and cancer

Cancer is a disease of uncontrolled cell proliferation. Most of the cancer therapies aimed to reduce the tumor cells and thus prevent their accumulation. However, the underlying mechanisms of division is same in tumor and normal cell proliferation thus, make it difficult to target the cancerous tissue. This section will provide a review on the current development of our understanding of the complex molecular mechanisms involved in the regulation of cell proliferation.

1.1.1 Cell cycle and tumor suppressor pathways

Cell cycle regulation is quintessential for development, and there are several genes and regulators that control cell fate by regulating this process. Cell cycle and signaling pathways that control cell division are tightly regulated to prevent developmental abnormalities and cancer (Sherr, 1996; Duronio and Xiong, 2013). During development, a cell undergoes multiple rounds of division before differentiation. But before entering cell division, a cell must pass through various checkpoints to ensure the adequate resources and ideal conditions for division (Malumbres and Barbacid, 2009). A somatic cell cycle comprises a series of events that involves Gap phases G1 and G2 which separates S and M phase during the cell cycle. S phase also known as the synthetic phase, represents precise duplication of genomic DNA in the cell, while the M phase represents the distribution of complete sets of chromosomes to each daughter cell. On successful completion of M phase cells enters in G1 phase before proceeding to the S phase of the next cycle. G2 phase allows the cell to confirm for the accuracy of genomic DNA before advancing to the M phase (Schafer, 1998; Levine, 2004; Budirahardja and Gönczy, 2009). Sometimes after S phase cells temporarily or permanently entered an arrested phase

known as quiescent or G0 phase (Schafer, 1998). The decision of leaving the cell cycle depends on environmental or developmental singles received by cell.

Studies in eukaryotes have demonstrated that the entire process of cell-cycle and cell division is controlled by several genes that encode for Cyclin-Dependent Kinases, cyclins, positive and negative regulators. The transition of cells from one phase to another is strictly controlled by a set of Cyclin-Dependent Kinases (CDKs). These CDKs activate and inactivate in different phases to ease the process of phase transition during cell-cycle (Sherr and Roberts, 2004). On the contrary, *Saccharomyces cerevisiae* and *Schizosaccharomyces pombe* use only single CDK, p34CDC28 and p34cdc2 respectively to interact with different cyclins to progress through cell-cycle. (Hartwell et al., 1974; Nurse et al., 1976; Mendenhall, 1993)

Cyclin-Dependent Kinases (CDKs) are inactivate serine/threonine protein kinases (Pines, 1999). Their activation requires the association with the other components of the cell cycle (Malumbres and Barbacid, 2009). A controlled expression of cyclins and their interaction with CDKs is required for the cell cycle progression (Budirahardja and Gönczy, 2009). CDKs bind with Cyclins and form Cyclin/CDK complex, though the complex remains inactivated as Cyclin-Dependent Kinase Inhibitors (CKIs) bind with the complex and induce the phosphorylation by Wee1/Myt1 kinases, which leads to the inactivation of the complex (Pines, 1999; Malumbres and Barbacid, 2005). The process of activation requires a particular subset of reactions within the cell. The activation of Cyclin/CDK complexes requires phosphorylation and dephosphorylation of CDKs and ubiquitinoylation of Cyclin-Dependent Kinase Inhibitors (CKIs) associated with Cyclin/CDK complexes or CDKs (Pines, 1999; Budirahardja and Gönczy, 2009).

The phosphorylation and dephosphorylation of CDKs are regulated by CDK-activating kinase (CAK) (Desai et al., 1995) and a Cdc25 phosphatase (Pines, 1999; Miller and Russell, 1992). Cdc25 dephosphorylates CDKs by removing the inhibitory phosphorylation from Wee1/Myt1 kinases (Pines, 1999; Miller and Russell, 1992). CDK-inhibitory proteins (CKIs) undergo ubiquitin-dependent proteolysis which leads to the activation of Cyclin/CDK complexes. Cyclin destruction marked as the completion of the phase. CDKs get recycled in all the phases of the cell cycle. Ubiquitinoylation of CDK-inhibitory proteins (CKIs) in late G1 and S involves E3 ligase SCF (Skp, Cullin, F-box) (Spruck and Strohmaier, 2002). while anaphase-promoting complex (APC) in M phase and early G1 is required for the proteolysis degradation of Cyclin (CYC) (Harper et al., 2002).

Progression through cell cycle requires the activation and inactivation of CDKs and multi-level regulation in all eukaryotes (de Nooji et al., 1996; Hong et al., 1998; Malumbres and Barbacid, 2005). There are certain regulators that control these cell cycle regulations. These regulators ensure the accuracy of the cell cycle,

any error or damages during the cell cycle lead these regulators to activate cell cycle checkpoints, instigate repair mechanisms and induce programmed cell death and/or apoptosis. Any mutation in these regulators which leads to their reduced or loss of function disrupts the entire cell cycle and may result in abnormal cell proliferation (Sherr, 1996). The adverse effect will cause an increase in tumor cells which leads to cancer. These suppressors negatively regulate cell proliferation and thus known as Tumor suppressors.

1.1.2 Rb/E2F pathway and other tumor suppressors

One of the well-studied tumor suppressors is pRb (Retinoblastoma) (Nevins, 1998; Harbour and Dean, 2000; Sears and Nevins, 2002). pRb represses the genes that are mainly involved in S phase progression. Loss of function mutations in pRb lead to retinoblastoma. pRb interacts mainly with heterodimeric transcription factors E2F and DP (Stevaux and Dyson, 2002). E2F promotes the expression of cyclin E. When pRb binds with and E2F/DP heterodimers, it inactivates the E2F transcription factor and thus represses the expression of cyclin E and other downstream genes (Dyson, 1998; Sears and Nevins, 2002). In a cancerous cell, loss of function of pRb results in the activation of E2Fs whichpromotes the transcription of cyclin E gene. Cyclin E forms a complex with Cdk2 and triggers mitogen-independent cell cycle progression which leads to intraocular cancer, retinoblastoma (Harbour and Dean, 2000). Thus, pRB plays a crucial role in regulating cell cycle and cell proliferation as the inactivation of pRB during cell cycle can cause a cell to remain in a proliferating state.

PTEN (Phosphatase and TENsin homolog) a tumor suppressor, encodes for phosphatidyl inositol-3, 4, 5-trisphosphate 3-phosphatase. It dephosphorylates phosphatidyl inositol-3, 4, 5-trisphosphate 3-phosphate in cells and plays a key role in G1 cell cycle arrest and apoptosis (Eng 2003). It negatively regulates PI3K-Akt Pathway and thus maintaining homeostasis between cell survival and apoptosis (Di Cristofano et al., 2000). A cell with mutated PTEN, prone to grow and divide rapidly to generate tumors. Individuals with PTEN mutation have a high risk of breast, endometrial and gastric carcinomas (Yang et al., 2003).

Another classic example of a tumor suppressor gene is TP53, which encodes for tumor suppressor protein p53. A loss of function of p53 has been identified in more than 50% of colon, breast, and lung cancer cases (Levine, 1997; Sigal and Rotter, 2000). Sometimes when cells undergo biochemical changes (transition between phases) during cell cycle resulted in genomic DNA fragmentation and/or nucleic acid damage, cells respond to the damage by initiating repair mechanism protocols. Repair mechanism involves arresting the cell cycle progression, activating cell

cycle checkpoints and DNA repair assembly and inducing programmed cell death if the damage is severe. A mutation in DNA or defects in repair mechanisms may result in an increased cell proliferation which leads to tumor formation (Hanahan and Weinberg 2000). On sensing DNA damage, it prevents the cell from dividing by ceasing the cell at the G1 phase checkpoint during the cell cycle (Goodsell, 1999). p53 encodes for a tumor suppressor protein which functions as a transcription factor and promotes the transcription of genes that involved in DNA repair. p53 interacts with other tumor suppressors (BRCA1 in Breast cancer cells) and stimulates p21 promotor (Chai et al., 1999). The p21 family has three proteins, p21, p27 and 57 (LaBaer et al., 1997). p21 is a CDK-inhibitory protein (CKIs) that functions by inhibiting CDKs during the cell cycle and thus negatively regulates cell proliferation (Levine, 1997). The cells with a mutation in p53 genes do not express inhibitory p21 and subsequently shown an increase in the activity of CDKs which results in excessive cell proliferation (He et al., 2005). Thus, cells with a reduced or loss of function of p53 do not commence to programmed cell death and lead to tumor development (Schumacher et al., 2001). p53 is one of the most significant tumor suppressors because it restricts the activity of multiple CDKs and therefore maintains a balance between cell proliferation and apoptosis.

Von Hippel–Lindau disease (VHL) is a multisystem cancer syndrome caused due to a mutation in the VHL gene (Maher and Kaelin, 1997). Hundreds of mutations in the VHL gene have been diagnosed in individuals with cancer (Kaelin and Maher, 1998). VHL gene encodes pVHL protein, a von Hippel–Lindau tumor suppressor (Lisztwan et al., 1999). pVHL interacts with other proteins and is responsible for ubiquitin-dependent proteolysis of Hypoxia-Inducible Factors (HIFs). HIFs are transcription factors and regulate the transcription of genes in the oxygen-dependent manner (Mahon et al., 2001). When VHL genes lost their ability to interact with ubiquitin ligase E3 complex as a result of the mutations, it causes cells to maintain a constant level of HIFs (Lisztwan et al., 1999). HIF interacts and activates cyclin D1 which prevents the cell from undergoing apoptosis and result in an increased cell survival rates and thus, maintain a cell to remain in a proliferating state (Bindra et al., 2002; Ortmann et al., 2014). Other examples of tumor suppressors include APC, Fas receptor - CD95, ST5, ST7 and ST14 (ST-Suppressor of Tumorigenicity). Mutation in the tumor suppressor gene contributes to the development of cancer (Levine and Puzio-Kuter, 2010).

Since the fundamental mechanism of normal cell proliferation and tumor cell growth are similar it is difficult to understand the distinctive characteristic of tumor cells. A study on the negative regulators of cell proliferation and tumor suppressor genes is thus necessary for understanding the fundamental mechanism of cancerous growth. Investigation of novel tumor suppressor genes is important not only to uncover the underlying mechanism but also for the discovery of drug

targets and effective medical treatment.

1.2 Model organisms and their role in understanding cancer

The development of mutation screening procedures and the feasibility of the sequencing technique allowed the revelation of novel tumor suppressors. The use of model organisms serves as an excellent approach for the identification of these novel factors and understanding their role and interaction in the signaling pathway. The animal model organisms that are used to study the genetic basis of development are *Mus musculus* (common house Mouse), *Rattus norvegicus* (Rat), *Xenopus laevis* (African clawed frog), *Danio rerio* (Zebrafish), *Gallus gallus domesticus* (Chicken), *Macaca mulatta* (Rhesus monkey), *Daphnia spp.* (Daphnia), *Drosophila melanogaster* (Fruit fly), and the nematode, *Caenorhabditis elegans* (Roundworm). Invertebrates models are also extremely useful tools for understanding tumor biology and have led to the discovery of a number of signaling pathways that play conserved roles in human development. Many of the components essential in the cell cycle network are conserved from yeast (*Saccharomyces cerevisiae*) to mammals. The most commonly used invertebrate models are the fruit fly, *Drosophila melanogaster*, and the nematode, *Caenorhabditis elegans*.

Both *C. elegans* and *D. melanogaster* have provided substantial platform for the milestone discoveries in the field of biological sciences. Genetic analyses of cell signaling pathway in both models, have led to the discovery of number of pathway components that are involved in cell development and division. Ras and Notch signaling pathway, Wnt pathway components, Mechanism of JAK/STAT pathway have been extensively studied in these two model organisms (Neidich 2005). Most of these signaling pathways are involved in cell division and cell cycle regulation in these animals. Any abnormality in the general mechanism of these pathways can lead to the tumor formation. Due to evolutionary conservation, these organisms serve as excellent animal models to understand cell signaling and signal transduction pathways. Model organism *C. elegans* and its congener *Caenorhabditis briggsae*, are used to investigate evolutionary changes in cellular and molecular mechanisms of animal development.

The evolution of genetic analysis, forward and reverse genetic screens in model organisms feature the importance of signal transduction in developmental pathways. Study of tumor suppressor genes in model organisms provide a better understanding of signal transduction and cell signaling pathway. Tumor suppressors interact or work in parallel with signaling pathways that regulate the cell cycle,

cell fate specification, cell proliferation, cell growth, cell differentiation, and cell death. The vast diversity of organisms and their developmental cycles have provided researchers all over the globe, the advantage to select a model organism to understand the genetic basis of cancer development.

1.3 *C. elegans* as a model organism

C. elegans is a leading nematode animal model that allows for simplified studies of diverse and complex fundamental processes. *C. elegans* has provided a means for investigating the genetic basis of development and gene function and provide insights into the cellular and molecular basis of organ formation.

C. elegans was first used as a model system by Sydney Brenner in the late 1960s to study cell division and differentiation during development (Hoffenberg 2003). The use of this model organism has led to important discoveries in diverse fields such as development, signal transduction, cell death, aging, and RNA interference (RNAi). Currently, over 400 labs throughout the world are using *C. elegans* not only to study development, but also neurobiology, aging, and innate immunity.

C. elegans offers a number of advantages as a model organism. The first of these advantages is the size of the organism, which is about 1 mm in length; this small size greatly reduces the cost of working with the organism as well as allowing work in minimal lab space with easy handling (Riddle et al., 1997). The relatively short life span - from egg to young adult in 3 days at 20°C, and a total life span of 2-3 weeks - combined with its ability to self-fertilize allows for the development of large clonal populations in short periods of time as well as allowing experiments carried out over the entire life span of the animal to be conducted in a timely manner (Riddle et al., 1997). The presence of males, in addition to self-reproducing hermaphrodites, allows for the utilization of genetic crosses between strains (Riddle et al., 1997). The small and completely sequenced genome of approximately 100 Mb allows for the utilization of genomic tools (Hodgkin, 2005). The ease with which RNA interference can be delivered in *C. elegans* allows for the selective knockdown of any specific gene of choice (Fire et al., 1998). Finally, the transparent nature of the nematode allows direct observation of cellular events and development. It also allows the use of cell markers and labeled reporters to understand the processes and expression pattern (Hutter, 2006).

C. elegans has a short lifespan of about 2-3 weeks (Byerly et al., 1976). When the conditions are unfavorable, animals can go through an alternative developmental stage in which a resistant dauer larval form is produced, surviving extreme conditions (desiccation and lack of food) for several months. In the laboratory, *C.*

elegans can be easily cultured and maintained with *Escherichia coli* (*E. coli*) as a food source, on an agar substrate in Petri dishes, in liquid culture, or even in microtiter plates, making it amenable to high-throughput approaches. Moreover, stocks can be frozen at -80°C or in liquid nitrogen for indefinite storage.

C. elegans is diploid and has five pairs of autosomal chromosomes (I-V) and one pair of sex chromosomes (X). Two sexes exist; a self-fertilizing hermaphrodite (XX) which produces both sperms and oocytes; and a male (X0) which occasionally appears at a frequency of 0.2%, as a result of spontaneous X chromosome loss (Corsi et al., 2015). This hermaphroditism facilitates genetic analysis as the strains are normally propagated asexually, giving rise to a large number of self-progeny (300), forming clones. However, males, which can be generated experimentally by heat shock, are capable of mating with hermaphrodites, producing mainly cross-progeny. *C. elegans* has a simple body structure and a small invariant number of 959 somatic cells and about 2000 germ cells in hermaphrodites (1031 somatic cells and about 1000 germ cells in the male) from which the complete cell lineage, from fertilize egg to adult, is known (Sulston and Horvitz, 1977).

Genome sequencing of *C. elegans* (Stein et al., 2003) revealed significant similarity with higher organism including vertebrates such as mice and humans. Moreover, many cell signalings and developmental pathways are conserved in nematodes. The feasibility of genetic analysis, forward and reverse genetic screens, and site-directed mutagenesis, sample preparation for sequencing have made *C. elegans* an excellent model to carry out molecular and genetic analysis.

1.4 *C. briggsae* as a comparative model to understand the genetic basis of development

Caenorhabditis briggsae serve as excellent animal models for comparative study of developmental mechanisms and gene function. Both *C. elegans* and *C. briggsae* animal models diverged from a common ancestor approximately 30 million years ago (Stein et al., 2003). In 1949, Dougherty and Nigon used *C. briggsae* as a model organism for biological sciences. A hermaphrodite strain of *C. briggsae* was isolated in Gujarat, India (Fodor et al., 1983). It was latter termed as wild-type *C. briggsae* strain, AF16. The behavior appearances and developmental phases are similar in both *C. elegans* and *C. briggsae*. *C. briggsae* worms are self-fertilizing hermaphrodite and have males. Each species contains five pairs of autosomal chromosomes (I-V) and one pair of sex chromosomes (X).

The life cycle of this nematode strain comprises four larval stages (L1 - L4), which are separated by molts. The embryonic development and hatching take about 1 day, and the larva grow to a fertile adult in about 3 days. The adult worms can live on average 2-3 weeks when it is grown on a lawn of *E. coli* at 20°C. When encountering environmental stress, nematode larvae enter a non-feeding, stress resistant, dauer diapause larval stage to survive adverse conditions. When the conditions become favorable, dauer resume development and proceed to L4 larval stage and subsequently to adulthood. Dauer larvae can survive up to 6 months, longer than the adult worm life span (2-3 weeks) (Braeckman et al., 2001).

The genome size for *C. briggsae* spans over 104 Mbp and is nearly identical to the genome size of nematode *C. elegans* (100.3 Mbp) (Stein et al., 2003). The total number of unique gene count in the protein set for *C. briggsae* has revealed over 21,700 genes (uniprot.org/proteomes/UP000008549). Roughly one third of *C. briggsae* genes have multiple alignments, mostly of which is a result of sequence repeats in *C. elegans* genome. Roughly 5% of genes have no sequence similarity in *C. elegans* genome, thus appear to be unique (Gupta et al., 2007). A comparison of protein coding genes between the two species has revealed one-third of total sequence differences and more than a thousand chromosomal rearrangements. It is interesting to study whether these genomic variations result into the divergence of developmental mechanisms and signaling pathways.

Examination of physiological processes in *C. briggsae* and *C. elegans* has revealed variations in gene function between the two species (Gupta et al., 2007). These differences may arise due to the changes in signaling network or gene function. Though, more work is needed to fully understand the influence on gene networks on development. Studies of signal transduction pathways in two nematode species, similarities and differences in gene function, can provide an insight on gene evolution and their role in development (Haag and True, 2001) and thus may help in understanding the underlying mechanism of cancer and tumor suppressors.

1.5 Vulva development as a model to understand signaling mechanism involved in cell proliferation

Vulva development in *C. elegans* present a simple yet powerful model for understanding the mechanisms of cell fate specification and cell proliferation during development. The comparative studies in *C. briggsae* and the feasibility to study the genetic mechanism make vulval development an excellent model to strengthen

our understanding of the organogenesis. Cell lineages during vulva development and the effects of numerous mutations on vulval development can be easily observed throughout the life of the animal. Within this system, multivulva mutants are important because they exhibit inappropriate division in VPCs. Understanding and comparing the mechanism of gene function in between *C. briggsae* and *C. elegans* provide valuable lessons in cancer biology.

1.5.1 Vulva Development in Nematodes

One of the important components of the reproductive system is vulva. Vulva formation in nematodes involved a series of signaling events that coordinate and give rise to a 22 cells organ (Sternberg, 2005). The vulva development mainly involves three vulval precursor cells (VPCs) (P5.p, P6.p, and P7.p), that are located on the ventral side of the worm and are induced by anchor cell (AC), a somatic gonad cell (Hwang and Sternberg, 2004). The anchor cell lies dorsal to the vulva precursor cells and secrets the epidermal growth factor (EGF) ligand, LIN-3, to initiate induction in the VPCs (Hill and Sternberg, 1992). Since P6.p is most proximal to the AC, it receives the most LIN-3/EGF inductive signal through the LET-23 (EGFR) receptor (Katz et al., 1996). The phosphorylation of LET-23 led to the initiation of MAP kinase cascade, which causes the P6.p VPC to adopt the primary cell fate (1°) and produce eight vulval progeny classified as vulE and vulF (Wang and Sternberg, 2000). Both P5.p and P7.p are located further away from the AC in comparison to P6.p thus, adopt the secondary fate (2°) and each gives rise to seven vulval progenies vulA, vulB1 and vulB2, vulC and vulD (Sharma-Kishore et al., 1999). Lower levels of LIN-3 in addition to the repressive lateral signal from P6.p mediated by LIN-12 (NOTCH) (Simske and Kim, 1995) results in their secondary cell fate (Sternberg and Horvitz, 1989). The other three VPCs P3.p, P4.p, and P8.p are more distal to AC and as a result, remain un-induced, and adopt a tertiary (3°) cell fate (Hill and Sternberg, 1992). These cells divide only a single time and fuse to the hypodermis (Hill and Sternberg, 1992). The number of cells and the cellular process is conserved in *C. briggsae*.

1.6 Signaling pathways involved in vulva development

Molecular genetic studies in *C. elegans* has led to the discovery of multiple genes involved in vulva development that encode the components of signal transduction

pathways. The evolutionary conserved pathways include RAS pathway, Notch pathway and Wnt pathway.

These pathways are summarized below

1.6.1 Ras Pathway

The Ras pathway has been studied extensively in nematode vulva development. LIN-3/EGF secreted from the AC binds and activates receptor tyrosine kinase (RTK), LET-23 (Aroian and Sternberg, 1991) by dimerizing and autophosphorylating tyrosine residues at the C-terminal region. The phosphorylated residue serves as a docking sites for adaptor proteins such as SEM-5/GRB-2, which recruit SOS-1, a Guanine Nucleotide Exchange Factor (GEF) (Clark et al., 1992). SOS-1 serves as a positive regulator of RAS and promotes the formation of LET-60-GTP. The active form of LET-60/Ras initiates MAP Kinase cascade consisting of the kinases LIN-45 (Han et al., 1993), MEK-2 (Church et al., 1995) and MPK-1 (Lackner et al., 1994). The active form of Ras binds to LIN-45 (Raf) (Han et al., 1993) and coordinate with other scaffolding kinase proteins KSR-1 and KSR-2 to phosphorylate and activate MEK-2, which in turn phosphorylates and activates MPK-1 (Lackner et al., 1994). The MPK-1 then further phosphorylates and stimulate or repress downstream target proteins (Figure 1.1).

Gain of function mutation in EGF/Ras results in the overactivation of signaling pathway which results in VPCs showing abnormal division pattern and thus give rise to Muv phenotype (Yoo et al., 2004). These abnormal patterns in cell divisions can be studied as a model of tumor formation. EGFR-Ras-MAPK pathway components are found to be mutated in most of the human cancers (Montagut and Settleman, 2009). In *C. elegans*, the Hyperactivation of EGF/LET-23 causes additional VPCs to divide (Fay and Yochem, 2007) which results in the formation of pseudovulva. Thus, studying signaling pathways in nematodes can give us an insight of how cell division alters in cancerous cells and the genes involved or mutated in these cells.

1.6.2 Notch Pathway

Many pathways interact and coordinate with each other to control cell fates. During vulva development, Ras pathway interacts with Notch pathway to carry out the vulval cell fates (Sundaram, 2004). Ras induces the transcription of DSL ligand genes in P6.p cell of *C. elegans* for LIN-12 and reduces the LIN-12 protein levels by promoting the transcription of LIN-12/Notch inhibitors. (Shaye and Greenwald,

2002). LIN-12/Notch mediates secondary (2°) cell fate in VPCs via lateral signaling (Greenwald et al. 1983). Notch controls the transcription of Ras inhibitors, *ark-1*, *lip-1*, *lst-1, lst-2, lst-3, lst-4* in the P5.p and P7.p cells of *C. elegans* thus, preventing them from gaining 1o cell fate (Hopper et al., 2000, Berset et al., 2001, Yoo et al., 2004). There are 10 ligands for LIN-12/Notch proteins in *C. elegans*. Out of these three ligands *lag-2*, *apx-1*, and *dsl-1* are mainly involved in lateral signaling (Chen and Greenwald, 2004). *lag-2* expresses in all VPCs, but its expression seen to be up-regulated in P6.p cell. *lag-2*, *apx-1*, and *dsl-1* ligands are mainly involved in cell fate decisions (Mello et al., 1994). For normal Vulva cells fate, LIN-12 targets a number of negative regulators of LET-23 signaling (Yoo et al., 2004). Overall Ras and Notch pathways interact to induce neighbors to achieve 2° cell fate, thereby inhibiting them from gaining 1° cell fate (Figure 1.2).

1.6.3 Wnt Pathway in vulva development

The Wnt pathway influences a variety of developmental processes in nematodes. In particular, the mechanism of Wnt signaling pathway, function and regulation were extensively studied in vulva development using *C. elegans* as a model organism (Eisenmann, 2005; Gleason et al., 2002; Myers and Greenwald, 2007). When Wnt signals are absent, Axin, Disheveled, APC, GSK3β, and CK1 homologs form a degradation complex which phosphorylates the transcriptional coactivator BAR-1/β-Catenin on phosphodegron sequence, thus targeting it for βTrcp-dependent ubiquitination and proteasomal degradation (Korswagen 2002). The *C. elegans* genome encodes five Wnt ligands and four Frizzled receptors. The presence of Wnt ligand at Frizzled receptor induces the recruitment of the degradation complex to the cell membrane thus, allowing unphosphorylated BAR-1/β-Catenin to translocate to nucleus, where it coactivates transcription driven by the TCF/LEF family TF POP-1 (Korswagen 2002). This canonical Wnt signaling pathway is an important regulator of cell fate and cell proliferation (Angers and Moon 2009) and regulate VPC competence and polarity (Figure 1.3).

Wnt-BAR-1/β-catenin along with LET-60/Ras-MPK-1/MAPK, LIN-12/Notch, are highly regulated for vulva developmental in hermaphrodites (Eisenmann, 2005; Sternberg, 2005). These pathways coordinate vulval formation to produce 3°-3°-2°-1°-2°-3° cell fate pattern of 6 Vulval Precursor Cells (VPCs), which gives rise to the mature vulva. Wnt signaling promotes 2° fate in P5.p and P7.p cells and controls cell polarity by regulating Hox gene *lin-39* (Eisenmann et al., 1998). During L1, P3.p to P8.p escape fusion to the surrounding hypodermal syncytium through a process mediated by *lin-39*. The expression of *lin-39* is positively regulated by BAR-1(β-catenin) mediated canonical Wnt signaling pathway (Eisenmann et al.,

1998). The Wnt ligands, CWN-1 and EGL 20, are involved in the Wnt-BAR-1/β-catenin pathway to promote *lin-39* expression. Mutations in Wnt pathway components leads to abnormal cell proliferation during vulval development in nematodes. The study of vulva development helps us in comprehending the process of signal transduction and communication between different signaling pathways that controls organ formation in nematodes (Sharma-Kishore et al., 1999; Gleason et al., 2002; Sternberg, 2005; Seetharaman et al., 2010) (Figure 1.4).

1.7 Vulvaless (Vul) and Multivulval (Muv) mutants

Gupta lab has an extensive collection of *C. briggsae* mutants that have defects in vulva development. They are either Vulvaless (lacking normal Vulva cells - Vul) or Multivulva (Extensive division of cells - Muv). The genes that promote vulva development are categorized as Vul genes. Any mutation in Vul genes results in fewer than the normal cells (Ferguson and Horvitz, 1985). It has been found that, when the EGF pathway is curtailed, less EGF ligand is produced and thus received by the vulval precursor cells (VPCs) (Fay and Yochem, 2007). As a consequence, there is the reduction in the division of vulva precursor cells and thus, gives rise to Vulvaless (Vul) phenotype. The Muv mutants are characterized by the presence of a normal vulva along with multiple tumor-like protrusions on the ventral surface of the animal body, known as pseudo-vulvae, (Ferguson and Horvitz, 1989). Muv genes negatively regulate vulva developments by inhibiting inappropriate division of vulva precursors. Mutation in these genes lead to the Muv phenotype (Ferguson and Horvitz, 1989). In these mutants, more VPCs divide than expected.

Within this system, multivulva mutants are important because they exhibit inappropriate division in vulva cells and may identify genes with tumor suppressor activity (Kirienko et al., 2010).

1.8 Aim of the thesis

There are many unknown genes that still need to be discovered in order to understand the signaling network involved in vulva developmental. We still have limited knowledge of how genes interact to sustain the process of development in nematodes. Further research needs to be carried out to fully understand the mechanism of gene regulation system in vulva development. This thesis aims to understand

the novel Muv-class of genes, identified in Gupta and Chamberlin labs which negatively regulate vulva development in *C. briggsae* and how these genes function to regulate cell proliferation. By studying the gene function and uncovering the potential species-specific differences and similarities between *C. elegans* and *C. briggsae*, the molecular mechanism and underlying genetics of *Cbr-ivp* genes in vulval cell differentiation can be comprehended. This thesis further focuses on the identification and characterization of two previously uncharacterized Muv strains isolated in Gupta lab.

1.9 Research Objective

The long-term goal of this research is to characterize novel Muv-class genes, which negatively regulate cell proliferation in vulva development in *C. briggsae* and to understand how these genes have evolved to specify vulval cell fates differently from *C. elegans*.

Thus, the specific objectives are:

• Functional characterization of *Cbr-ivp* class of genes and comparative studies of gene function in *C. elegans*.

• Mapping of *Cbr-lin(bh1)* and *Cbr-lin(bh3)* mutations and determination of candidate gene.

• Functional characterization of *Cbr-lin(bh1)* and *Cbr-lin(bh3)*.

1.10 Work done prior to initiate this thesis

AF16 animals were mutagenized by treating them with Ethyl Methane Sulfonate (EMS). Animals exhibiting Muv phenotype were isolated in the F2 generation, and their progenies were evaluated. The lines exhibiting a heritable phenotype were retained for further study. The two strains *Cbr-lin(bh1)* and *Cbr-lin(bh3)* showing Muv phenotype were selected. Each of these strains has been outcrossed to the parental strain (AF16) twice to eliminate unwanted secondary mutations prior to initiate genetic analysis.

A set of 14 *C. briggsae* Muv mutants corresponding to seven genes, were mapped to specific regions on chromosomes using phenotypic markers and molecular polymorphisms and their molecular identities were determined (Sharanya et al. 2012). 4 of these 7 genes had shown no known *C. elegans* orthologs and were found to

regulate vulva development and thus, were categorized as *Cbr-ivp* (*i*nappropriate *v*ulval *p*roliferation) class of genes. *CBG11849/Cbr-spr-4*, *CBG01691/Cbr-htz-1*, and *CBG18977/Cbr-gon-14* were found to be located on the chromosome I, IV, V respectively (Sharanya et al., 2015) and examined at Dr. Chamberlin's Lab at Ohio State University, USA. One of these Cbr-ivp genes was mapped on chromosome and studied by the previous graduate students in our lab. *CBG03376/Cbr-ivp-3(sy5216)* was found to be located on the chromosome IV in *C. briggsae* (Sharanya et al. 2015). *Cbr-spr-4(gu163)* allele was located on sixth exon and *Cbr-htz-1(gu167)* was found to be located on second exon. *Cbr-gon-14(gu102)* affects the 5' splice site of intron 8 in *Cbr-gon-14*. There are three known Cbr-ivp-3 mutant alleles, *Cbr-ivp-3(gu236)*, *Cbr-ivp-3(sy5392)* and *Cbr-ivp-3(sy5216)*. *Cbr-ivp-3(gu236)* allele was located on the fourth exon while *Cbr-ivp-3(sy5392)* and *Cbr-ivp-3(sy5216)* both were located in seventh exon of *Cbr-ivp-3 gene*. The precise location of all the alleles was determined by polymorphism mapping and followed by whole genome sequencing. DNA was extracted and genome samples were prepared. Alleles for *Cbr-gon-14(gu102)* were sequenced at Ohio State University Comprehensive Cancer Center Genomics Shared Resource while alleles for all the other three genes were sequenced at McGill University - Génome Québec Innovation Centre Montreal. Sequencing data was analyzed by Dr. Don Moermon's lab and candidate genes were identified based on the in-frame missense and nonsense mutation.

On the basis of protein domain, these genes are likely to function in the nucleus and are possibly involved in the regulation of chromatin-mediated gene expression (Chamberlin et al., 2020). *Cbr-ivp-3* mutant was found to exhibit severe multivulva (Muv) phenotype with 100% Muv penetrance, and so it was hypothesized that this gene is involved in the negative regulation of vulval development. Both *Cbr-ivp-3(sy5392)* and *Cbr-ivp-3(sy5216)* alleles were identified as nonsense mutations (Sharanya et al. 2015), leading to truncation of IVP-3, and therefore most likely affecting the protein's structure and function.

To understand the effect of these mutations in vulva development VPC induction was examined at mid-L4 stage. In *Cbr-ivp* Muv animals, some or all of the remaining three VPCs (P3.p, P4.p, and P8.p) were found to be induced in addition to P5.p, P6.p and P7.p. As a result of an increase in the vulval progeny, the induction score of these mutant animals were found to be greater than 3.0. Further, the four mutants were exposed to different concentration of a MEK inhibitor during L1 larval stage. A significant decrease in Muv phenotype suggested that *Cbr-ivp* class of genes act through EGF pathway to regulate vulva development in *C. briggsae* (Sharanya et al. 2015). The laser ablation experiments were carried out, and gonad was removed to understand if the Muv phenotype in the *Cbr-ivp* mutants is gonad dependent. Though it was demonstrated that *Cbr-ivp* genes can

bypass the requirement of gonad and Anchor Cell (AC) for the vulva development (Sharanya et al. 2015).

Previous work conducted in our lab, showed that mutations in *Cbr-ivp* genes leads to the Muv phenotype in *C. briggsae*. The mechanism and involvement of *Cbr-ivp* genes in the negative regulation the cell proliferation in vulval cell is still under investigation.

Table 1.1 The three alleles of *Cbr-ivp-3* mutant

Allele	Type of Mutation	Location	Nucleotide change	Codon change	Amino acid change
Cbr-ivp-3(gu236)	Nonsense	Exon 4	C to T	CGA to TGA	Arg to STOP
Cbr-ivp-3(sy5216)	Nonsense	Exon 7	G to A	TGG to TGA	Trp to STOP
Cbr-ivp-3(sy5392)	Nonsense	Exon 7	A to T	AAA to TAA	Lys to STOP

(Adopted from Pabla R. 2017)

1.11 Findings of the thesis

This thesis focuses on genes that negatively regulate the proliferation of vulva precursor cells. Molecular genetic analyses of *Cbr-ivp* class of genes and *Cbr-lin(bh)* alleles have been carried out. *Cbr-ivp* class of genes includes, *Cbr-spr-4*, *Cbr-htz-1*, *Cbr-ivp-3* and *Cbr-gon-14* genes. All the mutants of Cbr-ivp class displayed ectopic VPC induction and defects in gonad morphology. The molecular identities of these genes were determined previously, and their functional characterization were carried out in this thesis.

The RT-qPCR were carried out to analyze the level of *Cbr-lin-3* transcript in ivp class mutants. It was observed that the level of *Cbr-lin-3* in all the ivp class mutants were significantly higher compared to wild-type AF16. Thus, it was decided to knockdown *Cbr-lin-3* in all the four mutants to see if that would result in the suppression of Muv phenotype. *C. briggsae* does not support systemic RNAi and thus a functional copy of *sid-2* gene from *C. elegans* was introduced in *Cbr-ivp* mutants. The Muv mutants were crossed with *mfIs42[Cel-sid-2 (+); myo-2::dsRed]* and RNA interference was carried out. A *Cbr-lin-3* RNAi plasmid was constructed to knockdown *Cbr-lin-3* transcripts in Cbr-ivp mutants. The RNAi knockdown of *Cbr-lin-3* transcripts showed a significant decrease in VPCs induction and thus, suppressed the Multivulva phenotype in these animals. It was concluded that *Cbr-ivp* genes negatively regulate the vulva development in *C.*

briggsae by repressing the transcription of *Cbr-lin-3*/EGF, a role that is similar to SynMuv class of genes in *C. elegans*.

A knockout allele of *ivph-3*, the *C. elegans* ortholog of *Cbr-ivp-3* was kindly provided by Dr. Don Moerman. The molecular genetic analysis and phenotypic characterization was carried out. The data showed that the animals with homozygous allele for *ivph-3(gk3691)*, exhibited a protruding vulva phenotype and were found to be sterile. This implied that *ivph-3* is crucial for maintaining fertility in *C. elegans*. To further understand the role of *ivph-3* in *C. elegans* development, embryonic and larval lethality assay was carried out. To investigate if *ivph-3* gene functions as a SynMuv gene, double mutants were constructed with *lin-15A(n767)*, *lin-8(n111)* and *lin-56(n2728)* strains. The strains were confirmed by PCR and sequencing for the presence of mutant alleles. It was observed that double mutants did not exhibit a Muv phenotype. These results suggested that although *ivph-3* is required for the normal vulval development similar to *Cbr-ivp-3*, its mechanism of function appears to have diverged.

To analyze the expression profile of *Cbr-ivp-3* and *ivph-3*, transcriptional fusion reporters were constructed and injected into *C. briggsae* and *C. elegans* along with *myo-2::GFP*. It was expected that the expression pattern of the gene will provide insight into the function of *Cbr-ivp-3* and *ivph-3*. However, no GFP expression was observed in *C. briggsae*. *ivph-3::GFP* plasmid expressed in intestine cells, neurons and in vulva during F1. Though, expression was lost from vulval cells in subsequent generations.

RNAseq analysis, was carried out to identify differentially expressed genes. The RNA-Seq data for *Cbr-spr-4(gu163)* and *Cbr-htz-1(gu167)* mutants were analyzed extensively for the germline candidate genes whose expressions were found to be up regulated. RT-qPCR was carried out to analyze the level of *Cbr-mes-4* and *Cbr-pgl-1* transcript in all *Cbr-ivp* class mutants at both L1 and mid-L3 stages. The expression levels of transcripts were found to slightly up regulated compared to wild-type AF16.

In addition to *Cbr-ivp* class of genes, this thesis also describes genetic analysis of two previously uncharacterized Muv genes, *Cbr-lin(bh1)* and *Cbr-lin(bh3)*. Both *Cbr-lin(bh1)* and *Cbr-lin(bh3)* alleles affect the vulva development in *C. briggsae*. These alleles had not been characterized previously and thus a molecular genetic analysis and functional characterization was carried out. The penetrance assay was carried out to analyze the frequency of Muv phenotype in the population. The Muv penetrance in *Cbr-lin(bh3)* was found to be 43.85% while for *Cbr-lin(bh1)*, it was found to be 30.42%. The effect of temperature on multivulva penetrance was tested for both *Cbr-lin(bh1)* and *Cbr-lin(bh3)* mutants. It was observed that the temperature did not affect the Muv penetrance in *Cbr-lin(bh3)*, on the other hand

Cbr-lin(bh1) mutants showed sensitivity when the culture was exposed to various temperatures. *Cbr-lin(bh1)* mutants showed 17.39%, 30.42% and 43.19% of Muv penetrance when grown at 15°C, 20°C, and 25°C respectively. It was observed that *Cbr-lin(bh1)* is a slow growing strain as compared to the wild type strain of *C. briggsae*. The standard growth time was delayed by approximately 8-10 hours when the animals are grown at 20°C.

Polymorphism mappings were carried out to map the location of mutations on the chromosomes and to identify new genes that are involved in vulva development. After several rounds of mapping for *Cbr-lin(bh1)*, the gene appear to be linked to Chromosome I. For *Cbr-lin(bh3)*, the gene appear to be linked to Chromosome III. Complementation experiment revealed *Cbr-lin(bh1)* and Cbr-spr-4 are two distinct genes.

Cbr-lin(bh1) and *Cbr-lin(bh3)* mutants also displayed ectopic VPCs induction. Use of *egl-17::GFP* (*mfIs5*) marker indicated that both P4.p and P8.p VPCs adopted the 2° cell fate in Muv animals while P3.p also adopted 2° cell fate in very few *Cbr-lin(bh3)* mutants. In an another experiment, *Cbr-lin(bh3)* animals were found to exhibit the ectopic expression of *zmp-1::GFP* (*mfIs8*), in P4.p and P8.p vulval progenies. Very few animals with *Cbr-lin(bh3)* mutation showed defects in the gonad morphology.

The work described in this thesis provide a platform to carry out further experiments in order to understand the role and mechanism of *Cbr-ivp* and *Cbr-lin(bh)* genes in vulva development. These findings will advance our understanding on the negative regulation of vulva development in nematodes.

1.12 Concluding remarks

This thesis forms a basis to carry out further experiment that are needed to further understand the role and mechanism of a novel class of tumor suppressor genes in vulva development. The findings in this thesis will advance our understanding on the negative regulation of vulva development in nematodes.

The results demonstrated *C. briggsae* as an excellent experimental model system to identify tumor suppressor genes that impact cell signaling. Comparison of gene function in diverse genetic backgrounds can provide us insight on how genetic differences contribute to different responses during development. These findings will demonstrate that although the structure of vulva is similar in nematodes, the fundamental genetic mechanisms include both conserved and divergent functional components.

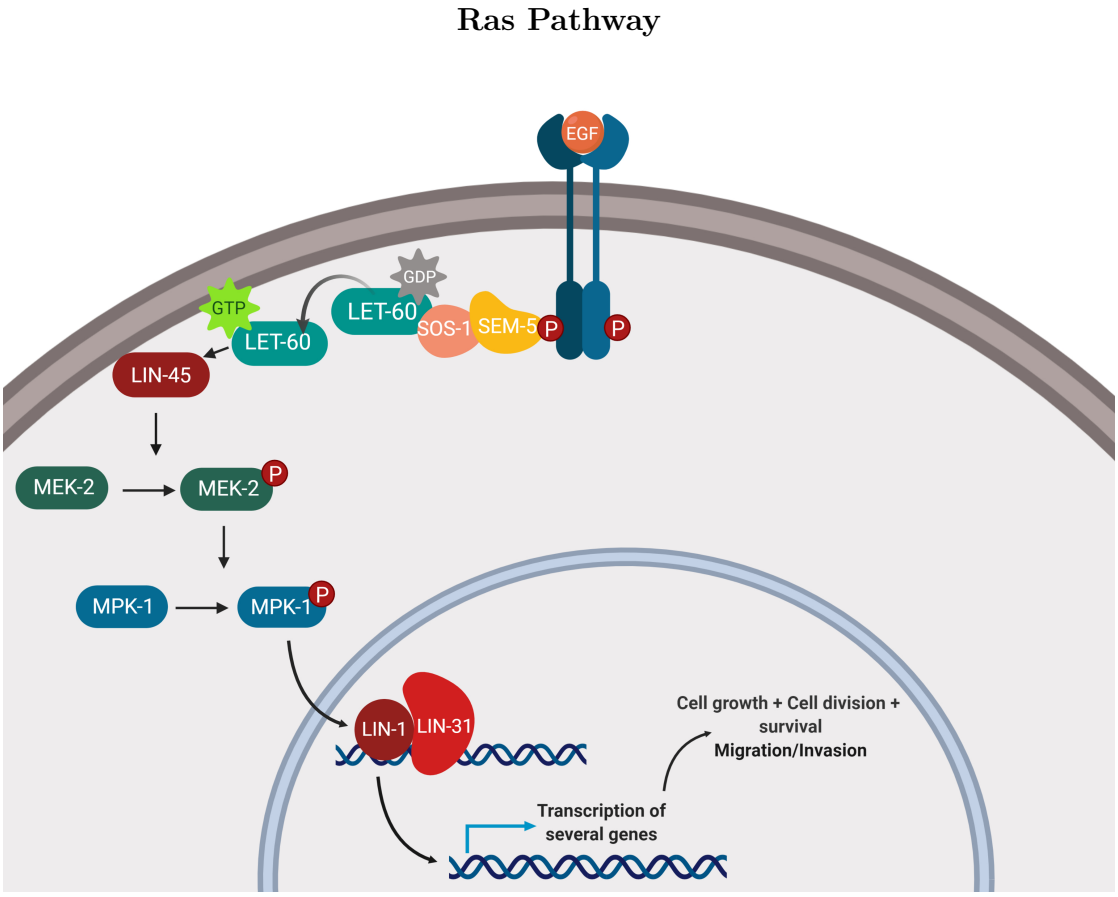

Figure 1.1 EGF/LIN-3 secreted from AC binds and induces receptor tyrosine kinase (RTK), EGFR/LET-23. Epidermal Growth Factor Receptor (EGFR) upon activation undergoes dimerization and autophosphorylating tyrosine residue at the C-terminal region. Autophosphorylated residue than serve as docking sites for adaptor proteins, GRB2/SEM-5, which recruit a Guanine Nucleotide exchange Factor SOS-1. SOS-1 then activates RAS, which activates the protein kinase activity of RAF kinase LIN-45. The active form of RAS binds to LIN-45 (Raf) and coordinate with other scaffolding proteins to phosphorylate and activate MEK/MEK-2, which in turn phosphorylates and activates ERK/MPK-1. The activated MPK-1 translocate into the nucleus and phosphorylates transcription factors (TFs) that regulate downstream target genes.

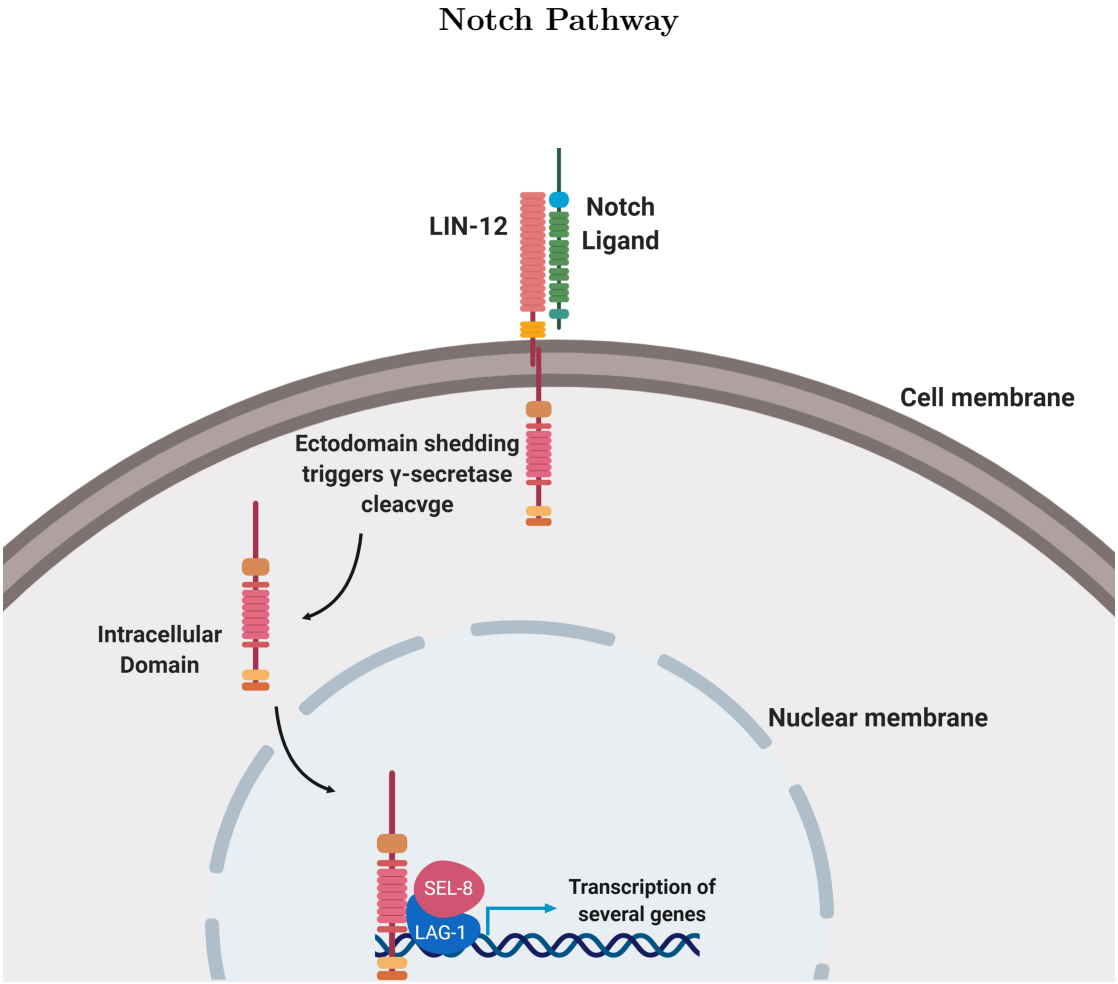

Figure 1.2 Ras induces the transcription of DSL ligand genes in P6.p cell. When a Notch ligand, such as LAG-2/DSL-1/APX-1, is present, it interacts with the Notch receptor. Binding of Notch ligand induces the extracellular cleavage in Notch receptor by ADAM-family. Shedding of ectodomain region triggers the intercellular cleavage of the receptor by γ-secretase. The released intracellular domain of Notch (NICD) translocated to the nucleus where it forms a complex with the transcription factors CSL and its co-activator, resulting in the transcription of target genes.

Wnt Pathway

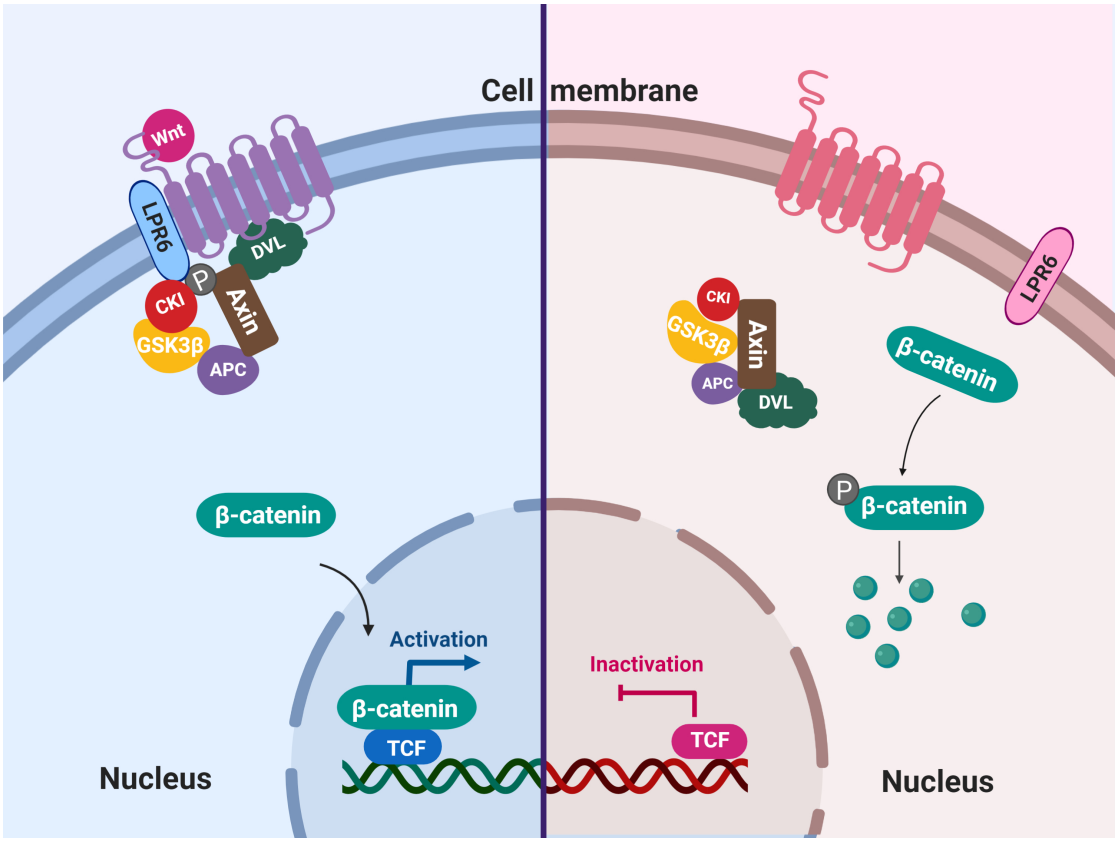

Figure 1.3 The canonical pathway is activated when a Wnt ligand binds to the Frizzled receptor. LPR6 binds with Wnt induced Frizzeled receptor. This binding triggers the recruitment of the degradation complex to the cell membrane. The β-catenin is stabilized in the cytoplasm and is translocated to nucleus where its interaction with with TCF family transcription factors activates the expression of target genes. However, when Wnt ligand is absent, APC (Adenomatous Polyposis coli), Disheveled and Axin scaffold proteins interact with β-catenin in the cytoplasm. β-catenin is further phosphorylated by CKIα kinase and GSK3β (Glycogen Synthase Kinase 3 beta), which leads to its ubiquitinoylation and degradation by the proteasome.

Integration and cross talk between cell signaling pathways during vulva development in nematodes

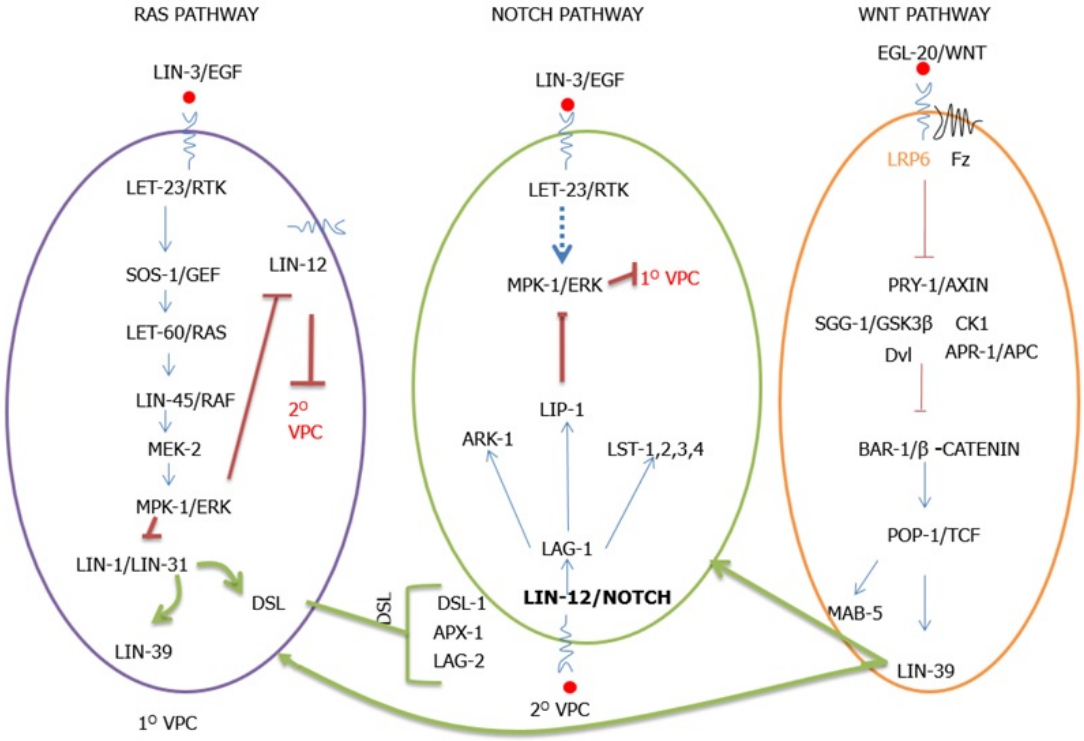

Figure 1.4 The anchor cell secretes the LIN-3/EGF inductive signal which binds to and activates LET-23/EGFR receptors. P6.p is most proximal to the AC; thus, receives higher LIN-3 inductive signal which causes P6.p to adopt 1° cell fate. P5.p and P7.p receive less LIN-3 gradient signals. Ras reduces the LIN-12 protein levels by promoting the transcription of LIN-12/Notch inhibitors. Notch ligands binds to the LIN-12/Notch receptors on P5.p and P7.p and induces the transcription of LIP-1, ARK-1 and LST. LIP-1 is a MAP Kinase Phosphatase, which negatively regulates MAP kinase activity in P5.p and P7.p during vulval induction. Lower levels of LIN-3/EGF signal in addition to the repressive lateral signals from P6.p mediated by LIN-12 (NOTCH) results in P5.p and P7.p to adopt 2° cell fate.

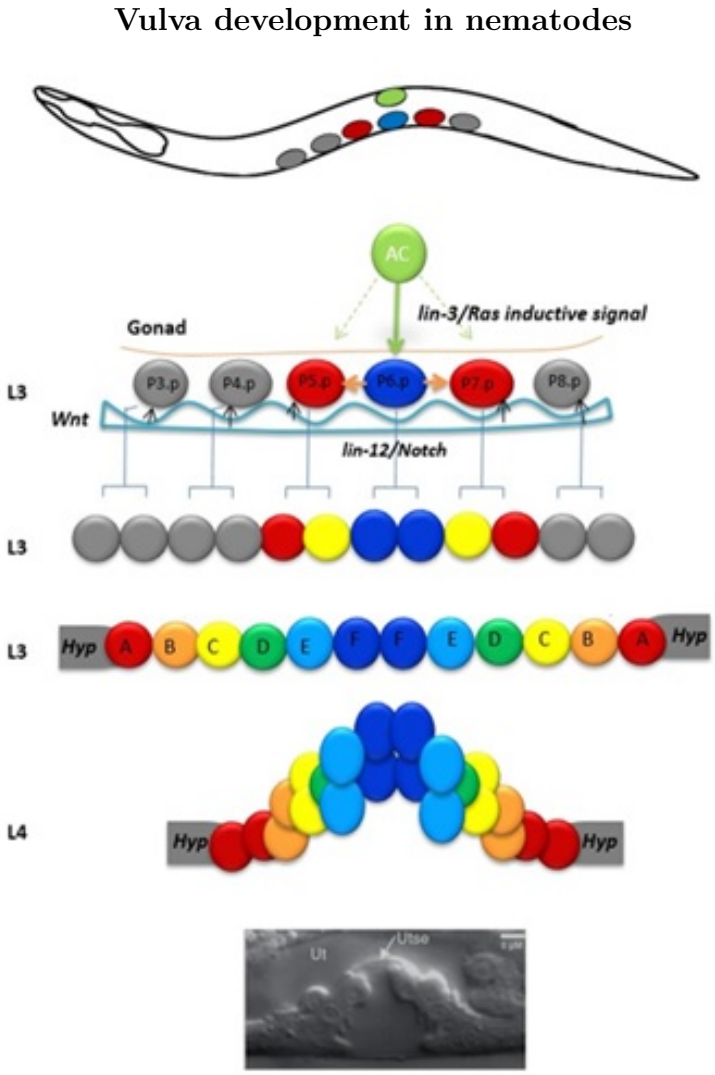

Figure 1.5 During vulva development Ras, Notch pathways and the Wnt pathway interacts with each other to determine the fate of 6 VPCs, P3.p to P8.p. Inductive signal released from the Anchor Cell (AC) leads to the division in 3 VPCs to give rise to 22 cells which undergo morphogenesis to form mature vulva. P6.p takes on a primary cell fate while P5.p and P7.p take on a secondary cell fate. The P3.p, P4.p and P8.p cells take on a tertiary sell fate, which divide one time and fuse to the hypodermis (Sternberg, 2005).

Chapter 2

Materials and methods

2.1 Worm maintenance and Genetics

Culture and maintenance of nematodes were carried out as described previously (Brenner, 1974). All experiments were carried out at 20°C, unless stated otherwise. Strains used in this study are,

C. briggsae: AF16 (wild-type), HK104 (Polymorphic wild-type), *bhEx117[mec-7::GFP + myo-2::GFP]*, *Cbr-spr-4(gu163)*, *Cbr-htz-1(gu167)*, *Cbr-ivp-3(sy5216)*, *Cbr-gon-14(gu102)*, *Cbr-lin(bh1)*, *Cbr-lin(bh3)*, *mfIs5[Cbr-egl-17::GFP + myo-2::GFP]*, *mfIs8 [Cbr-zmp-1::GFP + myo-2::GFP]*, *mfIs42[Cel-sid-2 (+); myo-2::dsRed]*, *mfEx32 [Cel-sid-2 (+); myo-2::dsRed]*, *Cbr-spr-4(gu163); mfIs42[Cel-sid-2 (+); myo-2::dsRed]*, *Cbr-htz-1(gu167); mfIs42[Cel-sid-2 (+); myo-2::dsRed]*, *Cbr-ivp-3(sy5216); mfIs42[Cel-sid-2 (+); myo-2::dsRed]*, *Cbr-gon-14(gu102); mfEx32[Cel-sid-2 (+); myo-2::dsRed]*, *Cbr-lin(bh1); mfIs5[Cbr-egl-17::GFP + myo-2::GFP]*, *Cbr-lin(bh1); mfIs8[Cbr-zmp-1::GFP + myo-2::GFP]*, *Cbr-lin(bh3); mfIs5[Cbr-egl-17::GFP + myo-2::GFP]*, *Cbr-lin(bh3); mfIs8 [Cbr-zmp-1::GFP + myo-2::GFP].*

C. elegans: N2 (wild-type), *ivph-3(gk3691)*, *lin-15A(n767)*, *lin-8(n111)*, *lin-56(n2728)*, *ivph-3(gk3691); lin-15A(n767)*, *lin-8(n111); ivph-3(gk3691)*, *lin-56(n2728); ivph-3(gk3691).*

2.2 Bleach synchronization

Bleach synchronization results in the synchrony of the worm larval stages. To obtain a synchronized population of worms, plates containing gravid hermaphrodites were washed using M9 buffer. Animals were collected and centrifuged in 15ml falcon tubes. The M9 buffer was then removed without disturbing the pellet and a new M9 buffer was added to the tube and the tube was then subjected to the

centrifuge. This process was repeated several times until the M9 buffer was clear. Multiple washes were carried out to remove residual *OP50* bacteria and other debris. The worms in M9 were then treated with a bleach solution containing 4N potassium hydroxide (KOH) and sodium hypochlorite (commercial bleach) in a 3:2 ratio. The tube was shaken vigorously until all the worms body disintegrated and released eggs in the solution. Fresh M9 buffer was added to prevent eggshells from getting harmed. The solution was then centrifuged, and the eggs were pelleted, the bleach solution was discarded without disturbing the pellet. The pellet was then washed with M9 buffer for three to four times (Stiernagle, 2006). The eggs were either placed on the plates for the further experiment or transferred in a 1.5ml Eppendorf tube along with M9 buffer and placed on a rotisserie overnight at room temperature. These eggs were hatched and arrested in the L1 stage until plated.

To double synchronize the culture, worms were bleached and placed on a rotisserie overnight at room temperature. The arrested L1 were plated onto the plates and allowed to reach the adult stage. Worms were washed after 6 hours of adulthood and bleached synchronize again. The culture thus obtained is defined as double synchronized culture.

2.3 Microscopy and Scoring

C. briggsae and C. elegans animals were examined for VPCs cell fate. The characterization of Muv phenotype was carried out using a Nikon Eclipse 80i microscope at 100X magnification. Mid-L4 animals were examined for the VPC induction under the Nomarski microscope. Animals were mounted on agar pads. 1mM Sodium Azide was used to immobilize the worms (Wood 1988). P5.p, P6.p, and P7.p VPCs are induced to divide and produce vulval cells. P6.p adopts the primary fate (1°) undergoes division and gives rise to eight vulval cell progeny. Both P5.p and P7.p adopt the secondary fate (2°) and each gives rise to seven vulval progenies. VPCs that exhibit complete induction, scored as 1.0 while a score of 0.5 would be assigned for every half induction. Thus, VPCs induction score for wild-type animals would be 3.0 . In multivulva animals additional VPCs, P3.p, P4.p, and P8.p induce and give rise to vulval progenies and thus, induction score in these animals are higher than 3.0.

Multivulva animals were examined for abnormalities in phenotype. Animals were analyzed and scored for the defects in the gonadal arm, direction, length, and orientation. Muv penetrance was calculated under a stereomicroscope. To carry out the penetrance assay, approximately 100 L3/L4 worms were transferred

on the plate and allowed to grow at 20°C. The Muv and Pvl phenotypes were scored in adults.

For transgenic worms, expressing reporter protein, images were captured on the Zeiss Axioimager D1 microscope equipped with the GFP filter HQ485LP (Chroma Technology). For the 100X magnification and VPCs pattern images were taken using a Nikon DXM1200F digital camera. The images were processed using NIH Image J software.

2.4 Genetic crosses

The genetic crosses were carried out on 15mm plates seeded with *E. coli OP50*. Cross plates were prepared by putting a drop of LB media containing bacterial strain. The plate was then swirled to spread the bacterial solution on the plate. Crossing works well when the bacterial spot is very small. The plates were then stored at room temperature overnight to allow the growth of the bacterial lawn. The plates were then used to set up the cross. To set up the cross, young adult males and young adult hermaphrodites were placed in a 3:1 ratio on cross plates. Animals were allowed to mate for 2 days to produce F1 animals. After two days, adult males (P0) were removed from the plate to prevent their accidental mating from F1 hermaphrodite progenies. L4 staged F1 heterozygous animals resulted from the cross (Cross progeny), were collected and cloned onto separate plates, different markers were used to distinguish cross progeny from the self-progeny. In the case where F1 males were collected, they were used to set up the subsequent crossed while F1 hermaphrodites were allowed to self-fertilize. F2 progeny worms were further observed for the phenotype.

For the mutants that exhibit maternal rescue effects, F2 animals were further cloned singly onto plates and allowed to produce F3 progenies. The F3 progenies were screened for the mutant phenotype. The plates which showed defective phenotype were retained while others were discarded. The penetrance of the Muv phenotype was monitored over the next several generations.

To carry out RNAi experiments in *C. briggsae*, the males from *mfIs42[sid-2::GFP; myo-2::dSRed]* strain were used to set up the cross with *Cbr-ivp* mutants hermaphrodite. The transgenic strain carries the wild-type copy of the *C. elegans sid-2* gene to generate strains sensitive to environmental RNAi.

2.5 Primer design and optimization

All the primers that were used for PCR and RT-qPCR experiments were designed using the NCBI Primer Blast tool (https://www.ncbi.nlm.nih.gov/tools/primer-blast) and ApE software available on http://jorgensen.biology.utah.edu/wayned/ape

The primers used for RT-qPCR were designed in a way that the primers spanned an exon-exon junction. The primers pairs were optimized for annealing temperature and specificity, based on melt curve analysis. Furthermore, the accuracy of the primer binding and amplification was examined by running the PCR products on an agarose gel to ensure that the correct amplicon size was produced. A list of oligonucleotide primers used in this study was described in table 2.1.

2.6 Construction of RNAi plasmids

The RNAi plasmids were generated to knock down the RNA transcripts of *C. briggsae* genes. The RNAi plasmids for *C. briggsae* were generated using PCR based cloning method. Genes of interest were amplified using primers specific to the gene. The amplicons were then inserted into the empty backbone of the *L4440* vector. The *L4440* vector was a gift from Andrew Fire (Addgene plasmid - 1654; http://n2t.net/addgene:1654 ; RRID:Addgene 1654).

Each primer designed for the construction of RNAi plasmid consists of three parts, an annealing region complementary and specific to the genes of interest, connected to a restriction site and followed by a buffer region of 2 to 3 base pairs. The length of the annealing sequence in each primer was approximately 20 bp each, the buffer region was added to the restriction site since many restriction enzymes do not cut DNA efficiently at the end of a linear piece. A pair of forward-reverse primers was used to amplify the gene of interest from AF16 genomic DNA. The PCR products were purified using GenepHlow^{TM} Gel/PCR Kit (DFH100, DFH300) from Geneaid. For the extraction of *L4440* plasmid, *pPD129.36* bacteria were inoculated in 3ml of LB media containing 3μl of Carbenicillin (100μg/ml) and allowed to grow overnight at 37°C. The plasmid was extracted using the Invitrogen miniprep kit (Cat No. K210011). Double digestion using restriction enzymes was carried out for 2 hours at 37°C for both the PCR amplicon and the *L4440* vector. The digested DNA products were then loaded and ran through electrophoresis on a 0.8% agarose gel. The bands were extracted from the gel and purification was conducted to isolate the digested product using GenepHlow^{TM} Gel/PCR Kit (DFH100, DFH300) from Geneaid.

A DNA ligation reaction was carried out to insert the PCR amplicon into the plasmid. The Invitrogen kit (Cat No. 15224-017) was used to carry out ligation. The insert to the plasmid ratio was 3:1. The total concentration was up to 100ng. A negative control reaction was set up alongside, contained only digested *L4440* vector but not the insert. The ligation reaction was carried out overnight at 26°C

1-5μl of the ligation reaction mixture was used to transformed NEB® 5-alpha Competent *E. coli* (High Efficiency). The transformation and incubation were carried out according to the manufacturer's instructions (Cat No. C2987H/C2987I). Individual bacterial colonies were picked and inoculated in 3ml of LB media containing 3μl of Carbenicillin (100μg/ml) and allowed to grow overnight at 37°C. The plasmid was extracted using the Invitrogen miniprep kit (Cat No. K210011) followed by diagnostic restriction digestion using restriction enzymes. The digested product was run and validated on a 0.8% agarose gel. The plasmid was transformed into *E. coli HT115* Electrocompetent cells through electroporation using Eppendorf® Electroporator 2510. The transformation was carried out according to the manufacturer's operating manual.

2.6.1 *Cbr-lin-3* RNAi plasmid

The RNAi plasmid to knockdown *Cbr-lin-3* transcript was constructed by inserting an 885 bp amplicon in the *L4440* vector (2,790 bp) using restriction enzymes SalI and SphI. The plasmid was transformed into *E. coli HT115* cells through electroporation.

2.6.2 *Cbr-mes-4* RNAi plasmid

To create the *Cbr-mes-4* RNAi plasmid, a 3,130 bp of *Cbr-mes-4* fragment was PCR amplified. The fragment was inserted into the *L4440* vector using restriction enzymes KpnI and SalI. *E. coli HT115* cells were transformed and the plasmid was extracted and confirmed by restriction digestions.

2.6.3 *Cbr-pgl-1* RNAi plasmid

Cbr-pgl-1 RNAi plasmid was created to knockdown the transcripts in *C. briggsae* animals. To achieve this, a 2638 bp of *Cbr-pgl-1* fragment was amplified using PCR and into the *L4440* vector using restriction enzymes NcoI and XhoI. *E. coli HT115* cells were electrocuted and plasmid was transformed.

2.7 RNA Interference

RNA interference was carried out to knock down the RNA transcripts of candidate genes in the worms. The worms were observed under Nomarski optics to analyze if RNAi resulted in the suppression of Multivulva phenotype in mutant animals. RNAi agar plates containing 100μg/ml Carbenicillin were used to carry out all the RNAi experiments. RNAi agar plates were prepared according to Dave Hansen's Lab protocol. 6gm of Na_2HPO_4, 3gm of KH_2PO_4, 1gm of NH_4Cl, 5gm of Casamino Acids and 20gm of Agar were added to water (bringing volume 1 liter). The media was autoclaved at 121°C for 40 minutes. The media was allowed to cool down to 55°C. 1ml of 1M $CaCl_2$, 1ml of 1M $MgSO_4$, and 1ml of 5mg/ml Cholesterol were added to the media and mixed well. 4gm of β-lactose and 1ml of 100mg/ml Carbenicillin was added to the media just before pouring the media into the plates. After transferring the media, the plates were allowed to dry at room temperature for overnight.

The *HT115* bacterial cultures containing RNAi plasmid to knockdown the candidate genes were inoculated in 3ml of LB media and 3μl of Carbenicillin (100μg/ml). The cultures were allowed to grow on an incubator-shaker at 37°C till the OD reached 0.6. The RNAi plates were seeded with 100μl of the HT115 bacterial culture that produces dsRNA of the gene of interest. The HT115 bacterial culture containing *L4440* empty vector was used as a negative control. The *HT115* bacterial culture containing the plasmid to knockdown *Cbr-pop-1* transcripts were used as positive control. Worms were bleached and eggs were plated on plates containing RNAi bacteria. The plates were stored at 20°C after plating the eggs. The worms were allowed to hatch and grow until the desired stages and collected for the analysis. To analyze the VPCs induction score, mid-L4 staged worms were mounted on a slide and observed under the Nomarski microscope. RNAi experiments were performed in multiple batches and analyzed for the phenotypes. The 3 batches (triplicates) that produced consistent results were considered.

To carry out the RNAi knockdown of specific genes in Cbr-ivp mutants, the transgenic strains contain *mfIs42[sid-2::GFP; myo-2::dSRed]* along with *Cbr-ivp* alleles, were generated.

2.8 RNA extraction

RNA was extracted from double synchronized animals using a standard TRIZOL method (Invitrogen). The animals were bleached and synchronized by transferring the eggs in a 1.5ml Eppendorf tube along with M9 buffer and placed on a rotisserie

overnight at room temperature. These eggs were hatched and arrested in the L1 stage until plated. L1 larvae were then plated onto the NGM plates and incubated at 20°C. The cultures were bleach synchronized again within a short period of time after the animals attained the young adult stage.

For examining the *Cbr-lin-3* transcript level, the double synchronized L1 worms were plated on NGM plates. The RNA was extracted at the mid-L3 stage. Exact staging of cultures was determined by mounting a sample of synchronized animals at different time intervals and observing them under the Nomarski microscope. RNA was extracted just prior to the stage when vulval precursors (Pn.p) were beginning to divide (Chamberlin et al., 2020). At this stage, vulval cells are most responsive to *Cbr-lin-3* levels (Felix, 2007), suggesting that at this stage the level of the *Cbr-lin-3* transcript should be high. For AF16 and *Cbr-spr-4(gu163)* animals, the RNA was extracted at L1+27 hours, for *Cbr-htz-1(gu167)* animals the RNA was extracted at L1+29 hours. Both *Cbr-ivp-3(sy5216)* and *Cbr-gon-14(gu102)* animals have shown extreme delayed in the growth thus, RNA was extracted at L1+41 hours and at L1+37 hours respectively.

For examining the transcript level of germline-specific genes, the RNA was extracted 16 hours after plating the double synchronized egg cultures for AF16, *Cbr-spr-4(gu163)* and *Cbr-htz-1(gu167)* while cultures were allowed to grow for 19 hours after plating the double synchronized eggs for *Cbr-ivp-3(sy5216)* and *Cbr-gon-14(gu102)*.

To extract RNA, worms grown on NGM plates were collected by washing the plates with M9 buffer. Animals were collected and centrifuged in 15ml falcon tubes. The M9 buffer was then removed without disturbing the pellet and a new M9 buffer was added to the tube and the tube was then subjected to the centrifuge. This process was repeated several times until the M9 buffer was clear. Multiple washes were carried out to remove residual *OP50* bacteria and other debris.

The pelleted worms were transferred to Eppendorf tubes. Three volume of TRIZOL (Invitrogen, cat. no. 15596-026) was added to the one volume of the pelleted worms. The pellet was then resuspended by vortexing, followed by flash freezing the sample in liquid nitrogen and thawing at 37°C and further vortexing it. The resuspension step was repeated multiple times resulting in the disintegration of the worm's cuticle to allow rapid RNA solubilization. The tubes were stored overnight at -80°C. The tube was thawed and two additional volumes of TRIZOL to the starting volume of the worms were added to the mixture and vortexed. The mixture was then left to stand at room temperature for 5 minutes. Two volumes of the chloroform to the original volume of worm pellet was added to the tube and mixed vigorously to form a uniform suspension. The mixture was allowed to incubate at room temperature for 3 minutes to disrupt nucleic acid

- protein complexes. The mixture was centrifuged at 12,000g for 15 minutes at 4°C. The upper aqueous layer containing the RNA and Nucleic acid residue was then transferred to a new tube, and an equal volume of isopropanol was added and mixed gently. The mixture was allowed to stand at room temperature for 15 minutes and was then centrifuged at 4°C at 12,000g for 20 minutes. The supernatant was discarded, the visible pellet of RNA was washed in 500μl of absolute alcohol followed by washing with 500μl of 75% ethanol and centrifuged at 12,000g for 5 minutes at 4°C to remove the traces of salts. The supernatant was removed, and the pellet was air-dried in Speed-vac to get rid of ethanol residual (three minutes). The pellet was dissolved in nuclease-free water that had been preheated to 65°C. The RNA was stored at -80°C until further used. The RNA integrity was determined by running electrophoresis on 0.8% agarose gel. The presence of two bands (28s and 18s) is indicative of intact RNA.

2.9 RNA-Seq data analysis and generation of plots

RNA was isolated and send for sequencing just prior to the stage when vulval precursors (Pn.p cells) were beginning to divide. The samples were processed and sequenced using Illumina HiSeq 2000 V3 Single Read system by Genome, Quebec (Chamberlin et al., 2020)

The raw files were extracted and RNA-Seq data were analyzed. *C briggsae* .gtf and genome.fa files were downloaded in addition to cb4 assembly from UCSC browser. We have used packages Cutadapt-1.12 and TrimGalore-master to process the sequencing read. The processed data were aligned to cb4 assembly (*C. briggsae* reference genome) using STAR2.5.1a. https://github.com/alexdobin/STAR/releases or the master branch from https://github.com/alexdobin/STAR.

2.9.1 Code to generate MA and volcano plot

Scattered plots of Differentially expressed genes were generated to display a global view of target genes from RNA-Seq data.

To install packages and accessing libraries

install.packages(“dplyr”)

install.packages(“tidyr”)

install.packages(“ggplot2”)

library("grDevices")

library("genefilter")

library("ggplot")

library("ggplot2")

MA Plot

mar.old < par('mar')

print(mar.old)

par(mar=c(w, x, y, z))

png("DESeq2MAplot.jpeg")

plotMA(dds, ylim = c(a,b), main = "RNAseq Experiment")

par(mar=mar.old)

dev.off()

dds is Distributed Data-Structure, it simplifies large-scale data analysis.

par is used to define the plotting parameters.

mar is for margin size.

Volcano Plot

with(res2, plot(log2FoldChange, log10(p-value), pch = 20, main = "Volcano plot, red = 0.05padj", ylim = c(a, b), xlim = c(c,d)))

with (subset (res2, padj<.05), points(log2FoldChange, log10(pvalue), pch = 20, col = "red"))

with(subset(res2, padj<.05 abs(log2FoldChange) > 1), points(log2FoldChange, log10(pvalue), pch = 20, col = "yellow"))

dev.copy(jpeg, 'Cbr-ivp-volcanoPlot.jpeg')

dev.off()

ylim and xlim are convenience function to set the limits of the y axis.

pch is plot character (value 0-20, by default color = black).

2.10 RT-qPCR

Quantitative reverse-transcription PCR (RT-qPCR) was used to quantify gene transcript levels and to compare the changes in gene expression in cells and tissue. Validation of RNA-Seq data requires the extraction of RNA from the worms followed by RT-qPCR analysis.

To examine *Cbr-lin-3* transcript levels in *Cbr-ivp* mutants, RNA was extracted from mid-L3 stage larvae. Animals were staged prior to harvesting by mounting a sample of worms and observing them under the Nomarski optics. (Refer Material and Methods 2.4). To examine the transcript levels of germline-specific genes the RNA was extracted from mid-L3 and early L1 larval stages. Primers for the candidate gene targets were designed and optimized using the NCBI Primer Blast tool and ApE software (Table 2.1). AF16 animals were used as control. Extracted RNA samples were treated with DNase (Quanta Biosciences PerfeCta® DNase I, RNase-free, Cat no. 95150-01K). The concentration of RNA was determined using the Nanodrop.

DNase treated RNA was used to prepare cDNA. SensiFASTTM cDNA Synthesis Kit (Bioline cat. no. BIO-65053) was used to synthesize cDNA from the purified RNA templates. The final concentration of RNA was 600ng/μl for all the strains. cDNA templates were used to carry out qPCR. For efficient quantification, SensiFASTTM SYBR R Hi-ROX Kit (Bioline cat. no. BIO-92005) was used. The reaction mix and cycling conditions and were followed as recommended by SensiFASTTM SYBR R Hi-ROX Kit. *Cbr-pmp-3* and *CBG22375* were used as the reference genes respectively for *Cbr-lin-3* and germline-specific genes transcript levels quantification. The reference genes were used to normalize the gene expression data to account for the differences in the amount of cDNA template between wild-type and mutants. Three biological and three technical replicates reactions were carried out for all the mutants and genes. For further validation, No Template Control (NTC) and No Reverse Transcriptase Control (NRT) reactions were carried out for at least 1 batch of data. BioRad CFX manager software 3.1 was used for the analysis of the data. Standard t-test was used for the calculations and data analysis.

2.11 Constructing the *ivph-3* rescue fragment

Rescue experiment was carried out to analyze if the wild-type copy of the gene from one species is able to restore the wild-type phenotype in another species. The

wild-type copy of the gene will rescue from the mutant phenotype caused by the mutated allele of the same gene.

Rescue experiment was carried out to analyze if the wild-type copy of the gene from one species is able to rescue from the mutant phenotype caused by the mutated allele of the same gene in another species. The wild-type copy of *C. elegans ivph-3* gene was amplified using primers GL1228 and GL1229 (Table 2.1). A 9357 bp fragment contained entire an 1899 bp of the 5' UTR region followed by entire *C. elegans ivph-3* gene including introns and a 1227 bp of 3'UTR.

To construct the rescue fragment, N2 genomic DNA (a total of 500ng in 50ml reaction) was used as the template. The reaction mix was prepared according to the NEB Long Range PCR Kit (cat no. 206401) protocol. The thermal cycling conditions were followed as recommended by NEB. Extension time PCR protocol was used to amplify a long fragment of DNA. For the initial ten cycles, an extension time of 1 minute per kilobase DNA was used. For the remaining 29 cycles, the extension time was increased by 10 seconds to the previous cycle, in each cycle. PCR product was analyzed by running the amplified product on 0.8% agarose gel. Invitrogen 1 kb Plus DNA Ladder (cat no. 10787018) was used as a reference. The sample ran for 7 hours at 60V. The product was further validated by digesting the amplicon using SpeI restriction enzyme digestion. The restriction digestion reaction was carried out by incubating amplicon, restriction enzyme and buffer mixture for 1 hour at 37°C. The digested DNA products were then loaded and ran on a 1% agarose gel for 7 hours at 50V. After confirmation, the PCR products were purified using GenepHlow^{TM} Gel/PCR Kit (DFH100, DFH300) from Geneaid. *ivph-3* gene fragment was then microinjected into wild-type *C. briggsae* AF16 and *Cbr-ivp-3(sy5216)* Muv mutants through microinjection technique (Mello et al., 1991). The injection mix contained 50ng/μl of the PCR product, 10ng/μl of *myo-2::GFP*, 100ng/μl of pBluescript SK (+) vector and nuclease-free water. F1 animals were screened for *myo-2::GFP* fluorescence. Fluorescing F1 animals were picked and cloned onto individual agar plates and plates were stored at 20°C. F2 generation animals were then screened for *myo-2::GFP fluorescence*. The penetrance of the *myo-2::GFP* and Muv phenotype were monitored over several generations.

2.12 Phenotypic analysis of *ivph-3(gk3691)*

The CRISPR allele *ivph-3(gk3691)* was kindly provided by the Don Moerman lab. The allele was generated by inserting a *myo-2::GFP* cassette in the open reading frame of *ivph-3*.

Details of the insertion sites

Y67D8C.3ab-1 Upstream Homology Arm (TCGCTTACATTGTCTGCGTTCTCCA)
Y67D8C.3ab-1 Downstream Homology Arm (AATGAACGAAAAGCGCCAATTTTTG)

2.12.1 Penetrance assay

Phenotypic analysis of *ivph-3(gk3691)* was carried out. Each experiment was carried out in triplicates. To carry out phenotypic analysis, a single L4 hermaphrodite larva with *myo-2::GFP* expression was cloned onto a single plate. Multiple plates with single L4 larva were stored at 20°C incubator. The worms were allowed to reach the young adult stage. The plates with young adult animals that had wild-type phenotypes were considered for further experiments. Animals with Protruding vulva (Pvl) phenotype were turned out to be sterile. Wild-type animals were allowed to lay eggs for 24 hours. The hermaphrodite animals were then transferred to a new plate to lay eggs for another 24 hours. The procedure was repeated, for two more times. The plates were stored at 20°C incubator and eggs were allowed to hatch.

The penetrance assay was carried out for F1 animals. F1 adult animals were scored for wild-type with no GFP, wild-type with GFP and Pvl with GFP phenotypes. Other phenotypes like defect in gonad, abnormal vulval morphology were noted. All animals with Pvl phenotype and *myo-2::GFP* expression were cloned onto individual plates and observed for sterility.

2.12.2 Embryonic and larval lethality assay

Embryonic and larval lethality were scored to determine if heterozygous *gk3691* worms produce a phenotype. Strain. To carry out embryonic and larval lethality assay young adult hermaphrodite, with GFP fluorescence and wild type phenotype, was allowed to lay eggs for 24 hours. The hermaphrodite animals were then transferred to a new plate to lay eggs for another 24 hours. The procedure was repeated, for two more times. The eggs were counted onto each plate and noted. The plates were then stored at 20°C incubator for 24 hours. After 24 hours the plates were observed for larvae and unhatched eggs. The hatched animals and unhatched eggs were counted. After 1 more day the unhatched eggs were removed and discarded. The remaining larvae on these plates were then scored each day until they reached adulthood. The wild-type *C. elegans* strain, N2, was analyzed as a control. The whole experiment was repeated 2 more times to prevent any biasness in the collected data.

2.13 Temperature-sensitivity assay for Muv penetrance in *Cbr-lin(bh1)* and *Cbr-lin(bh3)*

The effects of varying temperature on vulval development were examined in *Cbr-lin(bh1)* and *Cbr-lin(bh3)*. Specifically, the penetrance of the Muv phenotype was observed to determine if temperature affects the mutant gene expression leading to abnormal vulval development. *Cbr-lin(bh1)* and *Cbr-lin(bh3)* were maintained in individual plates at 15°C, 20°C, and 25°C for at least three generations to eliminate the effects of the temperature they were maintained at prior to the experiment.

If alleles are temperature-sensitive, the Muv penetrance will differ at 15°C and/or 25°C from 20°C.

2.14 Cell fate analysis of Vulval Precursor Cells during development

During normal vulval development, VPCs receive signals in order to adopt specific cell fates (Sundaram, 2006). Primary and secondary lineage marker, *mfIs5[Cbr-egl-17::GFP + myo-2::GFP]* and *mfIs8[Cbr-zmp-1::GFP + myo-2::GFP]* respectively, are used in *C. briggsae* to assess the induced cell fates of VPCs. Fluorescence of *egl-17::GFP* is seen in VPCs that adopt the 1° cell fate during early vulval development (Burdine et al., 1998). During late development (mid-L4), 2° cell fate VPCs exhibit *egl-17::GFP* fluorescence (Burdine et al., 1998). Similarly, the fluorescence of *zmp-1::GFP* is seen in VPCs that adopt the 1° cell fate.

Hermaphrodites of Muv mutants were crossed with *mfIs5[Cbr-egl-17::GFP + myo-2::GFP]* males. Fluorescing heterozygous hermaphrodites from the F1 generation were allowed to self-fertilize. Fluorescing Muv hermaphrodites in the F2 generation were picked and examined to identify the 2° cell fates in VPCs. The cross scheme is shown below in Figure 2.1. To examine 1° cell fates in Muv mutants, Multivulva hermaphrodites were crossed with *mfIs8[Cbr-zmp1::GFP + myo-2::GFP]* strain. Fluorescing heterozygous hermaphrodites from F1 generation were allowed to self-fertilize. Fluorescing Muv hermaphrodites in the F2 generation are picked and examined to identify the 1° cell fates in VPCs.

2.15 Genetic mapping using polymorphism markers

Verified polymorphism markers, such as SNPs, indels, and RFLPs, from Koboldt et al. (2010) are used to map genes on specific regions of the chromosome. The polymorphisms used in this experiment, including the chromosome number, indel ID, primer set, and length difference of each amplicon are listed in Table 2.1. The linkage of *Cbr-lin(bh1)* and *Cbr-lin(bh3)* were analyzed, with several phenotypic markers that were assigned to different chromosomes. Large indels are not used as there is a possibility of an error during the sequence assembly process. The polymorphisms scheme for the study involved small and medium indels (Koboldt et al., 2010), which has been verified previously based on genome sequencing. The website www.briggsae.org has the collection of a large number of markers that can be used for various mapping experiments.

Fluorescing HK104 males (*bhEx117[mec-7::GFP + myo-2::GFP]*) were crossed with mutants with AF16 background in order to genetically map the mutant gene loci. F1 cross-progeny (wild-type and having GFP fluorescence) were picked and cloned. The F2 offspring had shown both parental types and recombinants. Out of all the possible combinations, recombinants that are phenotypically mutant (20 each) were picked individually and subjected to genomic DNA isolation in order to genetically map the mutant gene loci in the F2 progeny.

Bulk Segregant Analysis (BSA) was performed using the previous protocol established for *C. elegans* and *C. briggsae* (Wicks et al. 2001, Koboldt et al., 2010). Genomic DNA from phenotypically mutant recombinants was isolated by placing 20 worms into 5μl of lysis buffer and Proteinase K mixture. The solution was stored in the freezer at -80°C for 30 minutes to overnight. For Proteinase K activation, the solution was incubated at 60°C for 1 hour followed by heat inactivation of Proteinase K at 95°C. The isolated genomic DNA is frozen at -20°C and used as a template in polymerase chain reactions (PCR). A PCR was carried out to amplify the sequences where the polymorphisms were present. The detailed indel mapping protocol was carried out using the set of primers and indel mapping protocols that have been published previously (Koboldt et al., 2010). The controls AF16 and HK104 (*bhEx117*) and F2 mutants are run using gel electrophoresis to determine possible linkages. The distance between the two loci was determined to be 10% (Koboldt et al., 2010). The recombinant frequency between the mutation and polymorphism can be used to identify the locus of the mutation on the chromosome. A lower recombinant frequency indicates a linkage between the indel-based polymorphism and the mutation. Single animal-based PCR assay was carried out to determine map distance which greatly facilitates the search for candidate gene.

Table 2.1 List of oligonucleotide primers used in this study

Primer name	Sequence (5'-3')	Description & notes
Experiment: RT-qPCR to estimate *Cbr-lin-3* transcript levels and Construction of *Cbr-lin-3* RNAi plasmid		
GL911	GTGGTTCCTTCTTGCCATTGTCC	GL911 and GL912 are the forward and reverse primers respectively, used to estimate the *Cbr-lin-3* transcript levels in Muv mutants through RT-qPCR.
GL912	GAACGAAGAGTTGCGCCGTG	
GL1242	CGGCTGCAGTGTCTCGTTATTCGGTTCCAG	GL1242 and GL1243 are the forward and reverse primers, respectively, used to amplify 885bp of *Cbr-lin-3* fragment. The amplicon was used to construct the RNAi plasmid
GL1243	AGACTCTCGAGCGTGCTGCTCATCGTGATC	
Experiment: RT-qPCR to estimate *Cbr-mes-4* transcript levels and Construction of *Cbr-mes-4* RNAi plasmid		
GL1400	TGGCTGAGTATGTCGGAGAGTTG	GL1400 and GL1401 are the forward and reverse primers, respectively, used to estimate the level of *Cbr-mes-4* transcript levels in Muv mutants
GL1401	ATTCCCATATCTGGCTGCATCC	
GL1410	ATGTCGACTCGCACCCAAGAAGCAAATC	GL1410 and GL1411 are the forward and reverse primers, respectively, used to amplify 3012bp of *Cbr-mes-4* fragment. The amplicon was used to construct the RNAi plasmid
GL1411	GCGGTACCATGGTGGCTACTGGTTCATC	
Experiment: RT-qPCR to estimate *Cbr-pgl-1* transcript levels and Construction of *Cbr-pgl-1* RNAi plasmid		

GL1402	CTTGCGGTTCTCAAAGAGTGC	GL1402 and GL1403 are the forward and reverse primers, respectively, used to estimate the level of *Cbr-pgl-1* transcript levels in Muv mutants
GL1403	AAACTGCTCAGAAATGCGGGTC	
GL1464	ATCTCGAGTCGTGGAAGTTGGTGGGATC	GL1464 and GL1465 are the forward and reverse primers, respectively, used to amplify 2638bp of *Cbr-pgl-1* fragment. The amplicon was used to construct the RNAi plasmid.
GL1465	ATCCATGGTGGAGAACCCGCAATAAGTG	
Experiment: *lin-15a(n767)* genotyping		
GL1346	AGTCCTATGCACTACGGATCTG	GL1346 and GL1347 are the set of forward and reverse primers, respectively, used to genotype the *n767* allele of *lin-15a*.
GL1347	CAGAACTTTAGTGGCGCAGA	
Experiment: *Cel-ivph-3(gk3691)* genotyping		
GL1128	CAAGCTTCACGCCTTCTTGTCATTCAAAATGTTTTG	GL1128 and GL1129 are the forward and reverse primers, respectively, used to amplify entire length of *ivph-3* gene
GL1129	TCGACAAAACATTTTGAATGACAAGAAGGCGTGAAGCTTGCATG	
GL1284	GTTGCATCACCTTCACCCTCTC	GL1287 is the forward primer binds just before the *Y67D8C.3ab* upstream homology arm, GL1328 (in the *Y67D8C.3ab* downstream homology arm) and GL1284 are the reverse primer.

		These primers were used in combination to validate the CRISPR allele *Y67D8C.3ab(gk3691)*
GL1287	CCTTCTGGCAATCGTCGTAGC	
GL1328	GTTCGGAGGTGGTTCATCCTG	
Experiment: *lin-8(n111)* genotyping		
GL1441	TGCAAACATCGTGGTAGGAAC	GL1441 and GL1442 are the set of forward and reverse primers, respectively, used to genotype the *n111* allele of *lin-8*.
GL1442	TAGACAACAGCAACCCTGTCC	
Experiment: *lin-56(n2728)* genotyping		
GL1443	TCGCTGCTGGAGACTTTATTCG	GL1443 is the forward primer binds the before the deletion site (11230bp region got deleted) GL1444 (binds within the deletion site) and GL1445 are the reverse primer. These primers were used in the combination to validate the allele *lin-56(n2728)*
GL1444	TCAGGCTTCATCATCCTCGCT	
GL1445	TCGACCTTCTTCCCACTATGAG	
Experiment: RT-qPCR for *C. briggsae* Reference (Positive control) genes		
GL767	CGGAATCGTTTCGAGGAATGC	GL767 and GL768 are the forward and reverse primers, respectively, used to estimate the level of *Cbr-pmp-3* transcript levels in Muv mutants
GL768	CGATGCGTGACTCCAGCAAG	
GL1406	GCTTCAAATCAGTCTCGCTGC	GL1406 and GL1407 are the forward and

		reverse primers, respectively, used to estimate the level of *CBG22375* transcript levels in Muv mutants
GL1407	GTGCCGACGTTCTTGTCGTTT	
Primers for Chromosomal Mapping		
GL588	AAGGCCTTAAAAATGAAGATAAT	GL588 and GL589 are cb-m142 medium indel mapping primer for Chromosome I. Expected product sizes are 700bp (AF16) and 905bp (HK104).
GL589	TGAAAATTGAAAAACCTAGAAAA	
GL1141	AACCAGTAAAAATAAGAGAAATTGA	GL1141 and GL1142 are cb-m21 medium indel mapping primer for Chromosome II. Expected product sizes are 900bp (AF16) and 700bp (HK104).
GL1142	TCTGATTCTGATGTTTTCAGTTC	
GL1143	AAACTGCTTGGAATTAAAAGATA	GL1143 and GL1144 are cb-m205 medium indel mapping primer for Chromosome III. Expected product sizes are 700bp (AF16) and 1000bp (HK104).
GL1144	TCAATGATTATCAAAGGAGGTC	
GL905	TTTGCTCTGCTGAATTTTTC	GL905 and GL906 are cb-m64 medium indel mapping primer for Chromosome IV. Expected product sizes are 539bp (AF16) and 412bp (HK104).
GL906	CAAAACAGTTCAAGCCTACG	
GL1145	AGCACATTTTCAGTTCTAACATC	GL1145 and GL1146 are cb-m105 medium indel mapping primer

		for Chromosome V. Expected product sizes are 800bp (AF16) and 520bp (HK104).
GL1146	GCATTTTATGTGTGCTGTGA	
GL666	CATTCTTCTAATTATCAATAAGGTCA	GL666 and GL667 are cb-m204 medium indel mapping primer for Chromosome X. Expected product sizes are 750bp (AF16) and 1000bp (HK104).
GL667	GCATCATTTCTTTTAATAACCAT	
GL590	TTAATGCTGGACCAAAAGTC	GL590 and GL591 are cb-m6 medium indel mapping primer for Chromosome I. Expected product sizes are 900bp (AF16) and 1000bp (HK104).
GL591	CCTGCAATTTTTGTGTTTTT	

Chapter 3

Functional characterization of *Cbr-ivp* class of genes

C. briggsae is an excellent experimental model system to identify genes that influence cell signaling and cell division during vulva development. *Cbr-ivp* genes were cloned and their molecular identity were determined previously. It has been shown that the Muv phenotype of *C. briggsae* mutants is dependent on RAS pathway (Sharanya et al., 2015). We analyzed the differential gene expression of different components of the pathway in these mutant and carried out interaction studies to understand the interaction between *Cbr-ivp* and *Cbr-lin-3*. The findings suggested that *Cbr-ivp* genes work through a well-established model in which *Cbr-lin-3*/EGF is found be overexpressed. A comparative analysis of the *Cbr-ivp*-3 and *ivph-3* was carried out in order to understand the functional differences that appear to have evolved between the two species. Further RNA-Seq analysis was carried out for the acquisition of gene expression profiles of the candidate target genes. Data obtained from RNA-Seq would be able to identify the targets of *Cbr-ivp* genes. Comparison of gene functions in *C. elegans* will elaborate our understanding on the role of these genes in vulva development. Further experiments need to be carried out to uncover the involvement of these genes in the negative regulation of cell proliferation and cell fate specification.

Vulval induction analysis in *Cbr-ivp* class of mutants

In wild-type *C. briggsae* animals P3.p, P4.p and P8.p divide only one time and fuse with hypodermis. Thus, the VPC induction score is 3.0 $\pm$ 0.0. In most Multivulva animals these 3 VPCs undergoes more than one round of division and thus give rise to Multivulva phenotype. The induction score in these animals found to be higher than 3.0. All *Cbr-ivp* class of mutants, exhibit a Multivulva phenotype. To analyze the induction in VPCs, mid-L4 stage animals were observed under Normarski microscope.

Table 3.1 Analysis of the VPC induction in *Cbr-ivp* mutants

	% Induction Score								
Genotype	P3.p	P4.p	P5.p	P6.p	P7.p	P8.p	Ave Ind	N	Muv%
Cbr-spr-4(gu163)	2.0	9.0	100.0	100.0	100.0	26.92	3.3	55	89.6
Cbr-htz-1(gu167)	5.0	13.2	100.0	100.0	100.0	54.0	3.9	55	66.7
Cbr-ivp-3(sy5216)	20.0	88.0	100.0	100.0	100.0	100.0	4.8	50	100.0
Cbr-gon-14(gu102)	17.0	90.0	100.0	100.0	100.0	97.0	4.9	60	96

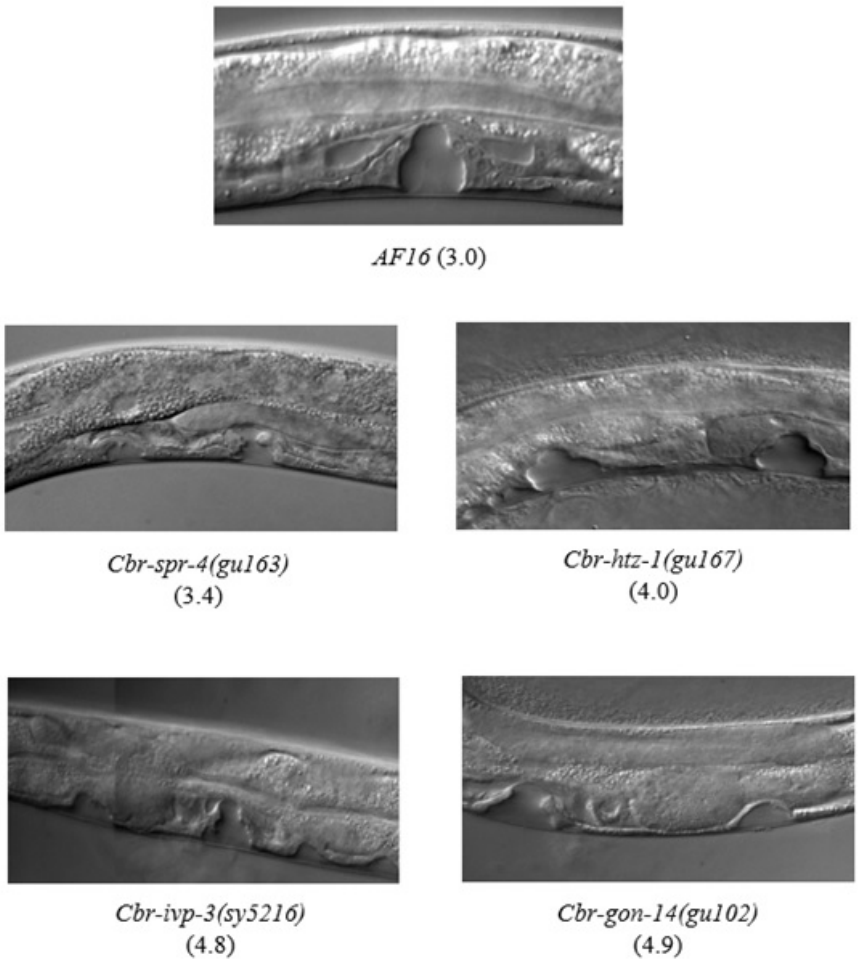

Figure 3.1 Vulval induction scores of *Cbr-ivp* mutants during mid-L4 stage. AF16 is the *C. briggsae* wild-type strain. The induction scores 3.0 indicated wild-type vulval induction in animals. *Cbr-ivp* mutants displayed induction scores higher than 3.0 which represents Multivulva phenotype.

3.1 Analysis of *Cbr-lin-3* expression in *Cbr-ivp* mutants

The anchor cell lies dorsal to the vulva precursor cells secrets the epidermal growth factor (EGF) ligand, LIN-3, to initiate induction in the VPCs (Hill and Sternberg, 1992). It has been shown that the MEK inhibitor U0126 suppressed the multivulva phenotype associated with *C. briggsae* ivp class of mutants (Sharanya et al., 2015). Thus, it was concluded that *Cbr-ivp* class of genes interact with Ras pathway to regulate vulva development. A high level of LIN-3/EGF signaling results in ectopic induction in VPCs which leads to multivulva phenotype in *C. briggsae* mutants (Sharanya et al., 2012). To investigate whether *Cbr-ivp* class of mutants exhibit similar expression of *Cbr-lin-3*, RT-qPCR was carried out to analyze the level of *Cbr-lin-3* transcripts in mutants. RT-qPCR quantified and compared the changes in the expression levels of *Cbr-lin-3* between wild-type and mutant strains.

Cbr-lin-3 transcripts were examined in synchronized mid-L3 stage worms. Exact staging of cultures was determined by mounting a sample of synchronized animals at different time intervals and observing them under the Nomarski microscope. RNA was extracted just prior to the stage when vulval precursors (Pn.p) were beginning to divide. At this stage, vulval cells are most responsive to *Cbr-lin-3* levels. RT-qPCR was then carried out to compare the changes in the expression levels of *Cbr-lin-3* transcript in wild-type and mutant worms.

The RT-qPCR data demonstrated a high level of *Cbr-lin-3* in *Cbr-spr-4(gu163)*, *Cbr-htz-1(gu167)*, *Cbr-ivp-3(sy5216)* and *Cbr-gon-14(gu102)*. It was found that the *Cbr-lin-3* transcript levels in *Cbr-ivp-3(sy5216)* were significantly increased (3.04 folds) in comparison to the wild-type, AF16. Both *Cbr-htz-1(gu167)* and *Cbr-gon-14(gu102)* exhibited high expression of *Cbr-lin-3* transcripts (2.21 folds and 2.43 folds respectively). While *Cbr-spr-4(gu163)* animals displayed 1.34 folds expression of *Cbr-lin-3* transcripts in comparison to AF16. For the thorough analysis all the extractions and other experiments were carried out in multiple batches. For the consistency in data, each step was optimized, and the parameters were kept constant throughout the batches (Table 3.1).

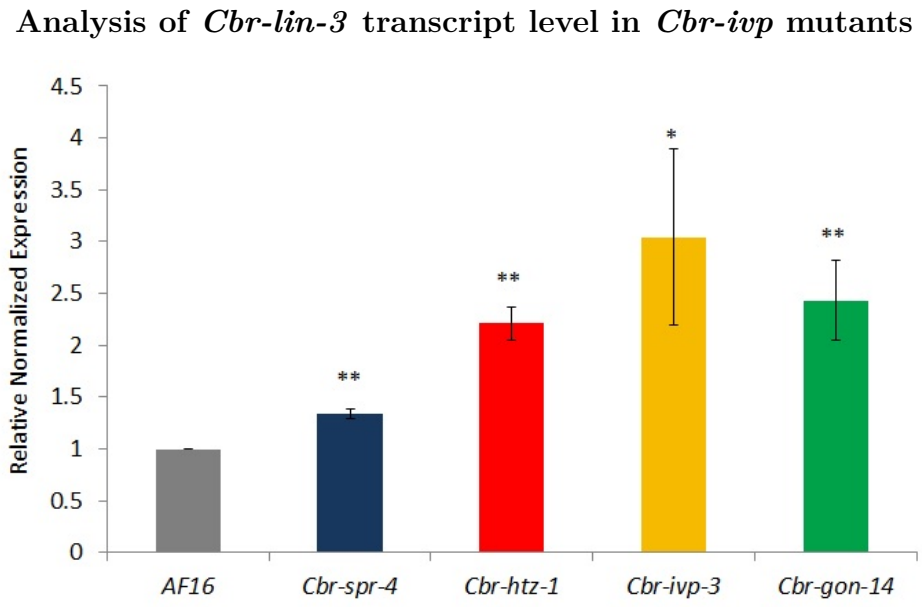

Figure 3.2 The expression of *Cbr-lin-3* transcripts in *Cbr-ivp* mutants determined by RT-qPCR. Relative fold changes of *Cbr-lin-3* transcripts have been plotted. AF16 was used as the positive control. *Cbr-pmp-3* was used for the normalization. Error bars represent standard error of the mean. Standard t-test was used for the statistical analysis. * $p<0.05$ and ** $p<0.01$.

Table 3.2 RT-qPCR data represents the relative normalized expression of *Cbr-lin-3* transcripts

Strains	Collection time	Relative Normalized Expression			Average Standard Deviation	P-value
		Batch 1	Batch 2	Batch 3		
AF16	~L1+27	1	1	1	1	0
Cbr-spr-4(gu163)	~L1+29	1.29462	1.4072	1.33314	1.344987	0.008376
Cbr-htz-1(gu167)	~L1+28	2.04862	2.21125	2.37389	2.211255	0.005063
Cbr-ivp-3(sy5216)	~L1+41	1.8781	3.36619	3.88674	3.043677	0.015115
Cbr-gon-14(gu102)	~L1+37	2.14462	2.17245	2.97624	2.431103	0.003345

3.2 RNAi knockdown of *Cbr-lin-3* in *Cbr-ivp* mutants

RT-qPCR results suggested that *Cbr-ivp* class of genes may regulate the expression of EGF/*Cbr-lin-3* and resulting in Muv phenotype. Thus, knocking down of *Cbr-lin-3* transcripts in Muv mutants should suppress the elevated levels of *Cbr-lin-3*/EGF and thus rescue the Multivulva phenotype. An RNAi plasmid was generated to knockdown *Cbr-lin-3* transcripts in *Cbr-ivp* mutants. The RNAi knockdown of *Cbr-lin-3* transcripts resulted a significant reduction in VPCs induction which led to the suppression of Multivulva phenotype in *Cbr-ivp* mutants (Figure 3.3 and Figure 3.4).

C. briggsae does not support environmental RNA interference (Winston et al., 2007). Thus, a functional copy of *sid-2* gene from *C. elegans* was introduced in all the *Cbr-ivp* mutant strains by crossing them with *mfIs42* and *mfEx32* strains. All *Cbr-ivp* mutants, sensitive to environmental RNAi were then exposed to *HT115* bacteria containing RNAi vectors. Wild-type *C. briggsae* strain, sensitive to environmental RNAi were exposed to control empty vector *L4440*, an induction score of 3.0 ± 0 was observed. While *Cbr-spr-4(gu163)*, *Cbr-htz-1(gu167)*, *Cbr-ivp-3(sy5216)* and *Cbr-gon-14(gu102)* animals, sensitive to environmental RNAi expressed an induction score of 3.2 ± 0.06, 3.7 ± 0.06, 4.8 ± 0.05 and 4.6 ± 0.2 respectively. The induction scores of these animals after their exposure to bacteria containing *L4440* vector were found relatively consistent with the data obtained previously in the penetrance analyses (Sharanya et al., 2015). Upon feeding the bacteria containing the *Cbr-lin-3* RNAi knockdown plasmid to the environmental sensitive RNAi mutants, the induction score was found to be reduced significantly for some mutants. The induction score of the rescued mutant was found to be 2.9 ± 0.09, 2.9 ± 0.08, 3.53 ± 0.2, 3.7 ± 0.2 for *Cbr-spr-4(gu163)*, *Cbr-htz-1(gu167)*, *Cbr-ivp-3(sy5216)* and *Cbr-gon-14(gu102)* mutant animals respectively. The induction score of the Muv mutant has been significantly reduced in *Cbr-htz-1(gu167)*, *Cbr-ivp-3(sy5216)* and *Cbr-gon-14(gu102)* animals, while a slight depression in the induction score was observed in the *Cbr-spr-4(gu163)* animals in comparison to that of the *L4440* control (Table 3.2 and Table 3.3).

The RNAi experiment confirmed that knocking down *Cbr-lin-3*/EGF expression in *Cbr-ivp* mutants led to the suppression of Muv phenotype. It implied that elevated level of *Cbr-lin-3*/EGF is responsible for the Muv phenotype in the *Cbr-ivp* mutants. The results and data from RT-qPCR and RNAi experiments suggested that high levels of *Cbr-lin-3*/EGF contribute to the Muv phenotype observed in *Cbr-ivp* mutants.

RNAi knockdown of *Cbr-lin-3* transcripts in *Cbr-ivp* mutants

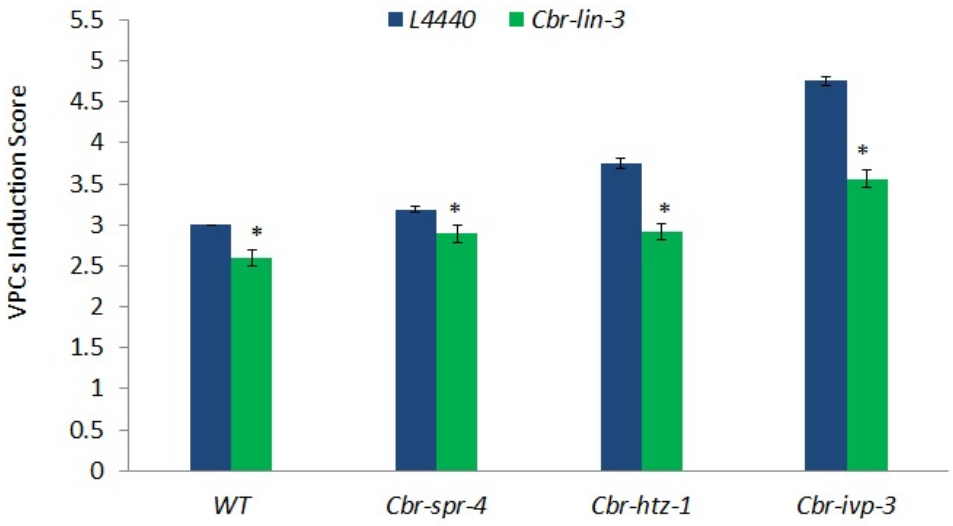

Figure 3.3 A comparison of the vulval induction scores between wild-type RNAi sensitive and *Cbr-ivp* RNAi sensitive animals that were exposed to bacteria containing empty vector *L4440* and RNAi plasmid *Cbr-lin-3*. It was found that *Cbr-lin-3* knockdown in *Cbr-ivp* animals show significant decrease in VPCs induction score and thus, reduction in multivulva phenotype in these animals. All the experiments were carried out in 3 individual batches. Wild-type *C. briggsae JU1018*, sensitive to environmental RNAi was used as a control strain. Standard t-test was used for the statistical analysis. * $p<0.01$

RNAi knockdown of *Cbr-lin-3* transcripts in *Cbr-gon-14(gu102)* mutants

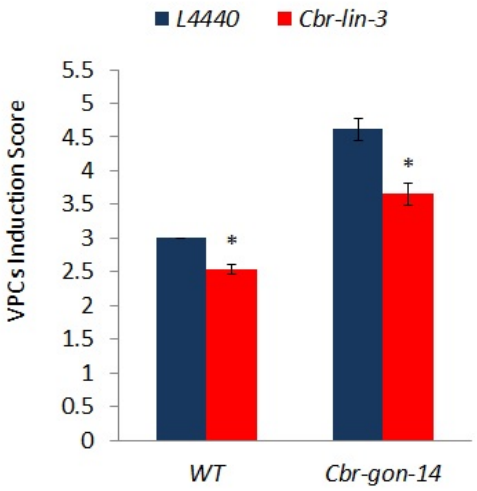

Figure 3.4 A comparison of the vulval induction scores between wild-type RNAi sensitive and *Cbr-gon-14(gu102)* RNAi sensitive animals that were exposed to bacteria containing empty vector *L4440* and RNAi plasmid *Cbr-lin-3*. The induction score of the Muv mutant has been significantly reduced when *Cbr-lin-3* transcript were knockdown in comparison to that of *L4440* control. A total of 131 *Cbr-gon-14(gu102)* RNAi sensitive animals were exposed to *Cbr-lin-3* RNAi bacteria. Standard t-test was used for the statistical analysis. * $p<0.01$

Table 3.3 Data representing VPC Induction Score of *Cbr-ivp* mutants after the knockdown of *Cbr-lin-3* transcripts

Genotype	RNAi Bacteria	VPC induction Score ± STD	N
mfIs42[sid-2::GFP + myo-2::dsRed]	*L4440*	3.0 ± 0.0	104
mfIs42[sid-2::GFP + myo-2::dsRed]	*Cbr-lin-3*	2.6 ± 0.08	107
Cbr-spr-4(gu163); mfIs42[sid-2::GFP + myo-2::dsRed]	*L4440*	3.2 ± 0.06	125
Cbr-spr-4(gu163); mfIs42[sid-2::GFP + myo-2::dsRed]	*Cbr-lin-3*	2.9 ± 0.09	130
Cbr-htz-1(gu167); mfIs42[sid-2::GFP + myo-2::dsRed]	*L4440*	3.7 ± 0.06	120
Cbr-htz-1(gu167); mfIs42[sid-2::GFP + myo-2::dsRed]	*Cbr-lin-3*	2.9 ± 0.08	118
Cbr-ivp-3(sy5216); mfIs42[sid-2::GFP + myo-2::dsRed]	*L4440*	4.8 ± 0.05	129
Cbr-ivp-3(sy5216); mfIs42[sid-2::GFP + myo-2::dsRed]	*Cbr-lin-3*	3.53 ± 0.2	140

Table 3.4 Data representing the VPC Induction Score of *Cbr-gon-14(gu102)* mutants after the knockdown of *Cbr-lin-3* transcripts

Genotype	RNAi Bacteria	VPC induction Score ± STD	N
mfEx32[sid-2::GFP + myo-2::dsRed]	*L4440*	3.0 ± 0.0	122
mfEx32[sid-2::GFP + myo-2::dsRed]	*Cbr-lin-3*	2.5 ± 0.07	130
Cbr-gon-14(gu102); mfEx32[sid-2::GFP + myo-2::dsRed]	*L4440*	4.6 ± 0.2	127
Cbr- gon-14(gu102); mfEx32[sid-2::GFP + myo-2::dsRed]	*Cbr-lin-3*	3.7 ± 0.2	131

N represents the total number of animals analyzed during the experiments.

3.3 The expression pattern of *ivph-3* and *Cbr-ivp-3*

Fusion reporter for both *ivph-3* (transcriptional) and *Cbr-ivp-3* (transcriptional/ translational) genes were constructed and injected into *C. elegans* and *C. briggsae* respectively to observe the expression pattern of the gene, providing some insight into the function of *ivph-3* and *Cbr-ivp-3*. It was hypothesized that these genes should express in reproductive assembly or hypodermis of these animals.

3.3.1 *ivph-3::GFP*

The expression pattern of *ivph-3* worms was analyzed under Nomarski microscopy. 31 worms that were expressing *myo-3::mcherry* were picked and observed. 7/31 worms exhibited GFP expression in vulva cells, 27/31 worms had shown GFP expression in intestine, 9/31 worms showed GFP expression in neurons (Figure 3.5). Though none of the worms result in the generation of stable lines.

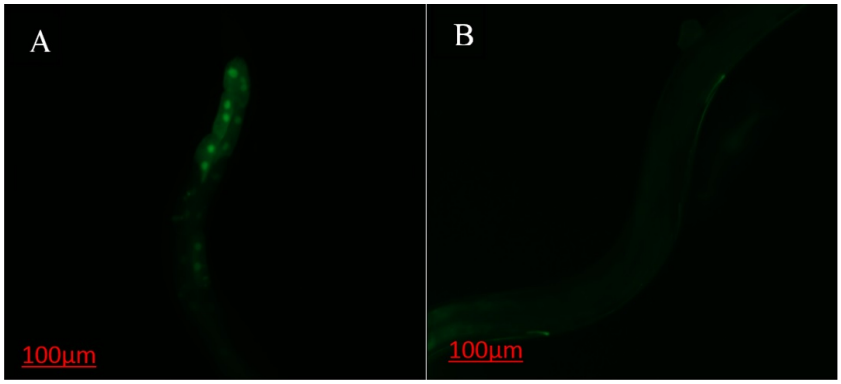

Figure 3.5 *ivph-3::GFP* expression in *C. elegans*.

3.3.2 *Cbr-ivp-3::GFP*

A Translational fusion reporter of *Cbr-ivp-3* gene were injected in *C. briggsae* animals. 23 worms with *myo-3::mcherry* expression were analyzed. 19/23 worms expressed GFP in vulva region (Figure 3.6). Though none of the worms result in generation of stable line.

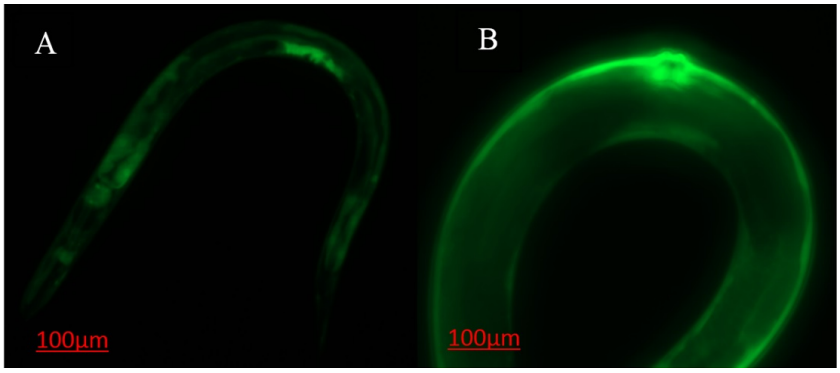

Figure 3.6 *Cbr-ivp-3::GFP* expression in *C. briggsae*.

3.4 Characterization of *ivph-3(gk3691)*

Y67D8C.3 (ivph-3) is a *C. elegans* ortholog of *Cbr-ivp-3* gene. After the molecular identification of *Cbr-ivp-3* in *C. briggsae*, the nucleotide blast was carried out to find the ortholog of *Cbr-ivp-3* in *C. elegans*. The nucleotide sequences revealed the 65% identity with the *ivph-3* gene in Wormbase (Pabla, 2017). A genetic and phenotypic characterization had been carried out in order to understand the significance of the gene in development. A comparative analysis of the two genes in sister species helped in uncovering the evolution of gene function and mechanism in the development.

C. elegans CRISPR strain, *VC3731* was kindly provided by Don Moerman lab, at the University of British Columbia. The *ivph-3(gk3691)* allele was generated by inserting an approximately 1 kb long *myo-2::GFP* cassette in the open reading frame of *ivph-3*. The strain has been validated by PCR carried out with the primer designed around the insertion site and in the cassette. The extensive phenotypic analysis followed by several round of PCR validation, confirmed the distinct genotypic population of animals in the culture. The animals that are homozygous for *gk3691* allele (homozygous for the insertion), expressed GFP and possessed a Protruding vulva (Pvl) phenotype and were sterile. Thus, the animals that were displaying the wild-type phenotype, expressing GFP and were heterozygous for the *gk3691* allele (heterozygous for the insertion with one wild-type copy of the gene) were used to maintain the culture. The heterozygous population produced animals that displayed wild-type phenotype, homozygous for wild-type copy of *ivph-3* (no insertion) and did not express GFP.

3.4.1 Penetrance, phenotypic and vulva induction analysis of *ivph-3(gk3691)*

ivp-3(gk3691) strains exhibit a mixed population in the culture, worms with wild-type phenotype, worms with wild-type phenotype with *myo-2::GFP* expression, and worms showing Pvl phenotype with *myo-2::GFP* expression. The phenotypic analysis, penetrance assay and the vulva induction analysis were carried out for the three observed phenotypes in culture. The penetrance assay was carried out by cloning single L4 hermaphrodite larva with *myo-2::GFP* expression onto multiple small plates. It was concluded that all the animals expressing GFP and displayed prominent Pvl phenotype were sterile and unable to produce eggs. The genomic DNA extraction and PCR validation confirmed that these animals were homozygous for *gk3691* allele. The DNA isolated from the egg laying, GFP expressing animals revealed that the animals are heterozygous for *gk3691* allele and have a wild-type copy of *ivph-3* gene along with the *myo-2::GFP* cassette insertion in the another copy of gene. The phenotypic and genotypic ratio of animals displaying the wild-type phenotype with wild-type copy of *ivph-3* gene (*+/+*), wild-type phenotype and heterozygous for the insertion cassette (*gk3691/+*) and homozygous for the insertion cassette site (*gk3691/gk3691*) were 26%, 61% and 13% respectively (Figure 3.7). This ratio differed from the expected Mendelian ratio.

To further analyze the defect in morphology and to calculate vulva induction score, L4 stage worms were mounted on slides and observed under Nomarski. Worms with defective vulva invagination were grown to have protruding vulva phenotype. Some of these worms also exhibited abnormal gonad morphology. 13% animals (*gk3691/gk3691*, further confirmed with PCR) were found to have vulva morphology defect (Figure 3.8). These worms turned out to be Pvl and sterile. The vulva induction for each of these worms were 3.0 ± 0.0 (Table 3.6).

Table 3.5 Penetrance analysis of the observable phenotype in *ivph-3(gk3691)* animals at plate level

Penetrance in *ivph-3(gk3691)*				
Phenotype	Batch 1	Batch 2	Batch 3	STD
WT	67	70	77	0.016599
WT-GFP	159	175	162	0.00605
Pvl-GFP	34	40	31	0.010553
Total	260	285	270	

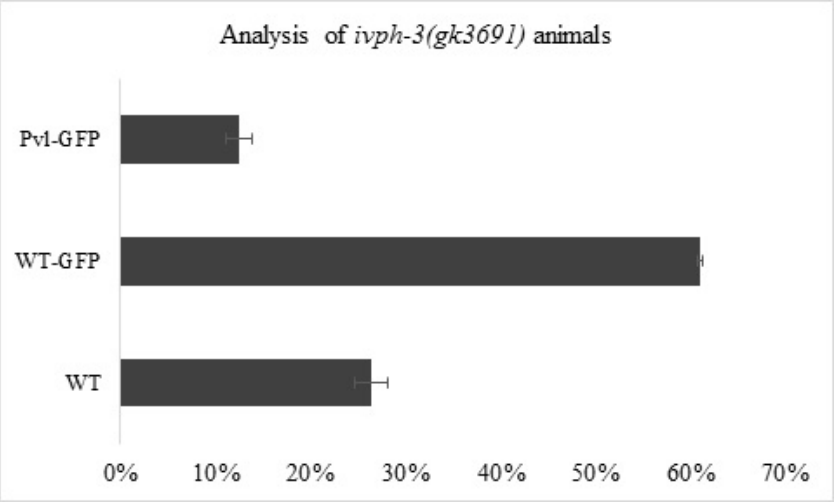

Figure 3.7 Analysis of the CRISPR allele, *ivph-3(gk3691)*, indicated that there were three populations of animals within the strain; Wild-type animals that did not express GFP, Wild-type animals with GFP and Sterile animals expressing GFP and had a Protruding (Pvl) phenotype. The observed phenotypic ratios for the three phenotypes were determined by scoring progenies of heterozygous hermaphrodites. Error bars represent standard error of the mean.

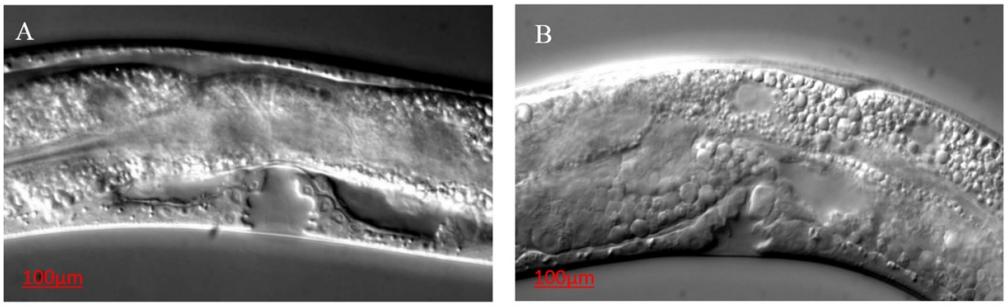

Wild-type *C. elegans* N2 at mid-L4 stage (L1+44)

ivph-3(gk3691) at mid-L4 stage (L1+52)

Figure 3.8 VPCs induction and vulva morphology in *ivph-3(gk3691)* mutants (B) when compared to wild-type N2 strain (A).

Table 3.6 Data representing the VPC Induction Score of *ivph-3(gk3691)*

Hours	L4 Worms	P3.p	P4.p	P5.p	P6.p	P7.p	P8.p	Induction Score	Vulva Morphology	Gonad	Phenotype of Adult worms	
L1+52	1	0	0	1	1	1	0	3	Defective	Defective	Pvl	Sterile
L1+54	1	0	0	1	1	1	0	3	Defective	Normal	Pvl	Sterile
	2	0	0	1	1	1	0	3	Defective	Normal	Pvl	Sterile
L1+56	1	0	0	1	1	1	0	3	Defective	Defective	Pvl	Sterile
	2	0	0	1	1	1	0	3	Defective	Normal	Pvl	Sterile
	3	0	0	1	1	1	0	3	Defective	Normal	Pvl	Sterile
L1+58	1	0	0	1	1	1	0	3	Defective	Defective	Pvl	Sterile
	2	0	0	1	1	1	0	3	Defective	Normal	Pvl	Sterile
	3	0	0	1	1	1	0	3	Defective	Defective	Pvl	Sterile
	4	0	0	1	1	1	0	3	Defective	Normal	Pvl	Sterile
	5	0	0	1	1	1	0	3	Defective	Defective	Pvl	Sterile
	6	0	0	1	1	1	0	3	Defective	Normal	Pvl	Sterile
L1+60	1	0	0	1	1	1	0	3	Defective	Normal	Pvl Subtle Pvl	Sterile
	2	0	0	1	1	1	0	3	Defective	Normal	(Swelling)	Sterile
	3	0	0	1	1	1	0	3	Defective	Normal	Pvl	Sterile
	4	0	0	1	1	1	0	3	Defective	Defective	Pvl	Sterile
	5	0	0	1	1	1	0	3	Defective	Defective	Pvl	Sterile
	6	0	0	1	1	1	0	3	Defective	Defective	Pvl	Sterile
L1+62	1	0	0	1	1	1	0	3	Defective	Normal	Pvl	Sterile
	2	0	0	1	1	1	0	3	Defective	Normal	Pvl	Sterile
L1+64	1	0	0	1	1	1	0	3	Defective	Normal	Pvl	Sterile
	2	0	0	1	1	1	0	3	Defective	Normal	Pvl	Sterile
	3	0	0	1	1	1	0	3	Defective	Defective	Pvl	Sterile
	4	0	0	1	1	1	0	3	Defective	Normal	Pvl	Sterile
	5	0	0	1	1	1	0	3	Defective	Normal	Pvl	Sterile
	Total - 25							**Ave - 3**	**Total - 25**	**Total - 9**	**Total 25**	**Total - 25**

3.4.2 Brood size assay in *ivph-3(gk3691)/+* animals

I have also carried out the brood size assay to determine if the insertion of *myo-2::GFP* cassette in *ivph-3* gene is responsible for any change in the brood size of *ivph-3(gk3691)* mutants. Single animals at L3/L4 stages were cloned on the different plates and the progenies were counted to analyze if the mutation in *ivph-3(gk3691)* results in decrease or increase in the brood size. Wild-type *C. elegans* strain N2 was used as control.

Table 3.7 Brood size assay in *ivph-3(gk3691)/+* animals

Phenotype	Worm 1	Worm 2	Worm 3	Average	STD
Wild-type (N2)	287	293	301	293.67	5.73488351
ivph-3(gk3691)	242	270	269	260.33	12.97005097

The results displayed a slight decrease in the brood size (P-value - 0.02927) (Table 3.7). Both homozygous *(gk3691/gk3691)* and heterozygous worms *(gk3691/+)* were found to be slow growing when compared to wild-type *C. elegans* strain N2.

3.4.3 Embryonic and larval lethality assays

To account for this deviation from the expected ratio of homozygous mutants, embryonic and larval lethality assays were carried out. The animals which are homozygous for the deletion site may have lethal phenotype. The disruption of *ivph-3* gene due to the insertion of *myo-2::GFP* cassette in the open reading frame might have prevented embryo to hatch or caused lethality in the hatched larvae. A large number of unhatched eggs is an indicator of embryonic lethality. The results indicated that the animals homozygous for *ivph-3(gk3691)* allele did not show embryonic lethality. The percentage of eggs hatched in the *ivph-3(gk3691)* animals were similar to that of the N2 control. The hatched larvae on these plates were then scored each day until they reached adulthood. The data obtained from the larval lethality assay demonstrated that all larval progenies were matured into adult worms. Overall results suggested that *ivph-3* is an important *C. elegans* gene necessary for maintaining the fertility and the disruption in gene function may result in sterility in nematode *C. elegans* (Table 3.8).

Table 3.8 Embryonic Lethality assay in *ivph-3(gk3691)/+* animals

	N2	*ivph-3(gk3691)/+*	
	Worm 1	Worm 1	Worm 2
Number of eggs laid	293	279	270
Number of eggs hatched	290	276	268
% eggs hatched	98.97%	98.92%	99.25%
Number of surviving larvae	290	274	268
% surviving larvae	98.97%	98.20%	99.25%

3.5 *ivp-3* genes accounts for functional differences in *C. elegans* and *C. briggsae*

RT-qPCR results suggest that *Cbr-ivp* class of genes regulate the expression *Cbr-lin-3*/EGF in *Cbr-ivp-3* mutants. Moreover, the RNAi knockdown of *Cbr-lin-3*/EGF transcripts in *Cbr-ivp-3* mutants results in the suppression of Multivulva phenotype. Thus, it was concluded that *Cbr-ivp-3* genes negatively regulate transcription of *Cbr-lin-3*/EGF during vulval development, a role that is similar to SynMuv class of genes in *C. elegans* (Cui et al., 2006). Thus, it was investigated if *ivph-3* has evolved as a SynMuv gene in nematode *C. elegans*. The previous data have shown that animals with homozygous allele (*gk3691/gk3691*) showed protruding vulva phenotype and were sterile. Microscopic analysis of VPCs induction helped us in understanding the involvement of *ivph-3* gene in vulva induction morphology in *C. elegans*.

Interaction studies were carried out to examine the possibility of *ivph-3* working as SynMuv genes in *C. elegans*. The crosses were set up to create double mutants of *ivph-3(gk3691)* with Class A synthetic multivulva genes. If the cross-progeny results in Muv phenotype then it is possible that *ivph-3* might be evolved as SynMuv genes in *C. elegans* and interact with SynMuv genes from other classes to restrict the tumor formation (Muv phenotype) in nematodes. Otherwise, it could be concluded that although *ivph-3* is required for the normal vulval development similar to *Cbr-ivp-3*, its mechanism of function appears to have diverged.

ivph-3 mutants were crossed with SynMuv mutants, *lin-15A(n767)*, *lin-8(n111)* and *lin-56(n2728)*, in order to analyze the interaction of *ivph-3* genes with class A SynMuv genes. The progenies of resultant double did not show Multivulva or any other phenotype. Moreover, the penetrance of Pvl phenotype was similar to

homozygous *ivph-3(gk3691)* allele (Figure 3.9, Figure 3.10 and Figure 3.11). In addition the interaction of the two genes did not augment embryonic and larval lethality, which suggested that *ivph-3* did not interact with class A SynMuv genes. *ivph-3(gk3691); lin-15A(n767)* mutants were scored and analyzed for the defective vulva morphology and to calculate vulva induction score (n = 254). 30/254 = 11.8110% of animals were found to have a defective vulva morphology. These animals showed Protruding vulva (Pvl) phenotype and turned out to be sterile. *lin-8(n111); ivph-3(gk3691)* mutants were analyzed under Nomarski microscope (n = 119). 14/119 = 11.7647% of animals were found to have a defective vulva morphology and later developed as sterile Pvl animals. 11/103 = 10.6796% of *lin-56(n2728); ivph-3(gk3691)* animals were found to have a defective vulva morphology. These animals also turned out to be Pvl and Sterile. These results were found to be parallel to homozygous *ivph-3(gk3691)* mutants. Thus, it was concluded that *ivph-3(gk3691)* double mutants carrying *lin-15A(n767)*, *lin-8(n111)* and *lin-56(n2728)* alleles have defective vulva morphology but none of them exhibit Muv phenotype (Figure 3.13). The vulva induction score for each of these strains were 3.0 ± 0.0 (Figure 3.12).

Table 3.9 Penetrance analysis of the observable phenotype in *ivph-3(gk3691); lin-15A(n767)* animals at plate level

Penetrance in *ivph-3(gk3691); lin-15A(n767)*				
Phenotype	Batch 1	Batch 2	Batch 3	STD
WT	71	68	72	0.012749
WT-GFP	164	180	168	0.008044
Pvl-GFP	35	39	32	0.007555
Total	270	287	272	

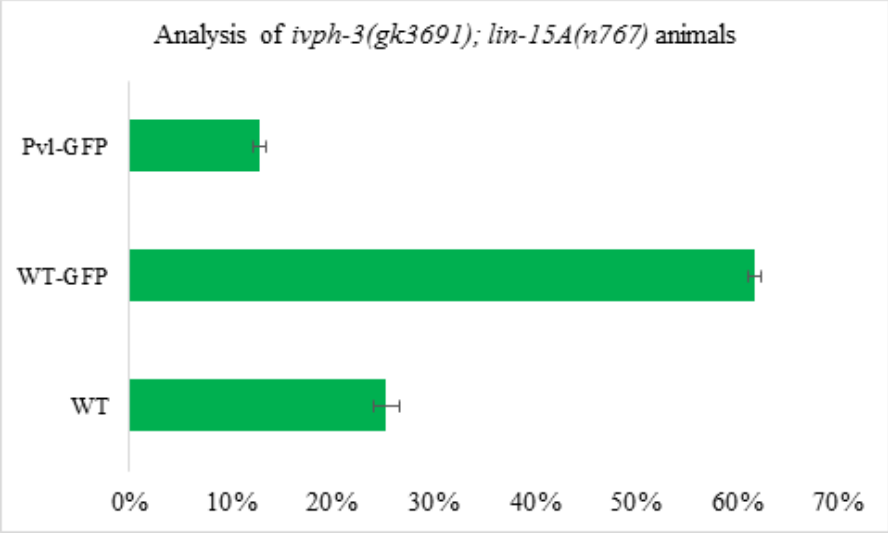

Figure 3.9 Analysis of *ivph-3(gk3691); lin-15A(n767)* animals, indicated that there were three populations of animals within the strain; Wild-type animals that did not express GFP, Wild-type animals with GFP and Sterile animals expressing GFP and had a Protruding (Pvl) phenotype. The observed phenotypic ratios for the three phenotypes were determined by scoring progenies of heterozygous hermaphrodites. Error bars represent standard error of the mean.

Table 3.10 Penetrance analysis of the observable phenotype in *lin-8(n111); ivph-3(gk3691)* animals at plate level

Penetrance in *lin-8(n111); ivph-3(gk3691)*				
Phenotype	Batch 1	Batch 2	Batch 3	STD
WT	68	78	82	0.018354
WT-GFP	180	170	181	0.011378
Pvl-GFP	39	30	40	0.012447
Total	287	278	302	

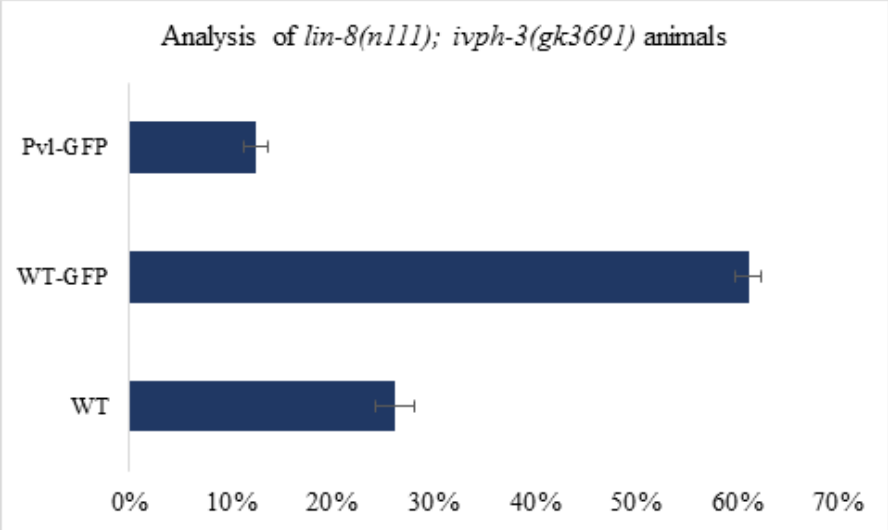

Figure 3.10 Analysis of *lin-8(n111); ivph-3(gk3691)* animals, indicated that there were three populations of animals within the strain; Wild-type animals that did not express GFP, Wild-type animals with GFP and Sterile animals expressing GFP and had a Protruding (Pvl) phenotype. The observed phenotypic ratios for the three phenotypes were determined by scoring progenies of heterozygous hermaphrodites. Error bars represent standard error of the mean.

Table 3.11 Penetrance analysis of the observable phenotype in *lin-56(n2728); ivph-3(gk3691)* animals at plate level

Penetrance in *lin-56(n2728); ivph-3(gk3691)*				
Phenotype	Batch 1	Batch 2	Batch 3	STD
WT	63	71	75	0.021141
WT-GFP	169	170	155	0.017173
Pvl-GFP	33	38	30	0.008534
Total	287	279	260	

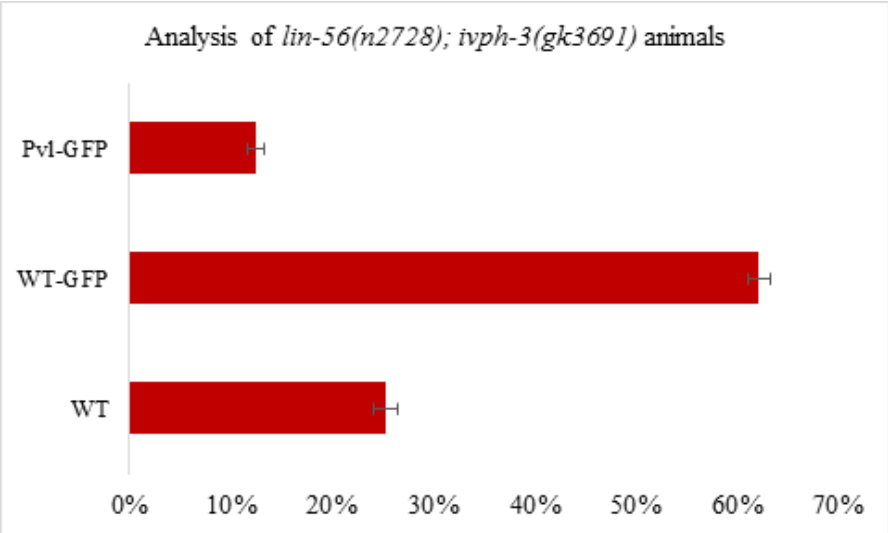

Figure 3.11 Analysis of *lin-56(n2728); ivph-3(gk3691)* animals, indicated that there were three populations of animals within the strain; Wild-type animals that did not express GFP, Wild-type animals with GFP and Sterile animals expressing GFP and had a Protruding (Pvl) phenotype. The observed phenotypic ratios for the three phenotypes were determined by scoring progenies of heterozygous hermaphrodites. Error bars represent standard error of the mean.

Table 3.12 Data representing the VPC Induction Score of *ivph-3(gk3691); lin-15A(n767)* mutants

Hours	L4 Worms	P3.p	P4.p	P5.p	P6.p	P7.p	P8.p	Induction Score	Vulva Morphology	Gonad	Phenotype of Adult worms	
L1+52	1	0	0	1	1	1	0	3	Defective	Normal	Pvl	Sterile
L1+54	1	0	0	1	1	1	0	3	Defective	Normal	Pvl	Sterile
	2	0	0	1	1	1	0	3	Defective	Defective	**Died**	**Died**
	3	0	0	1	1	1	0	3	Defective	Defective	Pvl	Sterile
	4	0	0	1	1	1	0	3	Defective	Normal	Pvl	Sterile
L1+56	1	0	0	1	1	1	0	3	Defective	Normal	Pvl	Sterile
	2	0	0	1	1	1	0	3	Defective	Defective	Pvl	Sterile
	3	0	0	1	1	1	0	3	Defective	Defective	Pvl	Sterile
	4	0	0	1	1	1	0	3	Defective	Defective	Pvl	Sterile
	5	0	0	1	1	1	0	3	Defective	Normal	Pvl	Sterile
L1+58	1	0	0	1	1	1	0	3	Defective	Normal	Pvl	Sterile
	2	0	0	1	1	1	0	3	Defective	Defective	Pvl	Sterile
	3	0	0	1	1	1	0	3	Defective	Defective	Pvl	Sterile
L1+60	1	0	0	1	1	1	0	3	Defective	Normal	Pvl	Sterile
	2	0	0	1	1	1	0	3	Defective	Normal	Pvl	Sterile
	3	0	0	1	1	1	0	3	Defective	Normal	Pvl	Sterile
	4	0	0	1	1	1	0	3	Defective	Defective	Pvl	Sterile
	5	0	0	1	1	1	0	3	Defective	Normal	Pvl	Sterile
L1+62	1	0	0	1	1	1	0	3	Defective	Defective	Pvl	Sterile
	2	0	0	1	1	1	0	3	Defective	Normal	Pvl	Sterile
	3	0	0	1	1	1	0	3	Defective	Normal	Pvl	Sterile
	Total - 25							**Ave - 3**	**Total - 21**	**Total - 9**	**Total 20**	**Total - 20**

Table 3.13 Data representing the VPC Induction Score of *lin-8(n111); ivph-3(gk3691)* mutants

	L4							**Induction**	**Vulva**		**Phenotype of**	
Hours	**Worms**	**P3.p**	**P4.p**	**P5.p**	**P6.p**	**P7.p**	**P8.p**	**Score**	**Morphology**	**Gonad**	**Adult worms**	
L1+54	1	0	0	1	1	1	0	3	Defective	Defective	Pvl	Sterile
	2	0	0	1	1	1	0	3	Defective	Normal	Pvl	Sterile
L1+56	1	0	0	1	1	1	0	3	Defective	Defective	Pvl	Sterile
	2	0	0	1	1	1	0	3	Defective	Defective	Pvl	Sterile
	3	0	0	1	1	1	0	3	Defective	Defective	Pvl	Sterile
L1+58	1	0	0	1	1	1	0	3	Defective	Normal	Pvl	Sterile
	2	0	0	1	1	1	0	3	Defective	Normal	Pvl	Sterile
L1+60	1	0	0	1	1	1	0	3	Defective	Normal	Pvl	Sterile
	2	0	0	1	1	1	0	3	Defective	Normal	Pvl	Sterile
	3	0	0	1	1	1	0	3	Defective	Normal	Pvl	Sterile
	4	0	0	1	1	1	0	3	Defective	Normal	Pvl	Sterile
L1+62	1	0	0	1	1	1	0	3	Defective	Defective	Pvl	Sterile
	2	0	0	1	1	1	0	3	Defective	Defective	Pvl	Sterile
	3	0	0	1	1	1	0	3	Defective	Defective	Pvl	Sterile
	Total - 14							**Ave - 3**	**Total - 14**	**Total - 7**	**Total - 14**	**Total - 14**

Table 3.14 Data representing the VPC Induction Score of *lin-56(n2728); ivph-3(gk3691)* mutants

Hours	L4 Worms	P3.p	P4.p	P5.p	P6.p	P7.p	P8.p	Induction Score	Vulva Morphology	Gonad	Phenotype of Adult worms	
L1+54	1	0	0	1	1	1	0	3	Defective	Defective	Pvl	Sterile
L1+56	1	0	0	1	1	1	0	3	Defective	Defective	Pvl	Sterile
	2	0	0	1	1	1	0	3	Defective	Defective	Pvl	Sterile
	3	0	0	1	1	1	0	3	Defective	Normal	Pvl	Sterile
L1+58	1	0	0	1	1	1	0	3	Defective	Normal	Pvl	Sterile
	2	0	0	1	1	1	0	3	Defective	Normal	Pvl	Sterile
L1+60	1	0	0	1	1	1	0	3	Defective	Normal	Pvl	Sterile
	2	0	0	1	1	1	0	3	Defective	Normal	Pvl	Sterile
	3	0	0	1	1	1	0	3	Defective	Defective	Pvl	Sterile
L1+62	1	0	0	1	1	1	0	3	Defective	Defective	Pvl	Sterile
	2	0	0	1	1	1	0	3	Defective	Normal	Pvl	Sterile
	Total - 11							**Ave - 3**	**Total - 11**	**Total - 5**	**Total - 11**	**Total - 11**

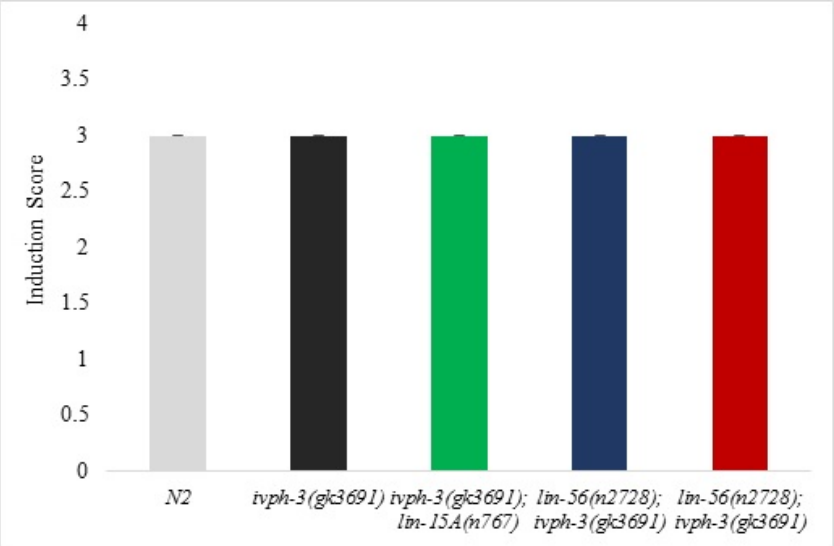

Figure 3.12 Data representing the VPC induction score of wild-type strain, N2 and mutant strains, *ivph-3(gk3691)*,*ivph-3(gk3691); lin-15A(n767)*, *lin-8(n111); ivph-3(gk3691)*, *lin-56(n2728); ivph-3(gk3691)*. The vulva induction score for each of these strains were 3.0 ± 0.0. The number of animals analyzed for each of the strains were given in the tables representing VPC induction data for these animals. Error bars represent standard error of the mean.

Vulva morphology of double mutants at mid-L4 stage

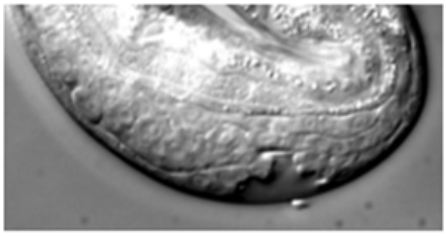

ivph-3(gk3691); lin-15A(n767) at mid-L4 stage (L1+56)

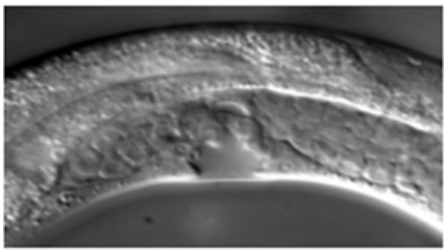

lin-8(n111); ivph-3(gk3691) at mid-L4 stage (L1+58)

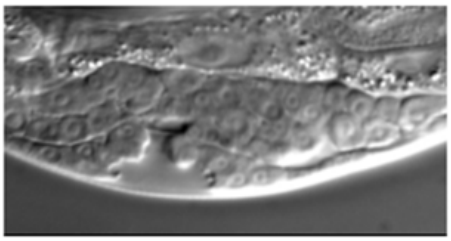

lin-56(n2728); ivph-3(gk3691) at mid-L4 stage (L1+60)

Figure 3.13 *ivph-3(gk3691)*,*ivph-3(gk3691); lin-15A(n767)*, *lin-8(n111); ivph-3(gk3691)*, *lin-56(n2728); ivph-3(gk3691)* mutants were analyzed under Normaski microscope. The vulva induction score of *ivph-3(gk3691)* and all the three double mutants were analyzed extensively. All the animals with defective vulval morphology had an induction score of 3.0 ± 0.0. These animals turned out to be Pvl and sterile.

3.6 Bioinformatics analysis of RNA-Seq data

RNA-seq experiments were performed to examine gene expression changes in Muv mutants in order to identify candidate genes that may mediate *Cbr-ivp* gene function in vulval development. The total RNA was extracted from the Muv mutants just prior to Pn.px stage. cDNA library was prepared and a high throughput RNA-Seq was carried out. Computational analysis was carried out to analyze the RNA-Seq data. Transcriptome profiling of *Cbr-spr-4(gu163)* and *Cbr-htz-1(gu167)* animals uncovered a total of 1,121 and 443 differentially expressed (DE) genes, respectively. RNA-Seq data were deposited with GEO (GSE133769) (Chamberlin et al., 2020). DE scattered plot to represent a global view of the target genes were generated. Volcano plots were developed to present the fold change of differentially regulated genes (Figure 3.15 and Figure 3.16).

Enriched GO terms in expression datasets

A GO analysis was performed to classify the function of all differentially expressed gene based on their GO term (http://amigo.geneontology.org/amigo). The results showed enrichment terms which are associated with a number of biological activities. The GO Term enrichment analysis allows for the identification of candidate target genes. The genes which are found to be up regulated and down regulated in the RNA-Seq dataset were considered for the further studies. Wormmine, a tool provided by Wormbase was used to study the involvement of the selected candidate genes in the vulva development pathway. Before studying the GO enrichment analysis of RNA seq dataset, the targets were filtered. The genes that were involved in molting and collagen and cuticle development were eliminated. It was necessary because the RNA was isolated at the L3 stage (Pn.px) and in developing larvae, the expressions of the genes that are involved in molting are readily oscillate (Hendriks et al. 2014). Gene Ontology (GO) enrichment analysis of DE genes revealed that while there are some differences in gene categories between the two mutants, both the *Cbr-spr-4(gu163)* and *Cbr-htz-1(gu167)* showed enrichment for genes involved in similar processes such as cell cycle and DNA repair.

A comparison of DE genes between the two mutants, revealed a significant overlap between the altered gene expression (197 genes, 181 upregulated and 7 downregulated; Hypergeometric score: 3.790918 e-129) (Figure 3.14). It is interesting to note that while both the *Cbr-spr-4(gu163)* and *Cbr-htz-1(gu167)* showed enrichment for chromosome organization involved in meiotic cell cycle. *Cbr-spr-4(gu163)* showed enrichment for meiotic nuclear division, mitotic cell cycle and mismatch repair and *Cbr-htz-1(gu167)* show enrichment for meiosis I, regulation

of cell cycle process, DNA repair and posttranscriptional regulation of gene expression (Figure 3.17 and Figure 3.18). Together, these results suggest that *Cbr-spr-4* and *Cbr-htz-1* may affect similar molecular processes to regulate cell proliferation in the vulva.

Venn diagram for Differentially Expressed genes in *Cbr-spr-4(gu163)* and *Cbr-htz-1(gu167)* mutants

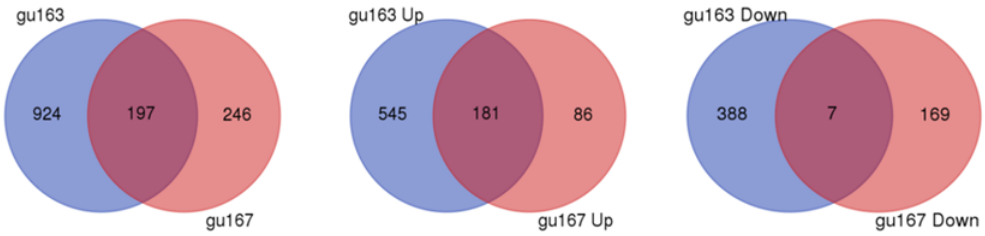

Figure 3.14 A comparison of DE genes between the two mutants, revealed a significant overlap between the altered gene expression (197 genes, 181 upregulated and 7 downregulated; Hypergeometric score: 3.790918 e-129).

MA Plot and Volcano Plot to represent Differentially Expressed genes in *Cbr-spr-4(gu163)* and *Cbr-htz-1(gu167)* mutants

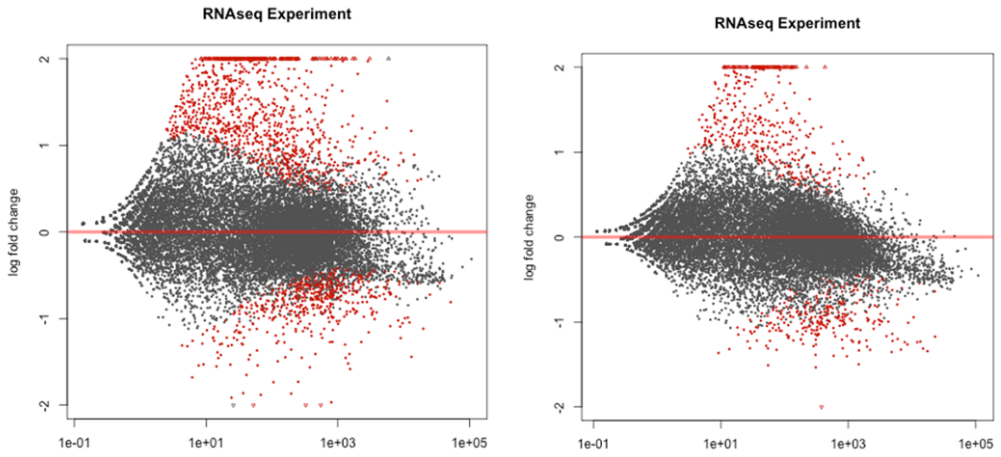

Figure 3.15 MA plots of differentially expressed genes in *Cbr-spr-4(gu163)* and *Cbr-htz-1(gu167)* mutants. Red dots represent transcripts with an FDR p-adj of <0.05 while black dots represent transcripts with FDR p-values of >0.05 (Chamberlin et al., 2020)

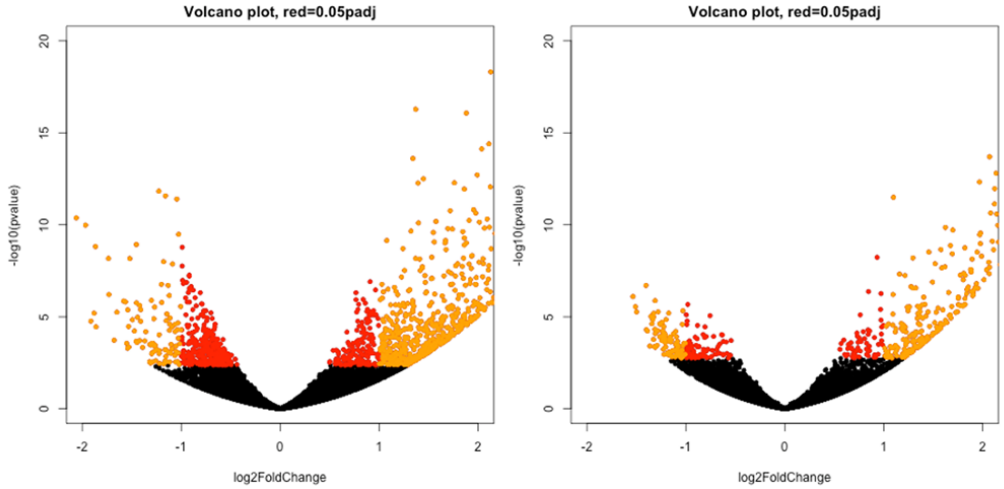

Figure 3.16 Volcano plot representing log2fold change in transcripts from *Cbr-spr-4(gu163)* and *Cbr-htz-1(gu167)* mutants plotted against their p-values. Each point represents an individual gene. Data points to the right of 0 represent up regulated genes, while data points to the left of 0 represent down regulated genes (Ranawade, 2017).

GO Amigo analysis of Differentially Expressed genes in *Cbr-spr-4(gu163)* mutants

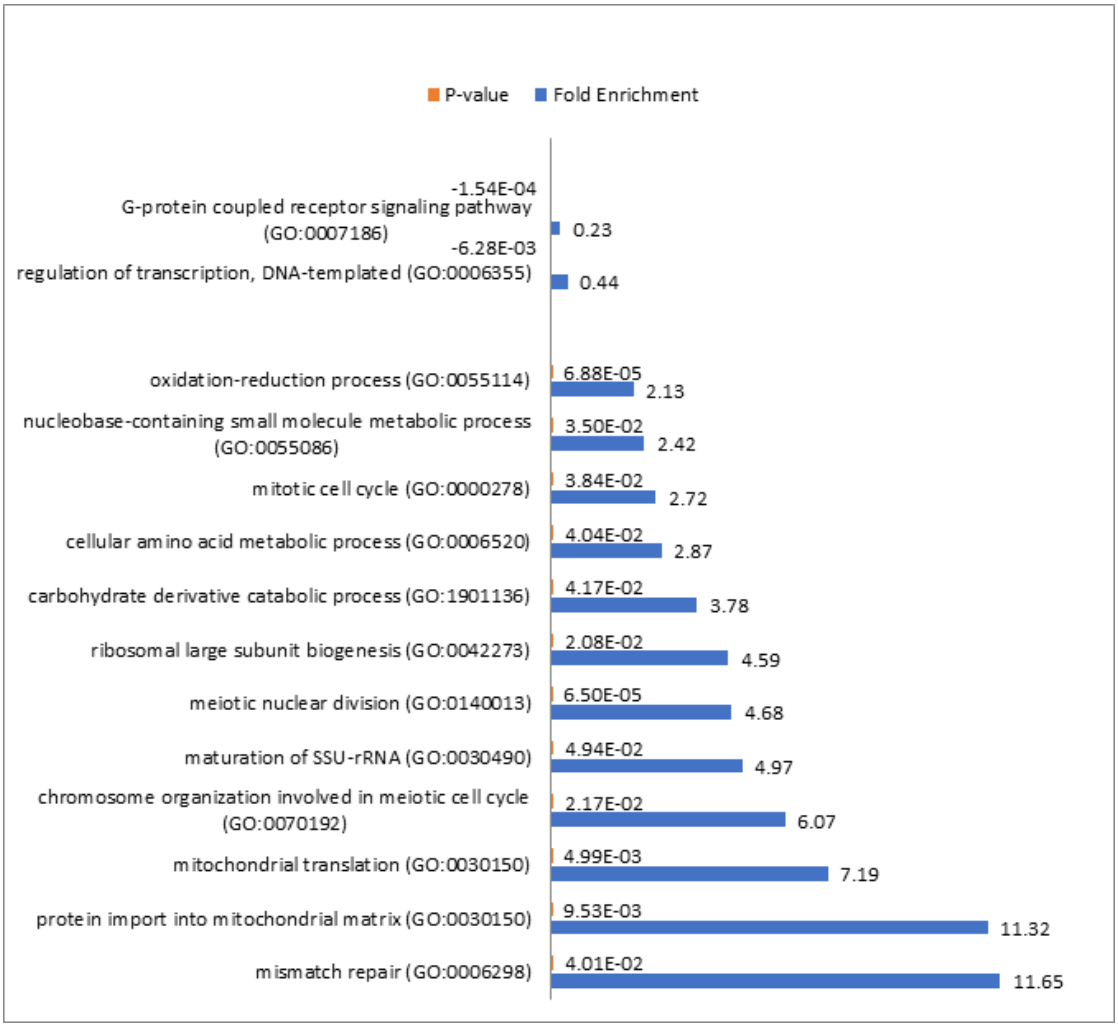

Figure 3.17 Selected biological functional GO categories enriched in *Cbr-spr-4(gu163)* targets, identified by GO Amigo (p-adj < 0.05). Differentially expressed genes for *Cbr-spr-4(gu163)* are enriched for cell cycle and cell proliferation genes.

GO Amigo analysis of Differentially Expressed genes in *Cbr-htz-1(gu167)* mutants

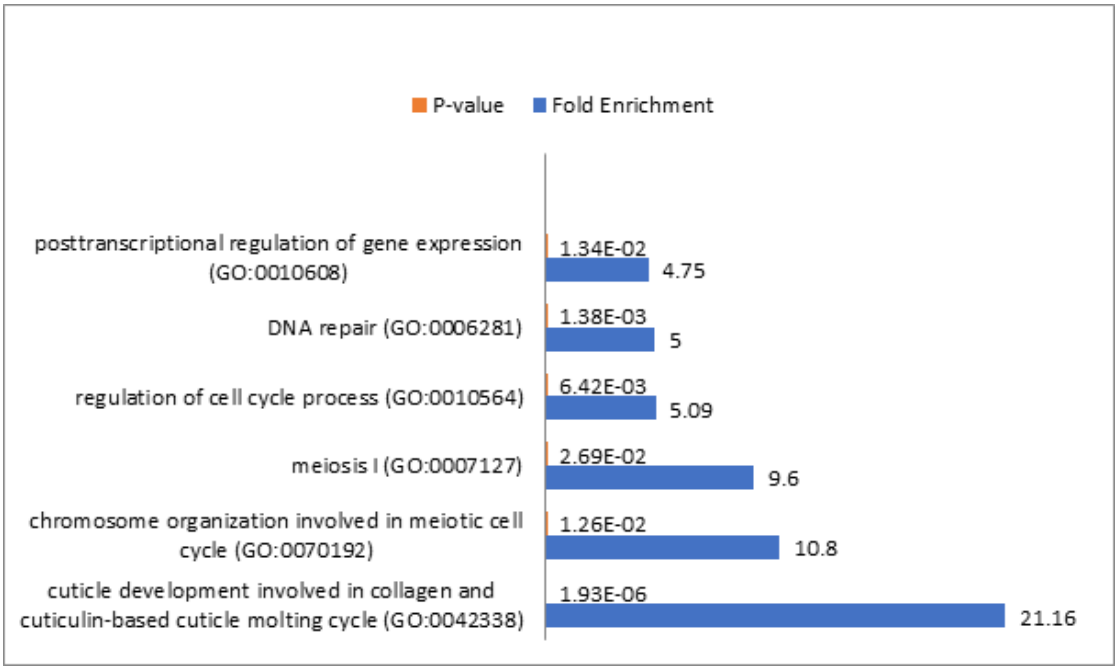

Figure 3.18 Selected biological functional GO categories enriched in *Cbr-htz-1(gu167)* targets, identified by GO Amigo (p-adj < 0.05). Differentially expressed genes for *Cbr-htz-1(gu167)* are enriched for cell cycle and cell proliferation genes.

3.7 Differentially Expressed germline specific genes in RNA-Seq data of *C. briggsae ivp* mutants

SynMuv genes repress *Cbr-lin-3*/EGF in hypodermis (hyp7), and thus restrict the multivulva development in nematodes. Our RT-qPCR data showed the increased level of *Cbr-lin-3* transcripts in *Cbr-ivp* class of mutants and RNAi knockdown of *Cbr-lin-3*/EGF showed a suppression of Muv phenotype in these animals. In addition, it has been shown that gonad ablation (Anchor cell) in *Cbr-ivp* mutants does not results in suppression of Muv phenotype (Sharanya et al., 2015). Thus, it can be concluded that *Cbr-ivp* class of genes also restrict *Cbr-lin-3*/EGF expression, a role that is similar to SynMuv class of genes in *C. elegans*.

It has been shown that SynMuv genes prevent the expression of germline specific factors in somatic cells (Lehner et al., 2006; Unhavaithaya et al., 2002; Wang et al., 2005). In SynMuv mutants, germline P granules were found to exhibit in somatic cells (Wang et al., 2005). Thus, it is possible that *Cbr-ivp* genes might regulate germline genes expression in *C. briggsae* and somatic cells might inherit the characteristics of germline in early developmental stages which leads to a mixed cell fate (driven by both somatic and germline factors) in *Cbr-ivp* mutants.

RNAi knockdown of genes that specifically express in germline suppresses the SynMuv phenotype in *C. elegans* (Cui et., 2006). The RNA-Seq data for *Cbr-spr-4(gu163)* and *Cbr-htz-1(gu167)* mutants were analyzed extensively for the germline candidate genes whose expressions were found to be up regulated. Expression of 62 germline specific genes in *Cbr-spr-4(gu163)* and 29 germline specific genes in *Cbr-htz-1(gu167)* mutants were found to be upregulated. Further, experiments need to be carried out to asses the interaction of these genes with *Cbr-ivp* class of genes. A global profile of germline genes expression in *C. elegans* was provided by Dr. Valerie Reinke (Reinke et al., 2000). The reference list "1063 germline-specific enriched genes (the entire dataset) identified by SAGE" used for the analysis was taken from Wang et al., 2009.

Table 3.15 A global profile of germ line genes in *C. elegans* (Reinke et al., 2000) and 1063 germline-specific enriched genes identified by SAGE (Wang et al., 2009)

	Number of genes in each data set	% of genes in genome
Reinke set of genes	1850	9.3%
Wang set of genes	1063	5.3%

Differentially Expressed germline specific genes in *Cbr-spr-4(gu163)* mutants

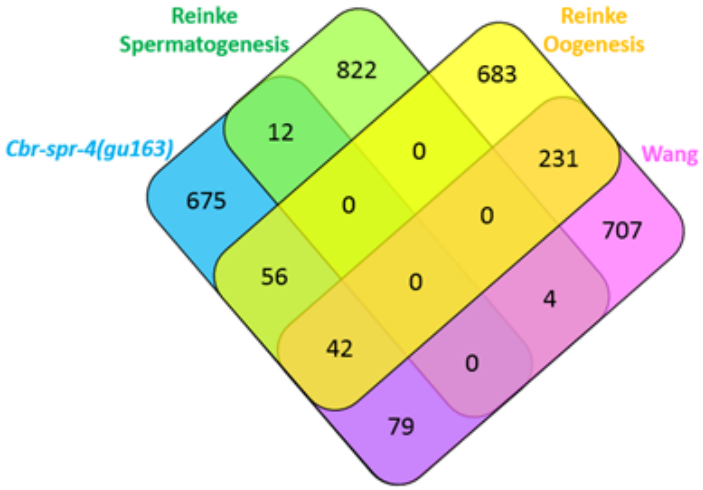

Figure 3.19 A comparison and overlap of germline-specific genes between the RNA-Seq data of *Cbr-spr-4(gu163)* animals and the germline data from Reinke et al., 2000 and Wang et al., 2009.

Table 3.16 Differentially Expressed genes in *Cbr-spr-4(gu163)* animals with increased abundance (up regulated) exhibit overlap between the two datasets

	% of genes	% of genes up regulated
Reinke germline genes in *Cbr-spr-4(gu163)*	12.7%	79.5%
Oogenesis genes	11.3%	77.0%
Spermatogenesis genes	1.4%	100.0%
Wang germline genes in *Cbr-spr-4(gu163)*	14.0%	52.4%

Differentially Expressed germline specific genes in *Cbr-htz-1(gu167)* mutants

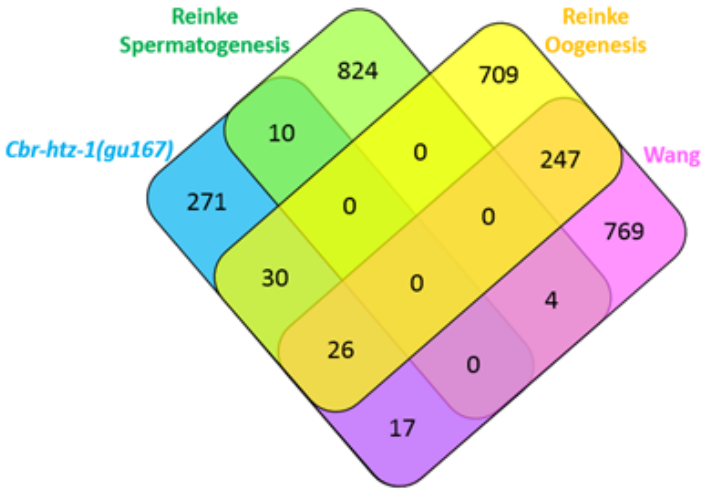

Figure 3.20 A comparison and overlap of germline-specific genes between the RNA-Seq data of *Cbr-htz-1(gu167)* animals and the germline data from Reinke et al., 2000 and Wang et al., 2009.

Table 3.17 Differentially Expressed genes in *Cbr-htz-1(gu167)* animals with increased abundance (up regulated) exhibit overlap between the two datasets

	% of genes	% of genes up regulated
Reinke germline genes in *Cbr-htz-1(gu167)*	18.6%	93.9%
Oogenesis genes	15.8%	96.4%
Spermatogenesis genes	2.8%	80.0%
Wang germline genes in *Cbr-htz-1(gu167)*	12.1%	88.4%

3.8 Examining the expression levels of germline specific genes in *C. briggsae ivp* mutants

It has been observed that many genes like *gld-3*, *mes-4* and *pgl-1* are required maternally for the germline development in *C. elegans* (Eckmann et al., 2004; Petrella et al., 2011; Cui et., 2006; Voronina et al., 2012). Thus, checking the expression level of these genes by RT-qPCR and knocking them down along with other candidate genes (expresses exclusively in germline) may be a good approach to examine the interaction of *Cbr-ivp* genes with germline specific genes.

RT-qPCR was carried out to quantify and compare the expression levels of *Cbr-pgl-1* and *Cbr-mes-4* transcript in wild-type and *Cbr-ivp* mutant worms. The RT-qPCR data for both *Cbr-pgl-1* and *Cbr-mes-4* demonstrated a high level of *Cbr-pgl-1* and *Cbr-mes-4* transcript level in *Cbr-spr-4(gu163)*, *Cbr-htz-1(gu167)*, *Cbr-ivp-3(sy5216)* and *Cbr-gon-14(gu102)* animals when compared to wild-type strain. Transcripts were examined at early L1 stage worms. Worm cultures were double synchronized in order to maintain the coherent stage in the worm culture. RNA was extracted just few hours after hatching the embryos (4 hours after hatching for wild-type animals and 6 hours after hatching for mutants). Our preliminary results suggested a higher level of *Cbr-pgl-1* and *Cbr-mes-4* transcript in *Cbr-spr-4(gu163)*, *Cbr-htz-1(gu167)*, *Cbr-ivp-3(sy5216)* and *Cbr-gon-14(gu102)*. The Differentially Expressed (DE) genes data obtained from RNA-Seq revealed slightly higher level of *Cbr-pgl-1* (log2fold change 1.0628198) and *Cbr-mes-4* (log2fold change 0.83946646) in *Cbr-spr-4(gu163)* mutants suggesting the misregulation of *Cbr-pgl-1* and *Cbr-mes-4* in *Cbr-spr-4(gu163)* mutant animals.

It was found that both *Cbr-pgl-1* and *Cbr-mes-4* transcript levels in *Cbr-spr-4(gu163)* were increased (1.58364 folds and 1.83709 folds expression respectively) in comparison to the wild-type, AF16. While, *Cbr-htz-1(gu167)* animals displayed 1.48229 folds and 1.15170 folds expression of *Cbr-pgl-1* and *Cbr-mes-4* transcripts respectively in comparison to AF16. Both *Cbr-ivp-3(sy5216)* and *Cbr-gon-14(gu102)* exhibited high expression of *Cbr-mes-4* transcripts (1.53528 folds and 1.49195 folds respectively) in comparison to AF16. *Cbr-pgl-1* transcript expression level in *Cbr-ivp-3(sy5216)* was recorded 1.48683 folds while only a slight increase in the level of *Cbr-pgl-1* transcript (1.28534 folds) was observed for *Cbr-gon-14(gu102)* mutant animals (Figure 3.21 and Figure 3.22). For the thorough analysis all the experiments were carried out in multiple batches (Table 3.18 and Table 3.19). For the consistency in data, each step was optimized, and the parameters were kept constant throughout the batches.

Analysis of *Cbr-pgl-1* transcript level in *Cbr-ivp* mutants

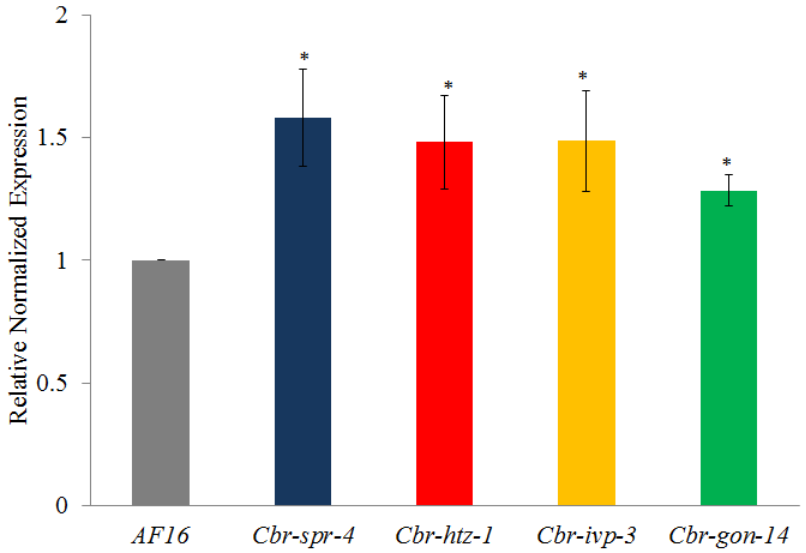

Figure 3.21 The expression of *Cbr-pgl-1* transcripts in *Cbr-ivp* mutants determined by RT-qPCR. Relative fold changes of *Cbr-pgl-1* transcripts have been plotted. AF16 was used as the positive control. *CBG22375* was used for the normalization. Error bars represent standard error of the mean. Standard t-test was used for the statistical analysis. * $p<0.05$.

Table 3.18 RT-qPCR data represents the relative normalized expression *Cbr-pgl-1* transcripts

Strains	Relative Normalized Expression			Average Standard Deviation	STDEVP
	Batch 1	Batch 2	Batch 3		
AF16	1	1	1	1	0
Cbr-spr-4(gu163)	1.38574	1.78154	-	1.58364	0.1979
Cbr-htz-1(gu167)	1.67253	1.29205	-	1.48229	0.19024
Cbr-ivp-3(sy5216)	1.25199	1.55765	1.78942	1.48683	0.206719
Cbr-gon-14(gu102)	1.34825	1.22242	-	1.28534	0.062915

Analysis of *Cbr-mes-4* transcript level in *Cbr-ivp* mutants

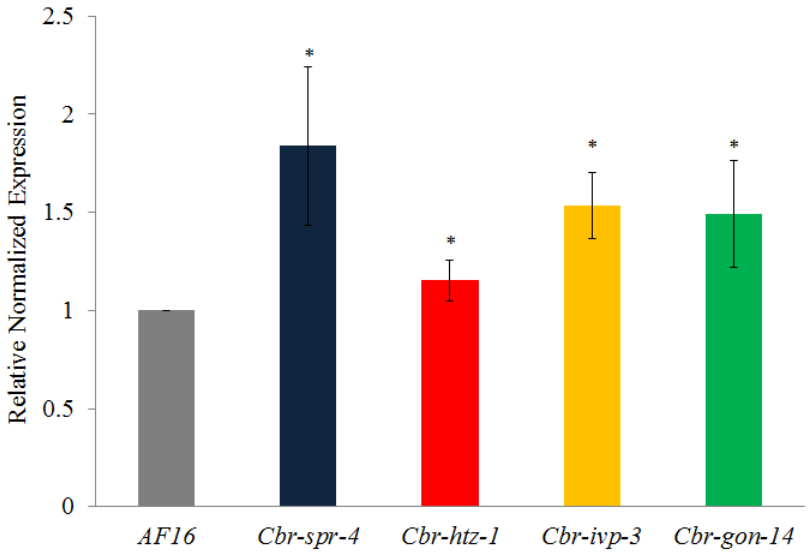

Figure 3.22 The expression of *Cbr-mes-4* transcripts in *Cbr-ivp* mutants determined by RT-qPCR. Relative fold changes of *Cbr-mes-4* transcripts have been plotted. AF16 was used as the positive control. *CBG22375* was used for the normalization. Error bars represent standard error of the mean. Standard t-test was used for the statistical analysis. * $p<0.05$.

Table 3.19 RT-qPCR data represents the relative normalized expression *Cbr-mes-4* transcripts

Strains	Relative Normalized Expression			Average	Standard Deviation	STDEVP
	Batch 1	Batch 2	Batch 3			
AF16	1	1	1		1	0
Cbr-spr-4(gu163)	1.43542	2.23875	-		1.83709	0.401665
Cbr-htz-1(gu167)	1.25279	1.19734	1.00497		1.15170	0.106195
Cbr-ivp-3(sy5216)	1.28825	1.56459	1.76475		1.53528	0.16932
Cbr-gon-14(gu102)	1.76475	1.21915	-		1.49195	0.2728

3.9 RNAi knockdown of *Cbr-pgl-1* and *Cbr-mes-4* transcripts in *Cbr-ivp* mutants

RT-qPCR results suggested that *Cbr-ivp* class of genes may regulate the expression of *Cbr-pgl-1* and *Cbr-mes-4* transcripts. Thus, consequences of knocking down *Cbr-pgl-1* and *Cbr-mes-4* transcripts in Muv mutants was investigated. It was hypothesized that reduced level of *Cbr-pgl-1* and *Cbr-mes-4* transcripts in Muv mutants would rescue the Multivulva phenotype. Thus, RNAi plasmid was generated to knockdown *Cbr-pgl-1* and *Cbr-mes-4* transcripts in *Cbr-ivp* mutants. The RNAi knockdown of *Cbr-mes-4* transcripts resulted the reduction in VPCs induction which led to the suppression of multivulva phenotype in *Cbr-spr-4(gu163)* and *Cbr-htz-1(gu167)* mutants.

Wild-type *C. briggsae* strain, sensitive to environmental RNAi were exposed to control empty vector *L4440*, an induction score of 3.0 ± 0 was observed. While *Cbr-spr-4(gu163)* and *Cbr-htz-1(gu167)* animals, sensitive to environmental RNAi expressed an induction score of 3.3 ± 0.02 and 4.1 ± 0.07 respectively when exposed to bacteria containing *L4440* vector. Upon feeding the bacteria containing the *Cbr-mes-4* RNAi knockdown plasmid to the environmental sensitive RNAi mutants, the induction score was found to be reduced. The induction score of the rescued mutant was determined to be 3.1 ± 0.08 and 3.2 ± 0.05 for *Cbr-spr-4(gu163)* and *Cbr-htz-1(gu167)* mutant animals respectively (Figure 3.23 and Table 3.20).

RNAi knockdown of *Cbr-mes-4* transcripts in *Cbr-spr-4(gu163)* and *Cbr-htz-1(gu167)* mutants

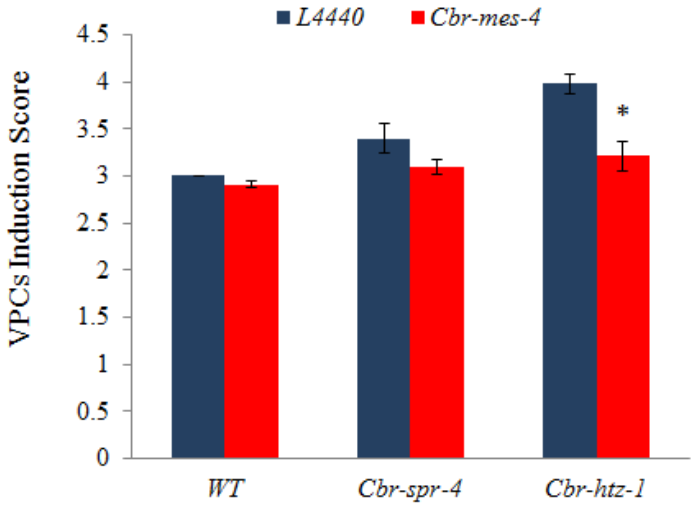

Figure 3.23 A representation of the vulval induction scores in environmental RNAi sensitive *Cbr-spr-4(gu163)* and *Cbr-htz-1(gu167)* mutant animals that were exposed to bacteria containing empty vector *L4440* and RNAi plasmid *Cbr-mes-4*. It was found that *Cbr-mes-4* knockdown in *Cbr-spr-4(gu163)* and *Cbr-htz-1(gu167)* mutant animals showed decrease VPCs induction score and thus, reduction in multivulva phenotype in these animals. All the experiments were carried out in two individual batches. Standard t-test was used for the statistical analysis. ** $p<0.01$.*

Table 3.20 Data representing VPC Induction Score of *Cbr-spr-4(gu163)* and *Cbr-htz-1(gu167)* mutants after the knockdown of *Cbr-mes-4* transcripts

Genotype	RNAi Bacteria	VPC induction Score ± STD	N
mfIs42[sid-2::GFP + myo-2::dsRed]	*L4440*	3.0 ± 0.0	45
mfIs42[sid-2::GFP + myo-2::dsRed]	*Cbr-mes-4*	2.9 ± 0.03	45
Cbr-spr-4(gu163); mfIs42[sid-2::GFP + myo-2::dsRed]	*L4440*	3.3 ± 0.02	45
Cbr-spr-4(gu163); mfIs42[sid-2::GFP + myo-2::dsRed]	*Cbr-mes-4*	3.1 ± 0.08	45
Cbr-htz-1(gu167); mfIs42[sid-2::GFP + myo-2::dsRed]	*L4440*	4.1 ± 0.07	45
Cbr-htz-1(gu167); mfIs42[sid-2::GFP + myo-2::dsRed]	*Cbr-mes-4*	3.2 ± 0.05	45

Evolution of Transcriptional Repressors Impacts *Caenorhabditis* Vulval Development

Helen M. Chamberlin,*[1] Ish M. Jain,[2] Marcos Corchado-Sonera,[1] Leanne H. Kelley,[1] Devika Sharanya,[2] Abdulrahman Jama,[1] Romy Pabla,[2] Adriana T. Dawes,[1,3] and Bhagwati P. Gupta*[2]

[1]Department of Molecular Genetics, Ohio State University, Columbus, OH

[2]Department of Biology, McMaster University, Hamilton, ON, Canada

[3]Department of Mathematics, Ohio State University, Columbus, OH

***Corresponding authors:** E-mails: chamberlin.27@osu.edu; guptab@mcmaster.ca.

Associate editor: Ilya Ruvinsky

Abstract

Comparative genomic sequence analysis has found that the genes for many chromatin-associated proteins are poorly conserved, but the biological consequences of these sequence changes are not understood. Here, we show that four genes identified for an Inappropriate Vulval cell Proliferation (*ivp*) phenotype in the nematode *Caenorhabditis briggsae* exhibit distinct functions and genetic interactions when compared with their orthologs in *C. elegans*. Specifically, we show that the four *C. briggsae ivp* genes encode the noncanonical histone HTZ-1/H2A.z and three nematode-specific proteins predicted to function in the nucleus. The mutants exhibit ectopic vulval precursor cell proliferation (the multivulva [Muv] phenotype) due to inappropriate expression of the *lin-3/EGF* gene, and RNAseq analysis suggests a broad role for these *ivp* genes in transcriptional repression. Importantly, although the *C. briggsae* phenotypes have parallels with those seen in the *C. elegans* synMuv system, except for the highly conserved HTZ-1/H2A.z, comparable mutations in *C. elegans ivp* orthologs do not exhibit synMuv gene interactions or phenotypes. These results demonstrate the evolutionary changes that can underlie conserved biological outputs and argue that proteins critical to repress inappropriate expression from the genome participate in a rapidly evolving functional landscape.

Key words: **developmental system drift, transcriptional repression, chromatin, developmental evolution.**

Article

Introduction

The genome of eukaryotes is assembled into chromatin, which allows for regulated packing and processing of the genetic material throughout the cell cycle. Especially important in chromatin are histones, which are highly conserved proteins that assemble with DNA into nucleosomes, the first-order structural feature of chromatin. In addition to chromatin's important role in packaging the genome, structural alterations by histone modifying and chromatin remodeling enzymes play a regulatory role and constrain the access other factors have to DNA (reviewed by Bracken et al. [2019]). Although many of the proteins that modulate or are part of chromatin are highly conserved across all eukaryotes, sequence analysis has identified other proteins that are less conserved or subject to positive selection, arguing that sequence conservation is not a uniform constraint (Calvo-Martín et al. 2016; Hemmer and Blumenstiel 2016; Ponte et al. 2017; Reddy et al. 2017; Baird 2018). Despite accumulating sequence evidence, it has not been demonstrated how these sequence changes relate to biological function.

One important chromatin modulating complex is the dREAM/MuvB complex, which recruits repressive cofactors to gene promoters (Burkhart and Sage 2008; van den Heuvel and Dyson 2008; Sadasivam and DeCaprio 2013). As the name suggests, founding members of this complex are encoded by "synMuvB" genes in *Caenorhabditis elegans*. Genes in this group were originally identified for their function with a second set of genes, termed synMuvA (Ferguson and Horvitz 1989; Fay and Han 2000; Fay and Yochem 2007). Double mutants between a synMuvA and a synMuvB gene exhibit inappropriate expression of the *lin-3/EGF* gene and give rise to a multivulva (or Muv) phenotype due to ectopic proliferation of cells that produce parts of the egg-laying apparatus, the vulval precursor cells (VPCs) (Cui et al. 2006). Single mutants for either type of gene are not Muv, indicating each class of genes can compensate for the other. This genetic redundancy arises from the participation of synMuvA and synMuvB genes in distinct compensatory processes, rather than direct (e.g., enzymatic) substitution, as they do not encode proteins with overt sequence similarity (Fay and Yochem 2007). Whereas many synMuvB genes encode nuclear proteins with clear human orthologs, canonical synMuvA genes encode worm-specific proteins, and how they modulate transcription is not known.

To better understand the evolution of developmental regulation, we are using genetics in the nematode *Caenorhabditis briggsae*, a species that diverged roughly 30 Ma from the better characterized *C. elegans* (Cutter 2008). The cell divisions and morphological processes underlying the development of the egg-laying system are essentially identical in these two species (Sulston and Horvitz 1977; Félix 2007), but a

number of experimental studies have identified differences between the two when signaling cells or pathway components are perturbed (Félix 2007; Sharanya et al. 2015; Mahalak et al. 2017). Using forward genetic screens, we isolated mutations in four genes that confer a Muv phenotype in *C. briggsae*, but that affected genes not known to participate in vulval development signaling processes in *C. elegans* (Sharanya et al. 2015). We have characterized these genes and find that although one encodes the noncanonical histone H2A.z (Cbr-HTZ-1), the other three are members of worm-specific gene families. For three of the four genes, comparable disruption in *C. elegans* does not confer a Muv phenotype, demonstrating functional evolution for these genes. RNAseq, site of action, and RNAi-knockdown experiments argue that these genes exhibit biological similarities to *C. elegans* synMuv genes, in that they function nonautonomously and alter *Cbr-lin-3/EGF* transcript accumulation. Our data support a model in which H2A.z/HTZ-1 coordinates with a rapidly evolving collection of proteins to repress inappropriate gene expression.

Results

Caenorhabditis briggsae Inappropriate Vulval Cell Proliferation Genes Encode Predicted Nuclear Proteins

To identify *C. briggsae* genes that impact vulval development, we performed a set of unbiased genetic screens for mutants with an Inappropriate Vulval cell Proliferation (*ivp*) phenotype. Our screens identified seven genes that, when mutant, confer the Muv phenotype to *C. briggsae* animals. Three of these genes were found to be orthologs of well-characterized *C. elegans* genes that participate in EGF or Wnt signaling pathways, but four mapped to regions without clear candidates (Sharanya et al. 2015). To molecularly identify these four genes, we used whole-genome sequencing, paired with polymorphism mapping of a representative mutant for each gene and focused on genes with sequence changes predicted to disrupt biological function. This approach identified a candidate gene affected in each mutant (fig. 1A and *B*); targeted sequencing of DNA from animals bearing additional alleles confirmed that they also affected each candidate. Gene identification was validated using transgenic rescue with wild-type DNA (fig. 1C). Based on sequence similarity to *C. elegans*, the four genes are predicted to encode nuclear proteins, including the noncanonical histone H2A.z, Cbr-HTZ-1, and three proteins exhibiting sequence similarity only within the *Caenorhabditis* genus. Two of these genes (*Cbr-spr-4* and *Cbr-gon-14*) have functionally characterized orthologs in *C. elegans* (Lakowski et al. 2003; Chesney et al. 2006). The third gene (*Cbr-ivp-3*/CBG03376) is orthologous to the *C. elegans* gene Y67D8C.3, which has been assigned the name *ivph-3* (*ivp-3* homolog). Although none of these genes have clear orthologs outside *Caenorhabditis*, *gon-14* and *ivp-3*/*ivph-3* from both species share sequence similarity and are classified as part of the same, relatively large gene family (Ruan et al. 2008).

Caenorhabditis elegans Mutants Exhibit Distinct Phenotypes Compared with *C. briggsae*

Since there are identified orthologs for all four *C. briggsae* genes in *C. elegans*, we asked whether *C. elegans* mutants exhibit a phenotype similar to those of *C. briggsae* (fig. 2). Loss-of-function *Cel-gon-14* mutants have been reported previously to exhibit a Muv phenotype (Chesney et al. 2006), but no such phenotype has been shown for the remaining orthologs. *Cel-htz-1* is an essential gene, and homozygous null mutants maternally rescued to adulthood do not exhibit a Muv phenotype (Whittle et al. 2008). However, *Cbr-htz-1(gu167)* is a missense mutation that may alter gene function in an unpredictable manner, and its Muv phenotype is likewise maternally rescued (Sharanya et al. 2015). Thus, we used CRISPR-mediated genome editing to engineer the orthologous change into *Cel-htz-1*. This mutation can be maintained in a homozygous strain, indicating that it is nonnull, and allowing mutant offspring from mutant parents to be evaluated. We likewise used CRISPR-mediated genome editing to generate a deletion of *Cel-sprp-4*, a paralog of *Cel-spr-4* that others have interpreted might compensate for some functions when *Cel-spr-4* is disrupted (Lakowski et al. 2003). A *Cel-ivph-3* deletion allele (also generated by CRISPR) was provided by the lab of Dr Don Moerman. We find that in contrast to *C. briggsae*, *Cel-htz-1* and *Cel-ivph-3* single mutants, and *Cel-spr-4; Cel-sprp-4* double mutants all exhibit normal vulval development (fig. 2). Thus, the phenotypic consequences of these mutations are distinct in the different species background. We also note that, whereas *Cbr-gon-14* and *Cbr-ivp-3* mutants are fertile, similarly disruptive alleles of *Cel-gon-14* or *Cel-ivph-3* result in a sterile phenotype. To ask whether this might reflect incomplete disruption of gene function or redundancy between the two genes, we constructed *Cbr-ivp-3(sy5216); Cbr-gon-14(gu102)* double mutants and find that doubles remain viable and fertile (supplementary table 5, Supplementary Material online). These results suggest that there are functional differences between the species for these genes in addition to variation in the vulval development process.

Due to these observed genetic distinctions in the two species, we asked whether the four genes exhibit any sequence features consistent with rapid evolution or positive selection. First, we tested for accelerated evolution using the codon substitution model of PAML (Yang 2007) and detected no difference in selection (ω) in the *C. briggsae* branch for these genes compared with the orthologs (supplementary table 6, Supplementary Material online). We then evaluated changes specifically between *C. elegans* and *C. briggsae* using the nonsynonymous substitution rate (K_A), which offers a signature for evolution of protein encoding genes (Wang et al. 2011). Compared with the genome-wide K_A of 0.121 (Cutter et al. 2019), K_A for *htz-1* is lower (0.007), whereas the values for *spr-4*, *gon-14*, and *ivp-3*/*ivph-3* are notably higher (0.608, 0.887, and 0.554, respectively). Altogether, we conclude that these sequence analyses do not predict the functional differences observed in vivo, as the identical mutation affecting the highly conserved *htz-1* confers a distinct vulval development phenotype in the two species, whereas mutation of the more divergent *gon-14* confers a Muv phenotype in both species.

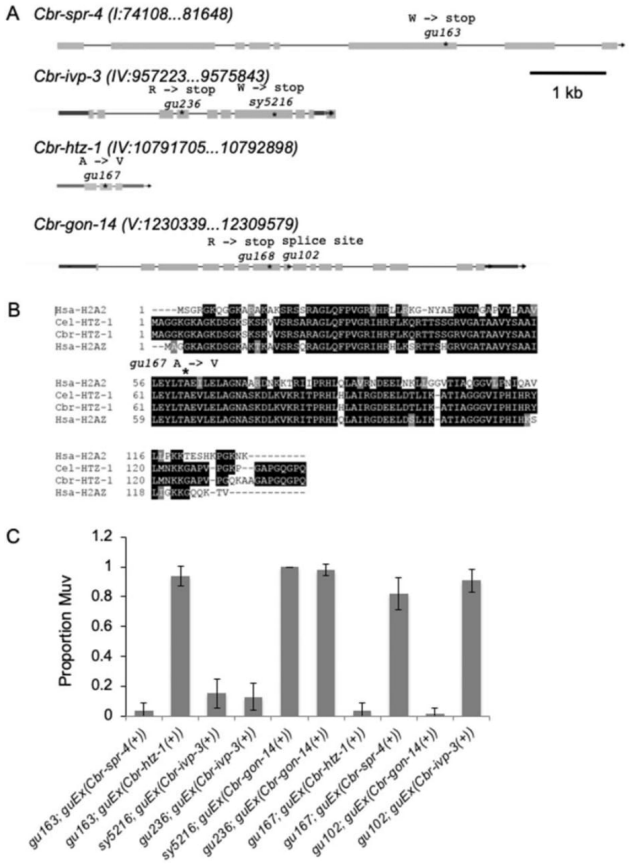

FIG. 1. Molecular cloning of *Caenorhabditis briggsae ivp* genes. (*A*) Gene models for *C. briggsae ivp* genes, based on Genome Browser annotation validated with publicly available RNAseq data. Each gene is represented to scale, with 5′ to the left. *gu163* (tgG [W] to tgA [stop]) is a nonsense mutation in *Cbr-spr-4*. *gu236* (Cga [R] to Tga [stop]) and *sy5216* (tgG [W] to tgA [stop]) are nonsense mutations in *Cbr-ivp-3*. *gu167* (gCc [A] to gTc [V]) is a missense mutation in *Cbr-htz-1*. *gu168* (Cga [R] to Tga [stop]) is a nonsense mutation, and *gu102* (G to A) affects the 5′ splice site of intron 8 in *Cbr-gon-14*. *gu102* results in transcripts which retain intron 8, leaving an in-frame stop codon. Genomic context of each mutation is listed in supplementary table 2, Supplementary Material online. Images modified from Wormbase.org (Lee et al. 2018). (*B*) Alignment of the predicted protein product of Cbr-HTZ-1 with orthologs from *Caenorhabditis elegans* (Cel-HTZ-1) and human (Hsa-H2AZ), and the canonical human histone H2A2 (Hsa-H2A2). The *gu167* mutation results in a substitution of Valine (V) for Alanine (A) in the a2 domain of the histone fold, a structural domain conserved across histones. (*C*) Transgenes (identified as *guEx*) including PCR fragments from wild-type DNA corresponding to each gene rescue the corresponding mutant but fail to rescue other mutants, even if the genes are from the same group (*Cbr-ivp-3* and *Cbr-gon-14* share sequence similarity and are from the same TreeFam group, TF317492). $n \geq 50$ for all genotypes. Full genotypes are listed in supplementary table 1, Supplementary Material online. Full data, exact sample sizes, and data from additional strains are listed in supplementary table 4, Supplementary Material online.

Evolution of synMuvA Genes Alters the In Vivo Function of *htz-1* but Not Other *ivp* Genes

We sought to test the hypothesis that the *ivp* genes have functional similarities between *C. elegans* and *C. briggsae*, but that their disruption is compensated by other genes in the *C. elegans* genome. We focused on the synMuv system, as synMuvB genes include *Cel-lin-35/Rb*, which has been shown to function with *Cel-htz-1* to repress transcription (Latorre et al. 2015). Since our *Cbr-htz-1* mutants exhibit a Muv phenotype but *Cel-htz-1* mutants do not, we asked whether this

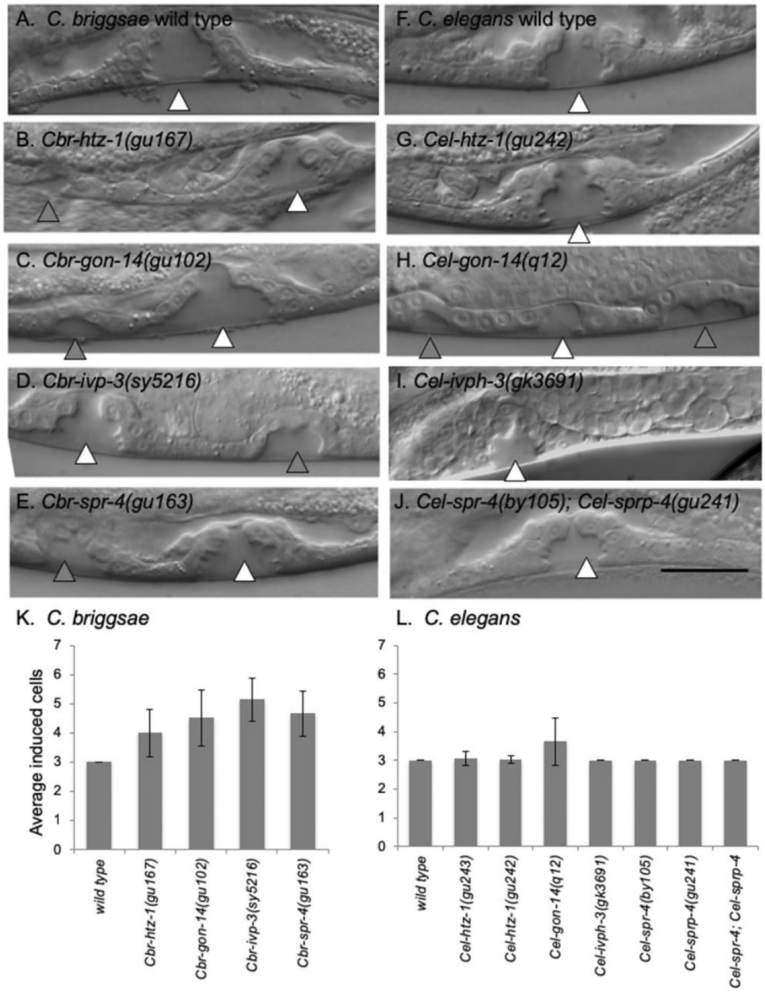

FIG. 2. *Caenorhabditis briggsae* and *C. elegans* mutants exhibit distinct phenotypes. Normal *C. briggsae* (*A*) and *C. elegans* (*F*) vulval development is very similar, with an identical pattern of cell divisions from three VPCs resulting in a single vulval structure in the L4 larval stage (white arrowhead). *Caenorhabditis briggsae* mutants of *htz-1*, *gon-14*, *ivp-3*, and *spr-4* (*B*–*E*) frequently exhibit the division of more than three VPCs (*K*), resulting in additional vulval-like structures (gray arrowheads). Although similar mutations in *Cel-gon-14* can induce the division of supernumerary VPCs (*H*), they result in little or no change to vulval development for *Cel-htz-1*, *Cel-ivph-3*, or *Cel-spr-4*; *Cel-sprp-4* (*G*, *I*, *J*, *L*). $n \geq 40$ for each genotype, except *Cel-ivph-3*, where $n = 24$. Full genotypes are listed in supplementary table 1, Supplementary Material online. Full data and exact sample sizes are listed in supplementary table 7, Supplementary Material online. Error bars correspond to the standard deviation. Scale bar, 20 μm.

might result from changes to synMuvA genes. Consistent with this idea, the *C. briggsae* genome appears to lack a *lin-15A* and a *lin-56* ortholog, based on Blast search, WormBase annotation (www.wormbase.org; Lee et al. 2018), and synteny (fig. 3*A* and *B*). Cel-LIN-15A and Cel-LIN-56 physically interact, and each protein is destabilized in mutants for the other, arguing they function together (Davison et al. 2011). Thus, we asked whether differences between the *C. elegans* and

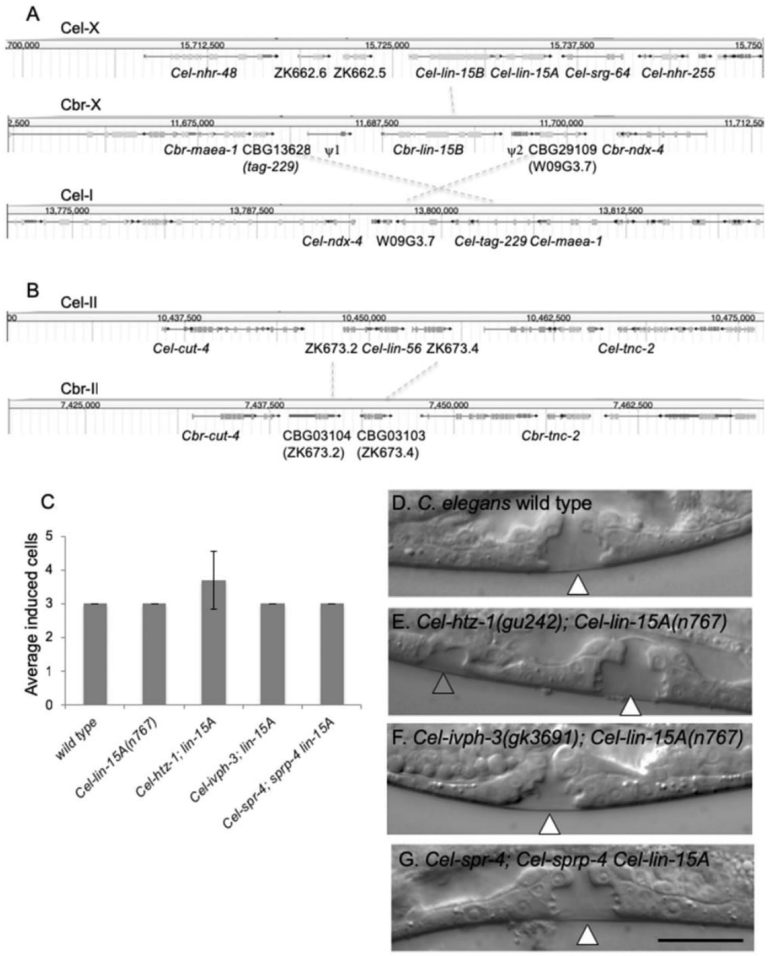

FIG. 3. Loss of synMuvA genes alters the in vivo function of *Cbr-htz-1*. (*A*) The *Caenorhabditis elegans lin-15* locus comprises an operon of *Cel-lin-15B* (upstream) and *Cel-lin-15A* (downstream). The *Caenorhabditis briggsae* genome lacks an annotated *lin-15A* ortholog, based on wormbase.org annotation and Blast search. The Chromosome X genomic region including the *Cbr-lin-15B* gene is not syntenic with the *Cel-lin-15B* region, but rather flanked by sequences syntenic with *C. elegans* Chromosome I. *Cbr-lin-15B* is flanked by two annotated psuedogenes, neither of which bears sequence similarity to *Cel-lin-15A* ($\psi 1 =$ CBG13630, annotated ortholog and top BlastX hit: T26E3.6; $\psi 2 =$ CBG13633, no ortholog annotated. Top BlastX hits: Y52B11A.12, *sdz-15*) (*B*) The *Cel-lin-56* locus is on Chromosome II. The *C. briggsae* genome lacks an annotated *lin-56* ortholog, based on wormbase.org annotation and Blast search. The syntenic region on *C. briggsae* Chromosome II likewise lacks a gene where *Cel-lin-56* is found. (*A*, *B*). Images modified from Wormbase.org (Lee et al. 2018). For *C. briggsae* genes not yet named based on orthology, each gene is followed by the *C. elegans* ortholog identified in wormbase.org, in parentheses. (*C*–*G*) *Cel-htz-1; Cel-lin-15A* double mutants exhibit increased numbers of induced VPCs, whereas no increase in induction is observed in *Cel-ivph-3; lin-15A* doubles and *Cel-spr-4; Cel-sprp-4 Cel-lin-15A* triples. $n \geq 40$ for each genotype, except *Cel-ivph-3; lin-15A*, where $n = 29$. Full genotypes are listed in supplementary table 1, Supplementary Material online. Full data and exact sample sizes are listed in supplementary table 7, Supplementary Material online. Error bars correspond to the standard deviation. Scale bar, 20 μm.

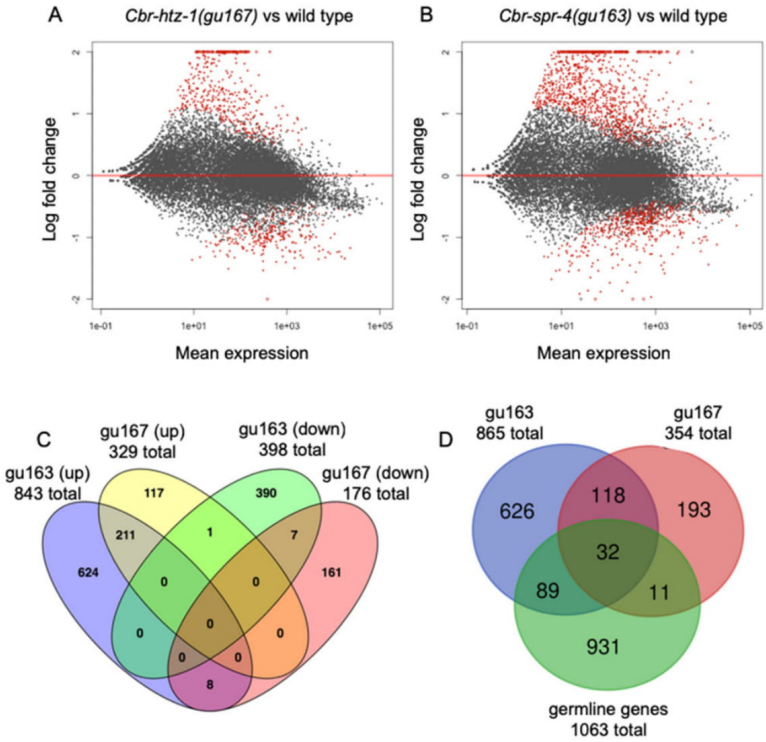

FIG. 4. *Caenorhabditis briggsae ivp* mutants exhibit increased transcript abundance of many genes. MA plots of DE genes in *Cbr-htz-1(gu167)* (A) and *Cbr-spr-4(gu163)* (B). DE genes in each strain are more likely to be increased (835 vs. 397 for *Cbr-htz-1(gu167)* and 328 vs. 168 for *Cbr-spr-4(gu163)*). Red dots represent transcripts with an FDR *P*-adj of <0.05, whereas black dots represent transcripts with FDR *P*-adj of >0.05. (C) DE genes with increased abundance ("up") exhibit overlap between the two data sets. Specifically, 211/952 (22%) of genes exhibiting increased abundance are shared between the two genotypes, whereas 7/558 (1.2%) of those with decreased abundance overlap. Also see supplementary workbook 1, Supplementary Material online. (*D*) Comparison of *Cbr-htz-1(gu167)* and *Cbr-spr-4(gu163)* DE gene orthologs with genes that are enriched in the germline of *Caenorhabditis elegans* ("germline genes" [Wang et al. 2009]). Also see supplementary workbook 2, Supplementary Material online. Sequence data submitted to GEO (GSE133769).

C. briggsae phenotypes can be explained by the absence of these synMuvA genes from the genome. Previous studies evaluated the functional consequences of disrupting *Cel-lin-15A* in the *Cel-gon-14* background and found no difference compared with *Cel-gon-14* alone (Chesney et al. 2006). We constructed double mutants with *Cel-htz-1* and *Cel-ivph-3*, and triple mutants for *Cel-spr-4* (fig. 3C–G). We find that *Cel-htz-1; Cel-lin-15A* double mutants indeed exhibit division of additional VPCs compared with single mutants, consistent with the idea that the presence of the *lin-15A* gene in the *C. elegans* genome can compensate for the *htz-1* mutation. However, a similar effect was not observed for *Cel-ivph-3* or *Cel-spr-4* (fig. 3C), indicating that the apparent loss of *lin-15A* from the *C. briggsae* genome is not sufficient to explain the functional differences for these genes.

Caenorhabditis briggsae ivp Mutants Exhibit Broad Misregulation of Transcripts, Including Germline Genes

Given that our *C. briggsae* genes are predicted to encode nuclear proteins, we evaluated gene expression changes in mutants using RNAseq. RNA was collected from two mutants, *Cbr-htz-1(gu167)* and *Cbr-spr-4(gu163)*, both synchronized to mid-L3 larval stage, and differentially expressed (DE) genes were compared with those from similarly staged wild-type animals (fig. 4A and B). The analysis revealed that in both mutants, twice as many DE genes exhibit an increased transcript abundance compared with those that exhibit a decreased transcript abundance (fig. 4C and supplementary workbook 1, Supplementary Material online). Furthermore, overlap between the *Cbr-htz-1(gu167)* and *Cbr-spr-4(gu163)*

data sets was prevalent among the genes with increased abundance, but negligible for those with decreased abundance. We conclude that an important normal function for these genes is to reduce transcript accumulation, such as through repression of inappropriate transcription from the genome.

We evaluated Gene Ontology (GO) categories enriched in DE genes in *Cbr-htz-1(gu167)* and *Cbr-spr-4(gu163)* mutants, and noted that these included several gene categories involved in meiosis. Since one defect in *C. elegans* synMuvB mutants is dysregulation of germline genes and related processes (Petrella et al. 2011; Rechtsteiner et al. 2019), this observation prompted us to evaluate how germline genes are represented among those altered in the *C. briggsae* mutants. From the genes with altered abundance, we identified those with direct (1:1) orthologs in *C. elegans*, and then looked for germline-expressed genes among these orthologs (Wang et al. 2009). Both *Cbr-htz-1(gu167)* and *Cbr-spr-4(gu163)* DE gene sets exhibit a significant enrichment of germline genes (fig. 4*D* and supplementary workbook 2, Supplementary Material online). For *Cbr-htz-1(gu167)*, the vast majority are upregulated compared with wild type, as is observed in *C. elegans* synMuvB mutants (Petrella et al. 2011) (supplementary workbook 2, Supplementary Material online). In contrast, the DE germline genes in *Cbr-spr-4(gu163)* include genes with both increased and decreased transcript abundance.

Caenorhabditis briggsae ivp Genes Function Nonautonomously to Repress Inappropriate Expression of the EGF Ligand Gene, *Cbr-lin-3*

Although the *C. briggsae ivp* mutants alter the transcript abundance of many genes, we wanted to better understand the specific contribution to vulval development. First, we asked where gene function is required by introducing cDNA under control of heterologous, cell-specific promoters. We found that introduction of either *Cbr-htz-1* or *Cbr-ivp-3* under control of a non-VPC, hypodermis-specific promoter can rescue each respective mutant (fig. 5*A* and supplementary fig. 1, Supplementary Material online). We then reasoned that one way to nonautonomously increase the number of VPCs that divide to produce vulval cells is to ectopically express genes that encode signals that promote vulval cell fates. Since the EGF, Notch, and Wnt pathways play an important role in vulval development in both species (Sternberg 2005), we evaluated the set of genes exhibiting increased transcript abundance in both *Cbr-htz-1(gu167)* and *Cbr-spr-4(gu163)* for ones encoding ligands for these three pathways. Only *Cbr-lin-3/EGF* (CBG05996) exhibited a significant increase in abundance in both strains, which is notable as the Muv phenotype in *C. elegans* synMuv mutants also results from an abnormal increase of *Cel-lin-3/EGF* (Cui et al. 2006). We used Reverse Transcriptase quantitative Polymerase Chain Reaction (RT-qPCR) to evaluate *Cbr-lin-3/EGF* gene transcripts and found that levels are elevated in all four mutant strains compared with wild-type animals (fig. 5*B*). Since the increase is modest (and not always detected [Sharanya et al. 2015]), we asked whether this observed difference is functionally relevant using RNAi to knock down *Cbr-lin-3* in each mutant. The vulval induction was found to be reduced in response to RNAi treatment, indicating that abnormal expression of this gene contributes to the observed Muv phenotype (fig. 5*C* and *D*).

Discussion

Here, we have characterized a set of genes in the nematode *C. briggsae* that act to prevent inappropriate proliferation and development of specialized epithelial cells, the VPCs. Altogether, the data support a model in which the gene products function in the nucleus to repress inappropriate transcription from the genome. The mutants exhibit increased transcript abundance of *lin-3/EGF* and of germline-associated genes, functionally similar to a class of genes defined in *C. elegans* as synMuv genes (Petrella et al. 2011). However, comparable genetic mutants in *C. elegans* result in a synMuvB phenotype for the conserved noncanonical histone gene *htz-1/H2A.z*, but not for the other genes that exhibit a similar phenotype in both species (*gon-14*) (Chesney et al. 2006) or distinct phenotypes (*spr-4* and *ivp-3/ivph-3*). Thus, even though the development, anatomy, and life history traits are similar between the two species, there are functional differences in the underlying networks that promote normal gene expression and development.

Nematode vulval development has been a focus of study by many evolutionary biologists and provides several examples of developmental system drift wherein there is evolutionary change in the underlying cellular and genetic processes that result in the production of overtly similar biological outcomes (True and Haag 2001; Sommer 2012). For example, nematodes across the Rhabditidae family share the common feature in which the vulva is formed from the offspring of three specialized epidermal cells (Sommer and Sternberg 1995). However, species differ with respect to the underlying developmental processes, such as the dependence of vulval development on cells in the gonad, and the molecular signals that are critical (Sommer and Sternberg 1994; Sigrist and Sommer 1999; Tian et al. 2008; Vargas-Velazquez et al. 2019). Specifically within *Caenorhabditis*, vulval development is identical in *C. elegans* and *C. briggsae*, but cell ablation experiments demonstrate that premature removal of the anchor cell can result in distinct patterning defects (Félix 2007). Likewise, genetic and pharmacologic experiments show that whereas the EGF signaling pathway is essential for *C. elegans* vulval development, *C. briggsae* animals still produce some vulval tissue under comparable conditions (Mahalak et al. 2017). Our current findings relate to the signaling processes that promote vulval development in that expression of a key signaling gene, *lin-3/EGF*, is affected. However, our findings are distinct from these other studies in that they uncover evolution of the processes that constrain transcription from the genome, rather than specific features of the underlying signaling networks that influence vulval development.

Importantly, our results demonstrate functional evolution of HTZ-1/H2A.z and the other *ivp* proteins. One important role for chromatin is in managing the genomic material from generation to generation, during which products of the

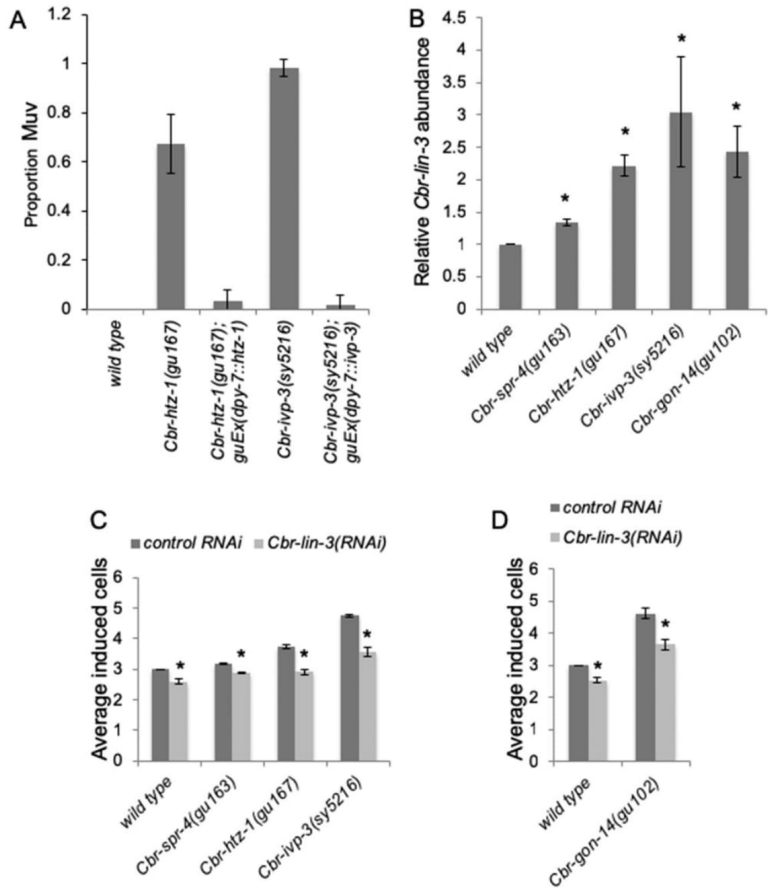

FIG. 5. The *Caenorhabditis briggsae* Muv mutant phenotype results from inappropriate expression of *Cbr-lin-3/EGF*. (*A*) Expression of cDNA for *Cbr-htz-1* or *Cbr-ivp-3* under control of a non-VPC hypodermis-specific promoter (*dpy-7*) rescues the Muv phenotype associated with mutants. Full genotypes are in supplementary table 1, Supplementary Material online. $n \geq 40$ for all genotypes. Full data and exact sample sizes are listed in supplementary table 8, Supplementary Material online. Additional transgenes tested are in supplementary figure 1, Supplementary Material online. (*B*) *Cbr-lin-3* transcripts exhibit increased abundance in the Muv mutants. * indicates statistically different from wild type (Student's *t*-test, $P < 0.01$). (*C*, *D*) RNAi-knockdown of *Cbr-lin-3* in the Muv mutants results in a decrease in the number of VPCs that divide to produce vulval tissue. Data are reported separately as the wild-type background strain is different in (*C*) (includes *Cel-sid-2* transgene *mfIs42*) compared with (*D*) (includes *Cel-sid-2* transgene *mfEx32*). Full genotypes are listed in supplementary table 1, Supplementary Material online. Data represent three independent trials for each, with $n \geq 30$ animals for each genotype in each trial. Full data and exact sample sizes are listed in supplementary table 9, Supplementary Material online. * indicates statistically different from wild type (Student's *t*-test, $P < 0.01$). Error bars correspond to the standard deviation.

maternal genome interact with those of the paternal genome in the one-cell zygote, and in the embryo following initiation of transcription from the zygotic genome. This process can result in genomic conflict, wherein there is competition between the maternal genome to repress expression of particular genes or genetic elements in the paternal genome, and the paternal genome to bypass those repressive effects (Johnson 2010; Crespi and Nosil 2013). Such conflict could drive rapid change in sequence and in the relative importance of different proteins in maintaining silenced chromatin states, in an effort to limit the genomic risks of outcrossing. Indeed, genome-wide sequence analysis identifies proteins predicted

to localize to the nucleus or participate in transcription as significantly enriched among rapidly evolving nematode genes (Castillo-Davis et al. 2004), and this is especially true for genes that are most abundant during early embryonic development (Cutter et al. 2019). Broadly, our results indicate that the function of proteins that impact access to the genome can evolve as part of developmental system drift. We anticipate that these may include critical regulatory factors that are understudied or yet to be discovered, as such proteins are refractive to canonical research approaches that emphasize sequence conservation and orthology to predict functional importance.

Materials and Methods

Worm Maintenance and Genetics

Methods for culturing and maintaining nematodes were as described for *C. elegans* (Brenner 1974; Stiernagle 2006). Specifically, worms were grown on NGM or NG-Agar plates seeded with *Escherichia coli* OP50 as a food source. All experiments were carried out at 20 °C, unless stated otherwise. The wild-type *C. briggsae* was AF16, and the wild-type *C. elegans* was N2. Specific strains and genotypes used are listed in supplementary tables 1 and 2, Supplementary Material online.

Generation of CRISPR Alleles

New alleles of *C. elegans* genes were generated using CRISPR-mediated genome editing methods. Standard procedure following recovery is to back-cross the strain 2× to wild type prior to phenotypic analysis.

Cel-htz-1(gu242) and *Cel-htz-1(gu243)* were generated using the method of Arribere et al. (2014). sgRNA targeting *Cel-htz-1* was introduced into pDD162 (Dickinson et al. 2015) and coinjected into the germline of wild-type *C. elegans* with a single-stranded repair template and a fluorescent reporter (*myo-2::gfp*) as a transformation marker (primers provided in supplementary table 3, Supplementary Material online). GFP-positive F1 animals were selected and allowed to self-cross. After each plate that was founded by an F1 parent depleted the bacteria, a portion was saved, and the remainder prepared to recover DNA and subject to PCR for genotyping. Animals were recovered from plates heterozygous for the introduced (silent) restriction enzyme site alteration and allowed to self to recover homozygotes.

Cel-sprp-4(gu241) was generated using the method and plasmids of Dickinson et al. (2015), with two sgRNAs each in pDD162 (one targeting the 5′ end of the gene, and one targeting the 3′ end of the gene), and a repair template in pDD285 consisting with flanking homology arms corresponding to sequences upstream and sequences downstream of the coding exons, resulting in a mutant allele in which the coding exons are replaced with the intervening sequence (mKate > SEC > FLAG). These plasmids were coinjected into the gonad of wild-type *C. elegans* animals together with a negative selection fluorescent marker (*myo-2::gfp*). Candidate repair events were selected (hygromycin^R GFP-), subjected to SEC excision, and validated with PCR and Sanger sequencing.

The *C. elegans ivph-3(gk3691)* allele was provided by the Moerman lab (UBC), and was also generated using a CRISPR/Cas9-based homology-directed repair and drug selection technique. Briefly, a GFP cassette (∼5.4 kb) containing *myo-2p::GFP* and *rps-27p::Neo* selection marker was inserted into the genomic region of *Y67D8C.3* using two ∼500-bp homology arms that flanked the first exon of *Y67D8C.3a*. The insertion of the cassette resulted in the deletion of the entire first exon and 9 bp of the second exon of *Y67D8C.3a*. These exons are common to all *Y67D8C.3* isoforms. The *gk3691* mutation is homozygous sterile and Pvl so it requires picking GFP fluorescing animals to maintain it. The strain was validated by PCR and Sanger sequencing.

Whole-Genome Sequencing, Candidate Gene Identification, and Mutation Confirmation

Genomic DNA was prepared for whole-genome sequencing from *Cbr-gon-14(gu102)*, *Cbr-spr-4(gu163)*, *Cbr-htz-1(gu167)*, and *Cbr-ivp-3(sy5216)* homozygotes and sequenced using the Illumina HiSeq platform by the Ohio State University Comprehensive Cancer Center Genomics Shared Resource (for *gu102*) and McGill University - Génome Québec Innovation Centre Montreal (for the remaining three strains). In general, paired read FASTQ files were aligned to the *C. briggsae* cb4 reference sequence using the Burrows–Wheeler Aligner BWA (Li and Durbin 2009) (version 0.6.2). SAMtools (Li et al. 2009) (version 0.1.19) was used to create the pileup file. Potential candidates with sufficiently high coverage (minimum four reads) were identified in the pileup file using custom Python scripts. Variants affecting genes on the chromosome to which each gene had been genetically mapped (Sharanya et al. 2015) were considered as prospective candidate genes. Although each mutation had been mapped against polymorphisms to particular chromosomal regions, we found that limiting our candidates to those regions excluded the (ultimately confirmed) affected gene in some cases, perhaps due to assembly errors in the reference genome (also supported by the data of others [Bi et al. 2015; Ren et al. 2018]). Nonsense mutations, splicing mutations, and alterations that disrupted reading frame were prioritized for further testing. No nonsense mutation was identified that affected genes in the *Cbr-htz-1(gu167)* strain. *Cbr-htz-1* was selected for further analysis based on the impact of the missense mutation on a highly conserved amino acid. The DNA mutations in strains evaluated by WGS, and those of strains not subject to WGS, were confirmed or identified by Sanger sequencing of PCR fragments (generated from DNA of each strain) that covered all exons and exon/intron boundaries. The sequence alteration for each allele is listed in supplementary table 2, Supplementary Material online.

RT-qPCR, Whole-Genome RNA Sequencing, and Data Analysis

RNA was recovered from synchronized L3 animals using a standard TRIZOL method (Invitrogen). Animals were staged prior to harvesting by mounting a sample and observing them under the Nomarski microscope. RNA was extracted just prior to the stage when vulval precursors (Pn.p cells)

initiate division. At this stage, vulval cells are responsive to *Cbr-lin-3* levels (Félix 2007). RT-qPCR used to validate abundance of *Cbr-lin-3* transcripts was carried out using the protocol described previously (Sharanya et al. 2015). For RNA sequencing (RNAseq) experiments, three independent biological replicates were prepared from AF16, *Cbr-htz-1(gu167)*, and *Cbr-spr-4(gu163)* strains, and the samples were processed, depleted for rRNA, and sequenced using Illumina HiSeq 2000 V3 Single Read system by Génome Québec.

RNAseq data were analyzed as follows. The package cutadapt/trimgalore was used to trim the adapters, and reads with QC values (Phred score) <30 bases were discarded (Martin 2011). The processed sequencing reads were mapped to the *C. briggsae* reference genome (cb3 assembly, UCSC genome browser) using STAR aligner v2.5 (Dobin et al. 2013). More than 95% of sequencing reads were successfully mapped to the genome. Transcript-level abundance was estimated using quantMode, a HTSeq-count package incorporated in the STAR 2.5 (Dobin et al. 2013). Gene counts were quantile normalized to avoid bias between samples (Bullard et al. 2010; Martin 2011). DE genes were called at a false discovery rate (FDR) of 0.05% using the R package DESeq2 that is based on the negative binomial distribution model (Love et al. 2014). The results revealed 1,241 DE genes in *Cbr-spr-4(gu163)* and 505 in *Cbr-htz-1(gu167)* animals. RNAseq data are deposited with GEO (GSE133769).

GoAmigo (Carbon et al. 2009) was used with default settings to perform GO analysis of candidate genes. A GO-term containing at least three genes with a *P* value (adjusted for multiple comparisons) of <0.05 (Benjamini–Hochberg method) was considered as significant (Carbon et al. 2009).

Cbr-spr-4(gu163) and *Cbr-htz-1(gu167)* transcriptomes were analyzed for germline, oogenesis, and spermatogenesis genes using available *C. elegans* data sets (Reinke et al. 2000; Wang et al. 2009). Sequence comparisons revealed a total of 865 and 354 1:1 unique *C. elegans* orthologs of DE genes for each genotype, respectively (supplementary workbook 2, Supplementary Material online). Germline and oogenesis genes were significantly overrepresented in the transcriptomes of each mutant (supplementary workbook 2, Supplementary Material online).

Generation of Transgenes and Plasmids

Genomic rescue DNA fragments were generated by PCR amplification of each gene, plus at least 500-bp flanking DNA, from AF16 (wild-type *C. briggsae*) genomic DNA. PCR fragments were confirmed based on size using gel electrophoresis, incorporated into injection mixes (5 ng/μl *myo-2::gfp*, 15 ng/μl *Cel-unc-119(+)*, and 50 ng/μl PCR product), and microinjected into the gonad of *Cbr-unc-119(st20000)* hermaphrodites using standard *C. elegans* methods (Mello et al. 1991). Males were induced in stable transgenic lines and crossed with hermaphrodites doubly homozygous for *Cbr-unc-119(st20000)* and the mutant to be tested for rescue. F1 non-Unc animals were selected individually and allowed to self. Animals homozygous for the Muv mutation were selected from among the offspring of the F1. Homozygotes were identified based on their Muv phenotype, or on the capacity of the non-Muv non-Unc parent to produce only non-Muv non-Unc or Muv Unc offspring. DNA from mutant rescued strains was recovered, subjected to PCR, and sequenced to evaluate the region including the mutation to verify that reversion of the mutant phenotype correlates with introduction of wild-type sequences into the genome and to confirm the identity of the DNA in the PCR product.

Plasmids for tissue-restricted rescue were generated in the pPD49.26 backbone (a gift from Dr A. Fire). *Caenorhabditis elegans* gene promoters that drive expression in the VPCs (*lin-31*), gonad (*ddr-2*), anchor cell (*lin-3* ACEL), and hypodermis (*dpy-7*) were used (Hwang and Sternberg 2004; Myers and Greenwald 2005; Liu et al. 2017). cDNAs for *Cbr-htz-1* and *Cbr-ivp-3* were generated by harvesting RNA from mixed-stage AF16 animals with TRIZOL, synthesizing first strand cDNA using random hexamers and Superscript III RT (Invitrogen), followed by PCR using gene-specific primers into which appropriate restriction enzyme sequences were incorporated to allow for cloning into the plasmid. Candidate plasmids were confirmed by restriction enzyme digestion and sequencing. Plasmids were incorporated into injection mixes (5 ng/μl *myo-2::gfp*, 15 ng/μl *Cel-unc-119(+)*, and 50 ng/μl PCR product(s)), and microinjected into the gonad of *Cbr-unc-119(st20000)* hermaphrodites using standard *C. elegans* methods (Mello et al. 1991). Transgenes were identified and tested for rescue activity using the methods outlined above for the genomic DNA rescue.

To create the *Cbr-lin-3* RNAi plasmid, a 885-bp *Cbr-lin-3* fragment was PCR amplified from genomic DNA using primers GL1242 and GL1243. The fragment was ligated into the *L4440* (pPD129.36; a gift from Dr A. Fire) vector using restriction enzyme sites *Sal*I and *Sph*I. *Escherichia coli* HT115 cells were transformed, and the plasmid was confirmed by restriction digestion. RNAi in *C. briggsae* animals was performed as described earlier (Seetharaman et al. 2010). *mfIs42* and *mfEx32* transgenes containing *Cel-sid-2* (necessary to introduce RNAi by feeding) (Nuez and Félix 2012) were introduced into mutant backgrounds through genetic crosses.

Microscopy and Phenotypic Scoring

Vulval development and VPC proliferation were assessed using two methods. Adult animals were evaluated for whether they exhibit two or more protrusions or growths on their ventral surfaces. To score adults, L4 worms were transferred on to a fresh plate and allowed to grow overnight at 20 °C. The next day, they were scored under a dissecting stereomicroscope for morphology and the presence of any ventral protrusions. Animals with two or more protrusions (or one protrusion in addition to the normal vulval opening) were scored as Muv.

Vulval induction was scored in early to mid-L4 animals under Nomarski optics. Animals were mounted on agar pads, with 1 mM Sodium Azide used to immobilize them. The overall morphology of the vulval cell pattern and the number of Pn.p cell progeny were counted, allowing an inference of whether each precursor cell divided multiple rounds to produce vulval cell types, or only once, as previously described (Sternberg and Horvitz 1986). In wild-type *C. elegans* and *C. briggsae* animals, normally three cells

(P5.p, P6.p, and P7.p) divide to produce vulval progeny, termed "induced." Muv mutants exhibit induction of greater than three cells.

Supplementary Material

Supplementary data are available at *Molecular Biology and Evolution* online.

Acknowledgments

We thank Ryan Johnson, Jennifer Patritti-Cram, Ayush Ranawade, Bavithra Thillainathan, Nagagireesh Bojanala, and members of the Sternberg lab (Caltech), in particular Shahla Gharib and Keith Brown, for technical assistance in the early phases of this project. We are grateful to Don Moerman and Mark Edgley for *ivph-3(gk3691)*, and Stephane Flibotte for assistance with genome sequence analysis to identify *Cbr-ivp* candidate genes. Wen Tang provided comments on a previous draft of the manuscript. Some strains were supplied by the *Caenorhabditis* Genetics Center, which is funded by the NIH Office of Research Infrastructure programs (P40 OD010440). Some plasmids were provided by Addgene.org. Some work was done with the OSU CCC Genomics Shared Resource, which is funded by the National Cancer Institute (P30 CA016058). We thank Wormbase.org for data and images. M.C.-S. was supported by the CMBP predoctoral training grant from the National Institutes of Health (T32-GM086252) and the Pelotonia Cancer Research Graduate Fellowship. This work was supported by the National Science Foundation (DMS-1361251) and NSERC Discovery (RGPIN-2014-05153) grants. RNAseq data are submitted to GEO (GSE133769).

References

Arribere JA, Bell RT, Fu BXH, Artiles KL, Hartman PS, Fire AZ. 2014. Efficient marker-free recovery of custom genetic modifications with CRISPR/Cas9 in *Caenorhabditis elegans*. *Genetics* 198(3):837–846.

Baird DM. 2018. Telomeres and genomic evolution. *Philos Trans R Soc B* 373(1741):20160437.

Bi Y, Ren X, Yan C, Shao J, Xie D, Zhao Z. 2015. A genome-wide hybrid incompatibility landscape between *Caenorhabditis briggsae* and *C. nigoni*. *PLoS Genet.* 11(2):e1004993.

Bracken AP, Brien GL, Verrijzer CP. 2019. Dangerous liaisons: interplay between SWI/SNF, NuRD, and Polycomb in chromatin regulation and cancer. *Genes Dev.* 33(15–16):936–959.

Brenner S. 1974. The genetics of *Caenorhabditis elegans*. *Genetics* 77(1):71–94.

Bullard JH, Purdom E, Hansen KD, Dudoit S. 2010. Evaluation of statistical methods for normalization and differential expression in mRNA-Seq experiments. *BMC Bioinformatics* 11(1):94.

Burkhart DL, Sage J. 2008. Cellular mechanisms of tumour suppression by the retinoblastoma gene. *Nat Rev Cancer* 8(9):671–682.

Calvo-Martín JM, Librado P, Aguadé M, Papaceit M, Segarra C. 2016. Adaptive selection and coevolution at the proteins of the Polycomb repressive complexes in *Drosophila*. *Heredity* 116(2):213–223.

Carbon S, Ireland A, Mungall CJ, Shu S, Marshall B, Lewis S, AmiGO H, Web Presence Working Group. 2009. AmiGO: online access to ontology and annotation data. *Bioinformatics* 25(2):288–289.

Castillo-Davis CI, Kondrashov FA, Hartl DL, Kulathinal RJ. 2004. The functional genomic distribution of protein divergence in two animal phyla: coevolution, genomic conflict, and constraint. *Genome Res.* 14(5):802–811.

Chesney MA, Kidd AR, Kimble J. 2006. gon-14 functions with class B and class C synthetic multivulva genes to control larval growth in *Caenorhabditis elegans*. *Genetics* 172(2):915–928.

Crespi B, Nosil P. 2013. Conflictual speciation: species formation via genomic conflict. *Trends Ecol Evol.* 28(1):48–57.

Cui M, Chen J, Myers TR, Hwang BJ, Sternberg PW, Greenwald I, Han M. 2006. SynMuv genes redundantly inhibit lin-3/EGF expression to prevent inappropriate vulval induction in *C. elegans*. *Dev Cell* 10(5):667–672.

Cutter AD. 2008. Divergence times in *Caenorhabditis* and *Drosophila* inferred from direct estimates of the neutral mutation rate. *Mol Biol Evol.* 25(4):778–786.

Cutter AD, Garrett RH, Mark S, Wang W, Sun L. 2019. Molecular evolution across developmental time reveals rapid divergence in early embryogenesis. *Evol Lett.* 3(4):359–373.

Davison EM, Saffer AM, Huang LS, DeModena J, Sternberg PW, Horvitz HR. 2011. The LIN-15A and LIN-56 transcriptional regulators interact to negatively regulate EGF/Ras signaling in *Caenorhabditis elegans* vulval cell-fate determination. *Genetics* 187(3):803–815.

Dickinson DJ, Pani AM, Heppert JK, Higgins CD, Goldstein B. 2015. Streamlined genome engineering with a self-excising drug selection cassette. *Genetics* 200(4):1035–1049.

Dobin A, Davis CA, Schlesinger F, Drenkow J, Zaleski C, Jha S, Batut P, Chaisson M, Gingeras TR. 2013. STAR: ultrafast universal RNA-seq aligner. *Bioinformatics* 29(1):15–21.

Fay DS, Han M. 2000. The synthetic multivulval genes of *C. elegans*: functional redundancy, Ras-antagonism, and cell fate determination. *Genesis* 26(4):279–284.

Fay DS, Yochem J. 2007. The SynMuv genes of *Caenorhabditis elegans* in vulval development and beyond. *Dev Biol.* 306(1):1–9.

Félix M-A. 2007. Cryptic quantitative evolution of the vulva intercellular signaling network in *Caenorhabditis*. *Curr Biol.* 17(2):103–114.

Ferguson EL, Horvitz HR. 1989. The multivulva phenotype of certain *Caenorhabditis elegans* mutants results from defects in two functionally redundant pathways. *Genetics* 123(1):109–121.

Hemmer LW, Blumenstiel JP. 2016. Holding it together: rapid evolution and positive selection in the synaptonemal complex of *Drosophila*. *BMC Evol Biol.* 16:91.

Hwang BJ, Sternberg PW. 2004. A cell-specific enhancer that specifies lin-3 expression in the *C. elegans* anchor cell for vulval development. *Development* 131:143–151.

Johnson NA. 2010. Hybrid incompatibility genes: remnants of a genomic battlefield? *Trends Genet.* 26(7):317–325.

Lakowski B, Eimer S, Göbel C, Böttcher A, Wagler B, Baumeister R. 2003. Two suppressors of sel-12 encode C2H2 zinc-finger proteins that regulate presenilin transcription in *Caenorhabditis elegans*. *Development* 130:2117–2128.

Latorre I, Chesney MA, Garrigues JM, Stempor P, Appert A, Francesconi M, Strome S, Ahringer J. 2015. The DREAM complex promotes gene body H2A.Z for target repression. *Genes Dev.* 29(5):495–500.

Lee RYN, Howe KL, Harris TW, Arnaboldi V, Cain S, Chan J, Chen WJ, Davis P, Gao S, Grove C, et al. 2018. WormBase 2017: molting into a new stage. *Nucleic Acids Res.* 46(D1):D869–D874.

Li H, Durbin R. 2009. Fast and accurate short read alignment with Burrows–Wheeler transform. *Bioinformatics* 25(14):1754–1760.

Li H, Handsaker B, Wysoker A, Fennell T, Ruan J, Homer N, Marth G, Abecasis G, Durbin R, 1000 Genome Project Data Processing Subgroup. 2009. The Sequence Alignment/Map format and SAMtools. *Bioinformatics* 25(16):2078–2079.

Liu H, Dowdle JA, Khurshid S, Sullivan NJ, Bertos N, Rambani K, Mair M, Daniel P, Wheeler E, Tang X, et al. 2017. Discovery of stromal regulatory networks that suppress ras-sensitized epithelial cell proliferation. *Dev. Cell* 41(4):392–407.e6.

Love MI, Huber W, Anders S. 2014. Moderated estimation of fold change and dispersion for RNA-seq data with DESeq2. *Genome Biol.* 15(12):550.

Mahalak KK, Jama AM, Billups SJ, Dawes AT, Chamberlin HM. 2017. Differing roles for sur-2/MED23 in *C. elegans* and *C. briggsae* vulval development. *Dev Genes Evol.* 227(3):213–218.

Martin M. 2011. Cutadapt removes adapter sequences from high-throughput sequencing reads. *EMBnet J.* 17(1):10–12.
Mello CC, Kramer JM, Stinchcomb D, Ambros V. 1991. Efficient gene transfer in *C. elegans*: extrachromosomal maintenance and integration of transforming sequences. *EMBO J.* 10(12):3959–3970.
Myers TR, Greenwald I. 2005. lin-35 Rb acts in the major hypodermis to oppose Ras-mediated vulval induction in *C. elegans*. *Dev Cell* 8(1):117–123.
Nuez I, Félix M-A. 2012. Evolution of susceptibility to ingested double-stranded RNAs in *Caenorhabditis* nematodes. *PLoS One* 7(1):e29811.
Petrella LN, Wang W, Spike CA, Rechtsteiner A, Reinke V, Strome S. 2011. synMuv B proteins antagonize germline fate in the intestine and ensure *C. elegans* survival. *Development* 138:1069–1079.
Ponte I, Romero D, Yero D, Suau P, Roque A. 2017. Complex evolutionary history of the mammalian histone H1.1–H1.5 gene family. *Mol Biol Evol.* 34(3):545–558.
Rechtsteiner A, Costello ME, Egelhofer TA, Garrigues JM, Strome S, Petrella LN. 2019. Repression of germline genes in *Caenorhabditis elegans* somatic tissues by H3K9 dimethylation of their promoters. *Genetics* 212(1):125–140.
Reddy PC, Ubhe S, Sirwani N, Lohokare R, Galande S. 2017. Rapid divergence of histones in Hydrozoa (Cnidaria) and evolution of a novel histone involved in DNA damage response in hydra. *Zoology (Jena)* 123:53–63.
Reinke V, Smith HE, Nance J, Wang J, Van Doren C, Begley R, Jones SJ, Davis EB, Scherer S, Ward S, et al. 2000. A global profile of germline gene expression in *C. elegans*. *Mol Cell* 6(3):605–616.
Ren X, Li R, Wei X, Bi Y, Ho VWS, Ding Q, Xu Z, Zhang Z, Hsieh C-L, Young A, et al. 2018. Genomic basis of recombination suppression in the hybrid between *Caenorhabditis briggsae* and *C. nigoni*. *Nucleic Acids Res.* 46(3):1295–1307.
Ruan J, Li H, Chen Z, Coghlan A, Coin LJM, Guo Y, Hériché J-K, Hu Y, Kristiansen K, Li R, et al. 2008. TreeFam: 2008 update. *Nucleic Acids Res.* 36(Database):D735–D740.
Sadasivam S, DeCaprio JA. 2013. The DREAM complex: master coordinator of cell cycle-dependent gene expression. *Nat Rev Cancer* 13(8):585–595.
Seetharaman A, Cumbo P, Bojanala N, Gupta BP. 2010. Conserved mechanism of Wnt signaling function in the specification of vulval precursor fates in *C. elegans* and *C. briggsae*. *Dev Biol.* 346(1):128–139.
Sharanya D, Fillis CJ, Kim J, Zitnik EM, Ward KA, Gallagher ME, Chamberlin HM, Gupta BP. 2015. Mutations in *Caenorhabditis briggsae* identify new genes important for limiting the response to EGF signaling during vulval development. *Evol Dev.* 17(1):34–48.
Sigrist CB, Sommer RJ. 1999. Vulva formation in *Pristionchus pacificus* relies on continuous gonadal induction. *Dev Genes Evol.* 209(8):451–459.
Sommer RJ. 2012. Evolution of regulatory networks: nematode vulva induction as an example of developmental systems drift. *Adv Exp Med Biol.* 751:79–91.
Sommer RJ, Sternberg PW. 1994. Changes of induction and competence during the evolution of vulva development in nematodes. *Science* 265(5168):114–118.
Sommer RJ, Sternberg PW. 1995. Evolution of cell lineage and pattern formation in the vulval equivalence group of rhabditid nematodes. *Dev Biol.* 167(1):61–74.
Sternberg PW. 2005. Vulval development. In: The C. elegans Research Community. WormBook.
Sternberg PW, Horvitz HR. 1986. Pattern formation during vulval development in *C. elegans*. *Cell* 44(5):761–772.
Stiernagle T. 2006. Maintenance of *C. elegans*. In: The C. elegans Research Community. WormBook.
Sulston JE, Horvitz HR. 1977. Post-embryonic cell lineages of the nematode, *Caenorhabditis elegans*. *Dev Biol.* 56(1):110–156.
Tian H, Schlager B, Xiao H, Sommer RJ. 2008. Wnt signaling induces vulva development in the nematode *Pristionchus pacificus*. *Curr Biol.* 18(2):142–146.
True JR, Haag ES. 2001. Developmental system drift and flexibility in evolutionary trajectories. *Evol Dev.* 3(2):109–119.
van den Heuvel S, Dyson NJ. 2008. Conserved functions of the pRB and E2F families. *Nat Rev Mol Cell Biol.* 9(9):713–724.
Vargas-Velazquez AM, Besnard F, Félix M-A. 2019. Necessity and contingency in developmental genetic screens: EGF, Wnt, and semaphorin pathways in vulval induction of the nematode *Oscheius tipulae*. *Genetics* 211(4):1315–1330.
Wang D, Liu F, Wang L, Huang S, Yu J. 2011. Nonsynonymous substitution rate (Ka) is a relatively consistent parameter for defining fast-evolving and slow-evolving protein-coding genes. *Biol Direct* 6(1):13.
Wang X, Zhao Y, Wong K, Ehlers P, Kohara Y, Jones SJ, Mara MA, Holt RA, Moerman DG, Hansen D. 2009. Identification of genes expressed in the hermaphrodite germ line of *C. elegans* using SAGE. *BMC Genomics*. 10(1):213.
Whittle CM, McClinic KN, Ercan S, Zhang X, Green RD, Kelly WG, Lieb JD. 2008. The genomic distribution and function of histone variant HTZ-1 during *C. elegans* embryogenesis. *PLoS Genet.* 4(9):e1000187.
Yang Z. 2007. PAML 4: phylogenetic analysis by maximum likelihood. *Mol Biol Evol.* 24(8):1586–1591.

SUPPLEMENTAL FIGURE 1. Expression of *Cbr-htz-1* and *Cbr-ivp-3* in non-VPCs rescues the mutant phenotype. Expression of cDNA for *Cbr-htz-1* (**A.**) or *Cbr-ivp-3* (**B.**) under control of a non-VPC hypodermis-specific promoter (*dpy-7*) rescues the Muv phenotype associated with mutants. Four different heterologous promoters were utilized for expression of *Cbr-htz-1* cDNA: *lin-31* (pB253), *ddr-2*, ACEL (Anchor Cell enhancer upstream of the Δ*pes-10* minimal promoter), *dpy-7* (Myers and Greenwald 2005; Liu et al. 2017). All of these promoters, except *lin-31* (pB253), were also used for expression of *Cbr-ivp-3* cDNA. For each transgene, the promoter driving expression of the cDNA corresponding to each gene is indicated in the parenthesis after the extrachromosomal designation, *guEx*. n>=40 for all genotypes. Full genotypes are in Supplemental Table 1. Full data and exact sample sizes are listed in Supplemental Table 8.

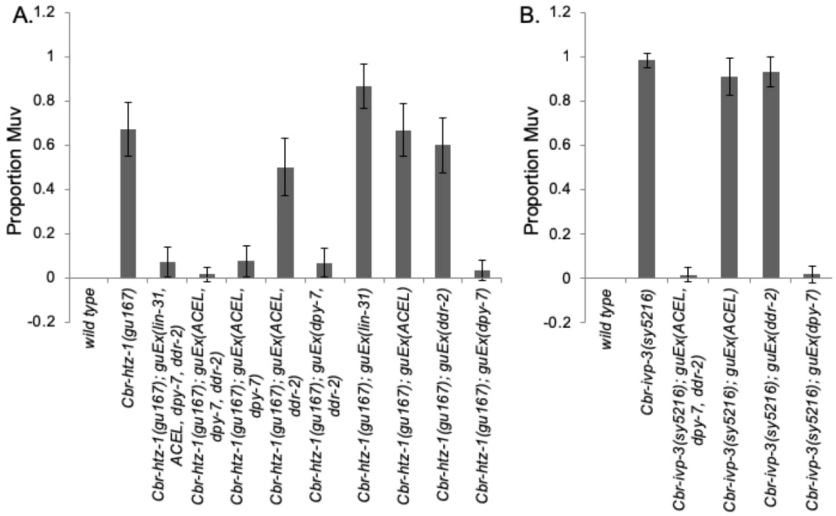

Chapter 4

Genetic analysis of *Cbr-lin(bh1)* and *Cbr-lin(bh3)* mutants

This research focuses on using *C. briggsae* as an experimental model system to identify novel genes that influence cell signaling and cell division during vulva development. *Cbr-lin(bh1)* and *Cbr-lin(bh3)*, exhibiting a heritable Muv phenotype and were obtained in a screening procedure, when AF16 animals were mutagenized by treating them with Ethyl Methane Sulfonate (EMS). Molecular and functional characterization of *Cbr-lin(bh1)* and *Cbr-lin(bh3)* alleles were carried out to understand their role in vulva development. Identification of novel genes and further characterization will help us understand the molecular function of genes and their involvement in the regulation of vulval cell differentiation. The findings in this thesis will provide a background for future studies to understand the role of novel genes in reproductive system development.

4.1 Genetic mapping

C. briggsae isolates have natural variability and carry a large number of single nucleotide polymorphisms (SNPs) and insertion-deletions (indels) which can be exploited to carry out genetic mapping (Koboldt et al., 2010). The linkage of *Cbr-lin(bh1)* and *Cbr-lin(bh3)* were tested with several polymorphic markers that were assigned to different chromosomes. These indels have been verified previously through genome sequencing and were classified as small (7 - 49 bp), medium (50 - 2000 bp), and large (>2 kb) indels (Koboldt et al., 2010). The polymorphisms scheme to map the *Cbr-lin(bh1)* and *Cbr-lin(bh3)* allele at the precise location on the chromosome, involved small and medium indels (Koboldt et al., 2010).

Out of all the many possible combinations, recombinants that are phenotypically mutant were selected to determine linkage of the mutation site to different

polymorphic loci in order to map the chromosomal location of the mutation. Unlinked markers (polymorphic loci) will be comprised of equal number of the wild-type AF16 and polymorphic HK104 amplicons. A higher ratio of AF16 amplicon to a particular marker indicates that the mutation has linkage to the marker. Since both *Cbr-lin(bh1)* and *Cbr-lin(bh3)* mutant alleles are in AF16 background, a higher number of AF16 amplicons compared to HK104, indicate that the mutations are close to polymorphic site. The frequency of recombination will be reduced in the region between indel and mutation if they are located closer to each other.

4.1.1 Genetic mapping of *Cbr-lin(bh1)* mutants

Indel cb-m142, a polymorphic marker on chromosome I (Koboldt et al., 2010), used to map the location of *Cbr-lin(bh1)* allele, showed possible linkage on chromosome I. After several rounds of mapping, the linkage seems to be consistent with chromosome I. Thus, additional mapping experiments were carried out to further narrowed down the location of *Cbr-lin(bh1)* allele on chromosome I.

Indel mapping of *Cbr-lin(bh1)* mutants

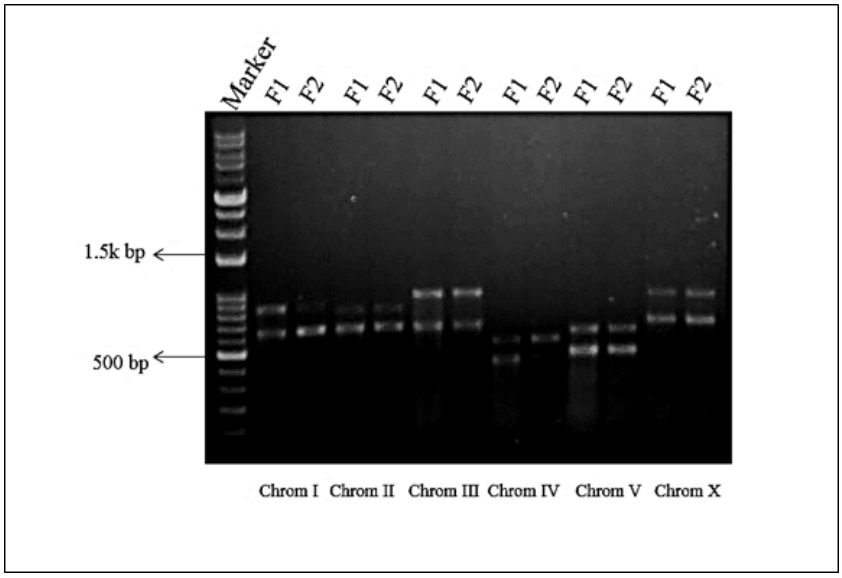

Figure 4.1 Genetic Mapping of *Cbr-lin(bh1)*. Lane 1: Ladder; Each subsequent lane shows chromosomal mapping for F1 progeny and F2 mutant. F1 represents the heterozygous cross-progeny of *Cbr-lin(bh1)* and polymorphic strain HK104, while F2 represents subsequent homozygous mutant progeny (multivulva) of F1. Indel cb-m142, used for mapping, is linked to chromosome I (Koboldt et al., 2010).

The additional polymorphism mapping showed the band sizes and intensities of the indel-based polymorphic markers on chromosome I for *Cbr-lin(bh1)* (Figure 4.2). Indel cb-m6 mapped on the right arm of chromosome I (Koboldt et al., 2010). The AF16 bands for cb-m6 indel appeared to be more intense than the band of polymorphic strain HK104. Therefore, this suggests that the mutation is located on the right arm of chromosome I. Further gene mapping must be completed to determine the precise location of the *Cbr-lin(bh1)* mutation on chromosome I.

Indel mapping of *Cbr-lin(bh1)* mutants on chromosome I

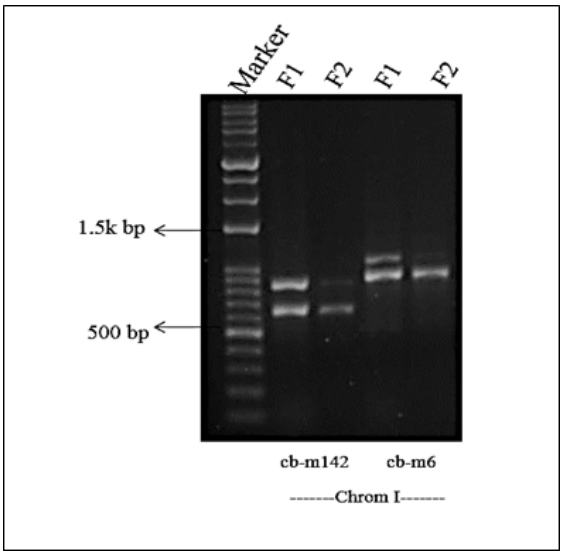

Figure 4.2 Indel cb-m6 mapped on the right arm of chromosome I. (Koboldt et al., 2010). Lane 1: Ladder; Each subsequent lane shows chromosomal mapping for (in the order) F1 progenies and F2 mutant. F1 represents the heterozygous cross-progeny of *Cbr-lin(bh1)* and polymorphic strain HK104, while F2 represents subsequent homozygous mutant progeny (multivulva) of F1.

4.1.2 Genetic mapping of *Cbr-lin(bh3)* mutants

Indel cb-m205, a polymorphic marker on chromosome III (Koboldt et al., 2010), used to map the location of *Cbr-lin(bh3)*, showed the linkage on chromosome III. After several rounds of mapping, the possible linkage seems to be consistent with chromosome III. The polymorphism mapping showed more intensity of indel-based polymorphic markers for AF16 based *Cbr-lin(bh3)* on chromosome III (Figure 4.3).

In terms of *Cbr-lin(bh3)*, linkage of the mutation to a specific region of the chromosome will be further determined using the additional indel-based polymorphisms mapping of chromosome III.

Indel mapping of *Cbr-lin(bh3)* mutants

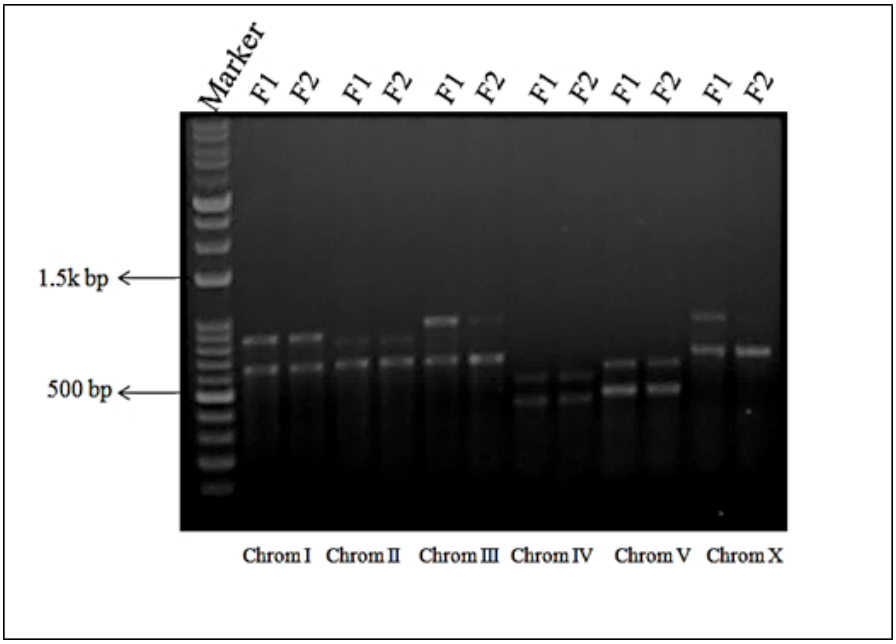

Figure 4.3 Genetic Mapping of *Cbr-lin(bh3)*. Lane 1: Ladder; Each subsequent lane shows chromosomal mapping for F1 progeny and F2 mutant. F1 represents the heterozygous cross-progeny of *Cbr-lin(bh3)* and polymorphic strain HK104, while F2 represents subsequent homozygous mutant progeny (multivulva) of F1. Indel cb-m205, used for mapping, is on the right arm of chromosome III (Koboldt et al., 2010).

4.2 Muv penetrance analysis in *Cbr-lin(bh)* mutants

The penetrance assay was carried out to determine the frequency of the mutant phenotype in the population. *Cbr-lin(bh1)* and *Cbr-lin(bh3)* alleles, exhibit a heritable Multivulva phenotype.

4.2.1 Muv penetrance analysis in *Cbr-lin(bh1)* animals

Multivulva Penetrance was carried out at 20°C for *Cbr-lin(bh1)* animals. Approximately 100 animals were scored in each batch. The penetrance of Multivulva phenotype for *Cbr-lin(bh1)* animals was found to be 30.42%. The animals showing protruding vulva (Pvl) phenotype have morphological defect but were considered at wild-type while determining the penetrance percentage.

Table 4.1 Penetrance of multivulva phenotype in *Cbr-lin(bh1)* mutants

Penetrance			
Phenotype	Plate 1	Plate 2	Plate 3
Multivulva (Muv)	33	30	27
Wild-type (WT)	63	64	58
Total	103	105	91
Muv %	32%	28.5%	30.76%
Protruding Vulva	7	11	6

4.2.2 Muv penetrance analysis in *Cbr-lin(bh3)* animals

Multivulva Penetrance was carried out at 20°C for *Cbr-lin(bh3)* animals. Approximately 100 animals were scored in each batch. The Muv penetrance was calculated by counting the number of animals that were displaying more than one protrusion. The penetrance of Multivulva phenotype for *Cbr-lin(bh3)* animals was found to be 43.85%.

Table 4.2 Penetrance of multivulva phenotype in *Cbr-lin(bh3)* mutants

Penetrance			
Phenotype	Batch 1	Batch 2	Batch 3
Multivulva (Muv)	45	38	49
Wild-type (WT)	37	40	35
Total	103	91	107
Muv %	42.7%	41.8%	45%
Protruding Vulva	21	13	23

Consolidate data summarizing the multivulva penetrance in both *Cbr-lin(bh1)* and *Cbr-lin(bh3)*.

Table 4.3 Consolidate data on multivulva penetrance in *Cbr-lin(bh)* mutants

Cbr-lin(bh1)			
Total	Multivulva (Muv)	Muv %	STD
299	90	30.42%	0.01448
Cbr-lin(bh3)			
Total	Multivulva (Muv)	Muv %	STD
301	132	43.85%	0.01347

4.3 Temperature-Sensitivity assay for Muv penetrance

Temperature is a critical factor in vulval development as it affects the gene expression that can alter the phenotype in *C. briggsae*. *C. briggsae* can be maintained between 16°C and 25°C (Stiernagle, 2006). It has been shown that temperature can affect the reproductive system development in certain *C. briggsae* strains (Sharanya et al., 2012). Certain mutant strains when grown at different temperatures displayed an increment or decline in abnormalities during vulva development. Such phenotypes are known as temperature-sensitive phenotypes.

As described above, the Muv penetrance at 20°C was found to be approximately 30% and 43% respectively for *Cbr-lin(bh1)* and *Cbr-lin(bh3)* mutants. *Cbr-lin(bh1)* and *Cbr-lin(bh3)* mutants were futher analyzed for Muv phenotype at 15°C and 25°C. If the alleles are temperature-sensitive, the Muv penetrance would be different at 15°C and/or 25°C. The strains were maintained at different temperatures and all the experiments were performed in three batches. L3/L4 animals were picked and transferred onto a fresh plate and allowed to grow. The phenotype was scored in adult worms.

4.3.1 Temperature-Sensitivity analysis in *Cbr-lin(bh1)* mutants at 15°C and 25°C

The penetrance of multivulva phenotype was carried out for *Cbr-lin(bh1)* animals at 15°C and 25°C. Approximately 300 animals were scored in each batch. The animals showing protruding vulva (Pvl) phenotype have morphological defect but were considered at wild-type while determining the penetrance percentage. The penetrance of multivulva phenotype for *Cbr-lin(bh1)* animals at 15°C was found to be 17.39%, while penetrance of multivulva phenotype for *Cbr-lin(bh1)* animals at 25°C was found to be 43.19% (Figure 4.4).

Table 4.4 Penetrance of multivulva phenotype in *Cbr-lin(bh1)* animals at 15°C

Penetrance			
Phenotype	Plate 1	Plate 2	Plate 3
Multivulva (Muv)	20	19	20
Wild-type (WT)	73	79	85
Total	108	110	122
Muv %	18.51%	17.27%	16.39%
Protruding Vulva	15	12	17

Table 4.5 Penetrance of multivulva phenotype in *Cbr-lin(bh1)* animals at 25°C

Penetrance			
Phenotype	Plate 1	Plate 2	Plate 3
Multivulva (Muv)	43	42	45
Wild-type (WT)	49	49	50
Total	102	98	101
Muv %	42.15%	42.85%	44.56%
Protruding Vulva	10	7	6

Table 4.6 Consolidate data on the effect of temperature in *Cbr-lin(bh1)* animals

***Cbr-lin(bh1)* at 15°C**			
Total	Multivulva (Muv)	Muv %	STD
340	59	17.39%	0.008696359
***Cbr-lin(bh1)* at 25°C**			
Total	Multivulva (Muv)	Muv %	STD
301	130	43.19%	0.010122692

Temperature-Sensitivity analysis in *Cbr-lin(bh1)* mutants

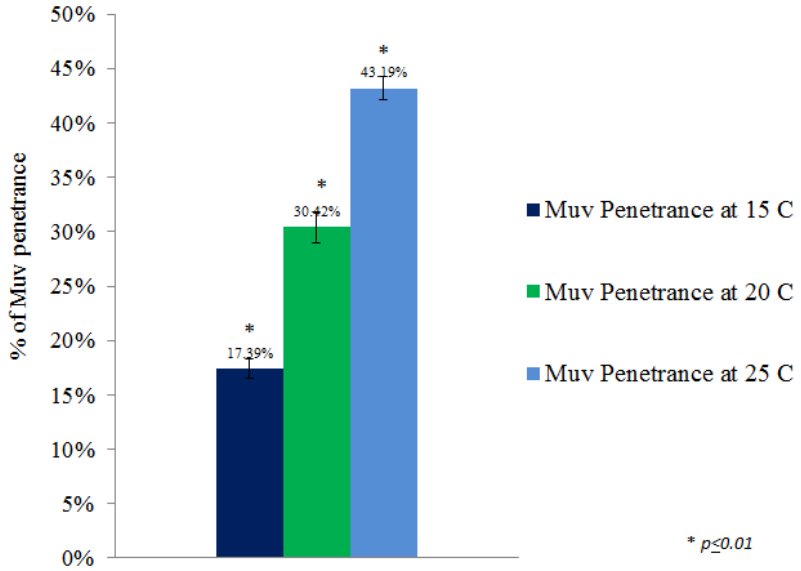

Figure 4.4 Muv penetrance at 15°C and 25°C in comparison to 20°C for *Cbr-lin(bh1)* animals.

4.3.2 Temperature-Sensitivity analysis in *Cbr-lin(bh3)* mutants at 15°C and 25°C

The penetrance of multivulva phenotype was carried out for *Cbr-lin(bh3)* animals at 15°C and 25°C. The animals showing protruding vulva (Pvl) phenotype have morphological defect but were considered at wild-type while determining the

penetrance percentage. The penetrance of Multivulva phenotype for *Cbr-lin(bh3)* animals was found to be approximately 40% at all three temperatures (Figure 4.5)

Table 4.7 Penetrance of multivulva phenotype in *Cbr-lin(bh3)* animals at 15°C

Penetrance			
Phenotype	Plate 1	Plate 2	Plate 3
Multivulva (Muv)	47	42	42
Wild-type (WT)	58	50	49
Total	114	99	96
Muv %	41.23%	42.42%	43.75%
Protruding Vulva	9	7	5

Table 4.8 Penetrance of multivulva phenotype in *Cbr-lin(bh3)* animals at 25°C

Penetrance			
Phenotype	Plate 1	Plate 2	Plate 3
Multivulva (Muv)	44	39	48
Wild-type (WT)	50	53	47
Total	101	92	106
Muv %	43.56%	42.39%	45.28%
Protruding Vulva	7	8	11

Table 4.9 Consolidate data on the effect of temperature in *Cbr-lin(bh3)* animals

***Cbr-lin(bh3)* at 15°C**			
Total	Multivulva (Muv)	Muv %	STD
309	131	42.47%	0.01029
***Cbr-lin(bh3)* at 25°C**			
Total	Multivulva (Muv)	Muv %	STD
299	131	43.75%	0.01186

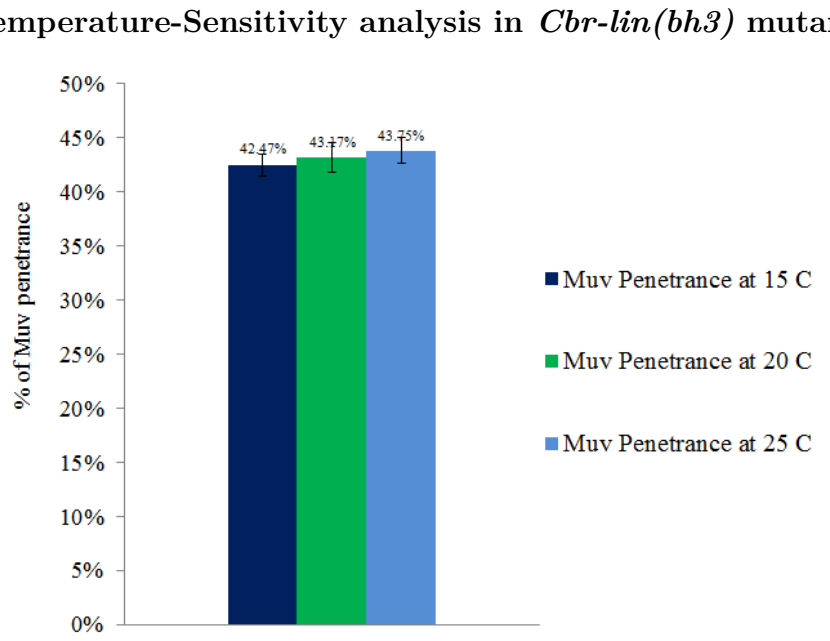

Figure 4.5 Muv penetrance at 15°C and 25°C in comparison to 20°C for Cbr-lin(bh3) animals.

4.4 Complementation assay for *Cbr-lin(bh1)* and *Cbr-spr-4(gu163)* mutants

Complementation assay indicates if the mutation is an allele of an existing gene. Mutant phenotype in the progenies suggests that the two alleles are the mutations in the same gene and thus fail to complement each other. Wild-type phenotype will be restored if the two alleles complement each other, indicating the mutant alleles are at different loci. As a result, the recessive mutations are alleles of different genes.

Cbr-spr-4(gu163) is found to be located on chromosome I (Sharanya et al., 2015). Mapping results suggested that the possible locus of *Cbr-lin(bh1)* is also on chromosome I. Thus, *Cbr-lin(bh1)* mutants were crossed with *Cbr-spr-4(gu163); mfIs5[Cbr-egl-17::GFP; myo-2::GFP]* animals (Figure 4.6). Heterozygous fluorescing F1 progenies were scored to determine whether the two genes complemented one another to restore the wild-type vulval phenotype.

Cross scheme

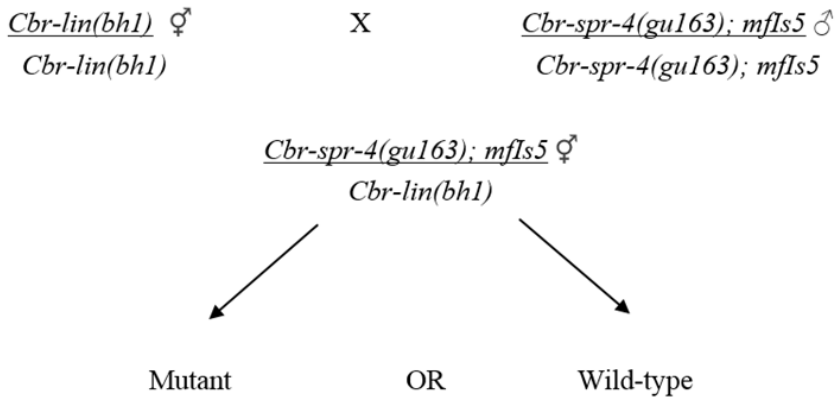

Figure 4.6 Cross scheme for complementation

The resultant F1 cross progeny did not display GFP fluorescing worms with Multivulva phenotype, which indicated that the two alleles complemented to restore the wild-type vulval phenotype. Thus, it is evident that both *Cbr-lin(bh1)* and *Cbr-spr-4(gu163)* genes are the located in different genomic region.

Table 4.10 Analysis of F1 cross-progenies for complementation

Phenotype	Batch 1 Number of Worms	Batch 2 Number of Worms
Wild-type (WT) GFP	45	72
Wild-type (WT)	37	48
Multivulva (Muv)	17	21
Multivulva (Muv) - GFP*	0	0
Total	99	141

F1 cross-progenies were observed for their vulval phenotype. Worms with multivulva phenotype and *myo-2::GFP* expression (Muv - GFP*) suggest that the two genes fail to complement each other. Thus, *Cbr-lin(bh1)* can be further characterized to determine novel gene responsible for the Muv phenotype.

4.5 Vulval induction in *Cbr-lin(bh1)* and *Cbr-lin(bh3)* mutants

In wild-type *C. briggsae* animals P3.p, P4.p and P8.p divide only one time and fuse with hypodermis. Thus, the VPC induction score is 3.0 ± 0.0. In most multivulva animals these 3 VPCs undergoes more than one round of division and thus give rise to Multivulva phenotype. Both *Cbr-lin(bh1)* and *Cbr-lin(bh3)* alleles, exhibit multivulva phenotype. The induction score in these animals was found to be higher than 3.0. *Cbr-lin(bh)* mutants were observed under Normarski microscope to analyze induction in VPCs.

Table 4.11 Analysis of the VPC induction pattern in *Cbr-lin(bh)* mutants

	% Induction Score								
Genotype	P3.p	P4.p	P5.p	P6.p	P7.p	P8.p	Ave Ind	N	Muv%
Cbr-lin(bh1)	0.0 (52)	21.15 (11)	100.0 (52)	100.0 (52)	100.0 (52)	26.92 (14)	3.5	52	32.69
Cbr-lin(bh3)	6.38 (3)	25.53 (12)	100.0 (47)	100.0 (47)	100.0 (47)	34.04 (16)	4.0	47	42.55

Mid-L4 stage worms were analyzed for VPCs induction (Invagination). It was observed that in *Cbr-lin(bh1)* mutants, P4.p, P5.p, P6.p, P7.p, and P8.p were induced while P3.p remained uninduced. Gonad seems normal. While, in *Cbr-lin(bh3)* mutants, P4.p, P5.p, P6.p, P7.p, and P8.p were induced while in some animals P3.p were found to be induced additionally. Very few *Cbr-lin(bh3)* mutants show abnormal gonad morphology.

However, the sample size for the experiment was small and the analysis was carried out in a single batch. Thus, the experiments should be repeated in order to establish the credibility of the data.

4.6 Cell fate analysis in *Cbr-lin(bh)* mutants

The expression of *egl-17::GFP* was used to investigate the divergence in the signaling and regulatory pathways during vulval development. *zmp-1*, an ortholog between *C. elegans* and *C. briggsae* that encodes a zinc metalloproteinase (Kirouac and Sternberg, 2003) was used as a primary cell fate marker to analyze vulval cell fate in Muv mutants.

In the early stages of vulval development (early to mid L3), *egl-17::GFP* expression can be seen in P6.p and its progenies. Subsequently, *egl-17::GFP* expression was observed in P5.p and P7.p progenies, vulC and vulD cells during late vulval development at mid-L4 stage (Burdine et al., 1998). The early expression of *egl-17::GFP* indicates a 1° cell fate, while a late expression signifies a 2° cell fate (Sharanya et al., 2015).

zmp-1::GFP is expressed in vulD and vulE vulva cells in late L4, and in vulA cells in adult worms (Inoue et al., 2002). As a 1° cell fate marker, *zmp-1::GFP* can be used for cell fate analysis in mutant vulval phenotypes. It has been observed in animals displaying Muv mutants that in addition to P6.p adopting a 1° cell fate, other precursor cells are also capable of developing 1° cell fates (Sharanya et al., 2015).

Thus, *egl-17::GFP* and *zmp-1::GFP* were used as markers to determine VPC fates in Muv animals.

4.6.1 Cell fate anlysis in *Cbr-lin(bh1)* mutants

Cell fate analysis was carried out in *Cbr-lin(bh1)* mutants. *zmp-1::GFP* expression was observed in young adult animals, while *egl-17::GFP* expression was observed at mid-L4 stage. Young *Cbr-lin(bh1)* adult worms did not display the ectopic expression of *zmp-1::GFP* in VPCs besides P6.p, thus in these animals only P6.p adopt the 1° cell fate. The worms examined at mid-L4 almost always show *egl-17::GFP* expression, thus adopting the 2° cell fate.

Analysis of 1° cell fate in *Cbr-lin(bh1)* mutants

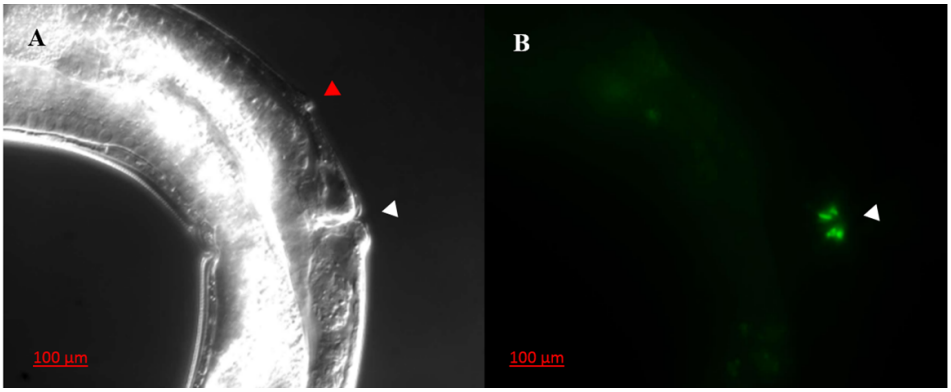

Figure 4.7 *zmp-1::GFP (mfIs8)* marker expressed in vulE and vulF cells in *Cbr-lin(bh1)* Muv animal. The strain *mfIs8[Cbr-zmp-1::GFP+ myo-2::GFP]* was used to generate *Cbr-lin(bh1); mfIs8[Cbr-zmp-1::GFP+ myo-2::GFP]* strain for the analysis of the 1° cell fate in mutants. The white triangle indicates the functional vulva, the red triangle indicates pseudovulva. Head is upward.

Analysis of 2° cell fate in *Cbr-lin(bh1)* mutants

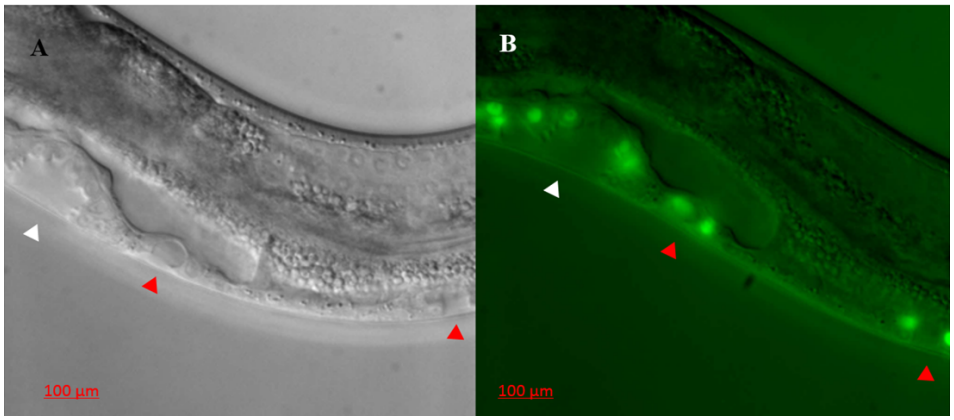

Figure 4.8 *Cbr-lin(bh1)* Muv animal with P8.p invagination. *egl-17::GFP (mfIs5)* marker indicating VPCs that adopted the 2° cell fate. The strain *mfIs5[Cbr-egl-17::GFP+ myo-2::GFP]*, was used to generate *Cbr-lin(bh1); mfIs5[Cbr-egl-17::GFP+ myo-2::GFP]* strains for the analysis of VPCs adopting 2° cell fate in these mutants. The white triangle indicates the functional vulva, the red triangle indicates abnormally induced VPCs. Anterior is on the left.

Cell fate in *Cbr-lin(bh1)* mutants

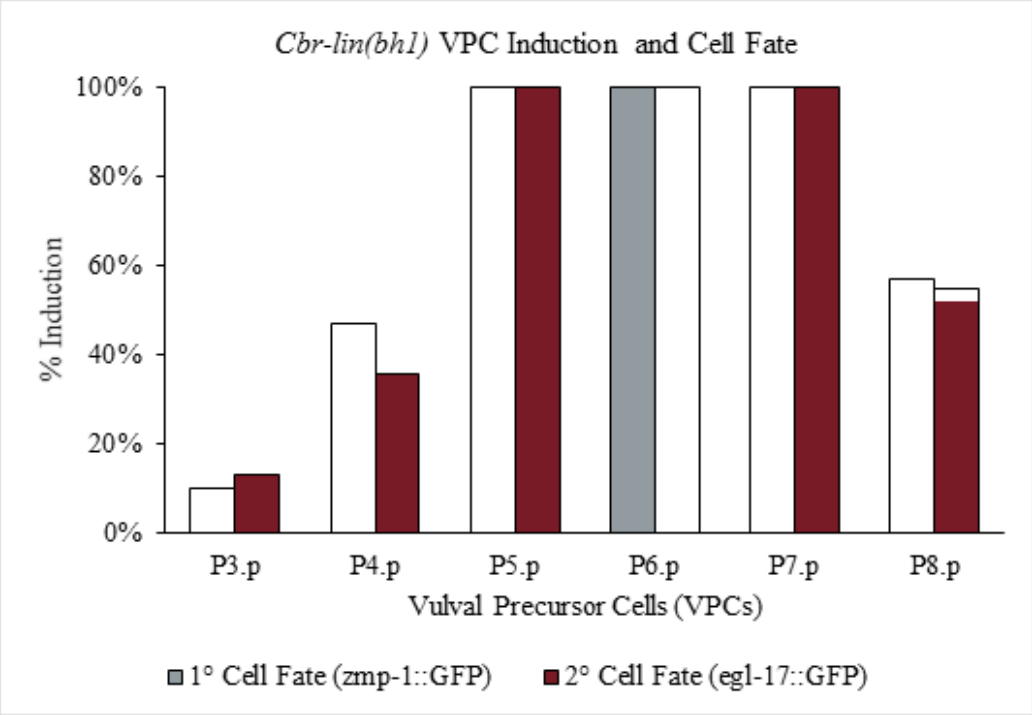

Figure 4.9 Analysis of 1° and 2° cell fate in *Cbr-lin(bh1)* mutants

Table 4.12 Frequency of VPC induction and cell fate fluorescence in *Cbr-lin(bh1)* mutants

Cbr-lin(bh1)							
mfIs8	P3.p	P4.p	P5.p	P6.p	P7.p	P8.p	N
% Induction	8.0 ± 0.11	45 ± 0.04	100 ± 0.0	100.0 ± 0.0	100 ± 0.0	62.0 ± 0.13	91
% GFP	0.0	0.0	0.0	100.0 ± 0.0	0.0	0.0	
mfIs5	P3.p	P4.p	P5.p	P6.p	P7.p	P8.p	N
% Induction	11.0 ± 0.06	42.0 ± 0.20	100.0 ± 0.0	100.0 ± 0.0	100.0 ± 0.0	60.0 ± 0.14	148
% GFP	100.0 ± 0.0	100.0 ± 0.0	100.0 ± 0.0	0.0	100.0 ± 0.0	93.0 ± 0.1	

4.6.2 Cell fate analysis in *Cbr-lin(bh3)* mutants

Cell fate analysis was carried out in *Cbr-lin(bh3)* mutants. *zmp-1::GFP* expression was observed in young adult animals, while *egl-17::GFP* expression was observed at mid-L4 stage. Young *Cbr-lin(bh3)* adult worms occasionally showed the ectopic *zmp-1::GFP* expression in VPCs along with P6.p which indicated the additional VPCs adopting the 1° cell fate in *Cbr-lin(bh3)* mutants. The worms examined at mid-L4 almost always showed *egl-17::GFP* expression, thus adopting the 2° cell fate. Thus, the ectopic expression of both the 1° and 2° cell fates were observed in *Cbr-lin(bh3)* mutants.

Strain *Cbr-lin(bh3); mfIs8[Cbr-zmp-1::GFP+ myo-2::GFP]* was used for the analysis of the 1° cell fate in mutants and strain *Cbr-lin(bh3); mfIs5[Cbr-egl-17::GFP+ myo-2::GFP]* was used for the analysis of VPCs adopting 2° cell fate in these mutants.

It was observed that the Muv mutants exhibit both 1° and 2° cell fates in ectopic VPCs other than P5.p, P6.p and P7.p.

Analysis of 1° cell fate in *Cbr-lin(bh3)* mutants

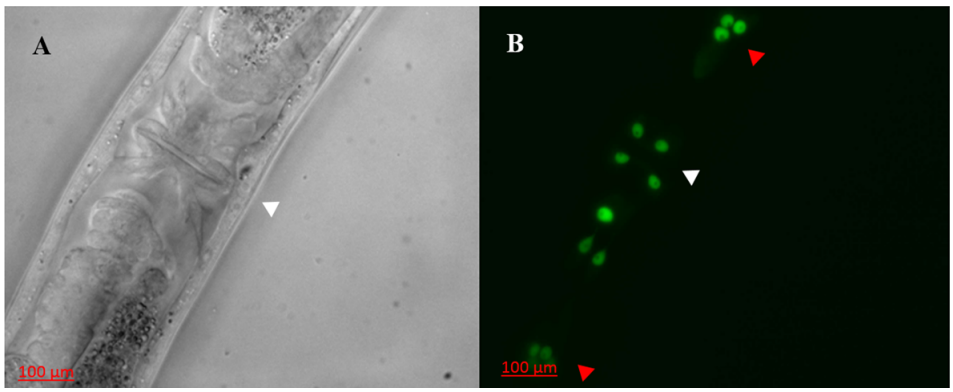

Figure 4.10 *zmp-1::GFP (mfIs8)* marker expressed in VPCs progenies. The strain *mfIs8[Cbr-zmp-1::GFP+ myo-2::GFP]* was used to generate *Cbr-lin(bh3); mfIs8[Cbr-zmp-1::GFP+ myo-2::GFP]* strain for the analysis of the 1° cell fate in mutants. The white triangle indicates the functional vulva, the red triangle indicates psuedovulva. Head is upward.

Analysis of 2° cell fate in *Cbr-lin(bh3)* mutants

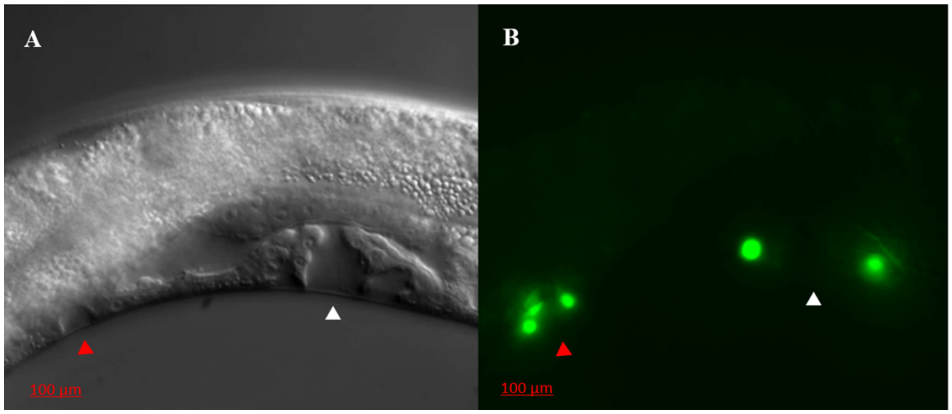

Figure 4.11 *Cbr-lin(bh3)* Muv animal with P8.p invagination. *egl-17::GFP (mfIs5)* marker indicating VPCs that adopted the 2° cell fate. The strain *mfIs5[Cbr-egl-17::GFP+ myo-2::GFP]*, was used to generate *Cbr-lin(bh3); mfIs5[Cbr-egl-17::GFP+ myo-2::GFP]* strains for the analysis of VPCs adopting 2° cell fate in these mutants. The white triangle indicates the functional vulva, the red triangle indicates abnormally induced VPCs. Anterior is on the right.

Cell fate in *Cbr-lin(bh3)* mutants

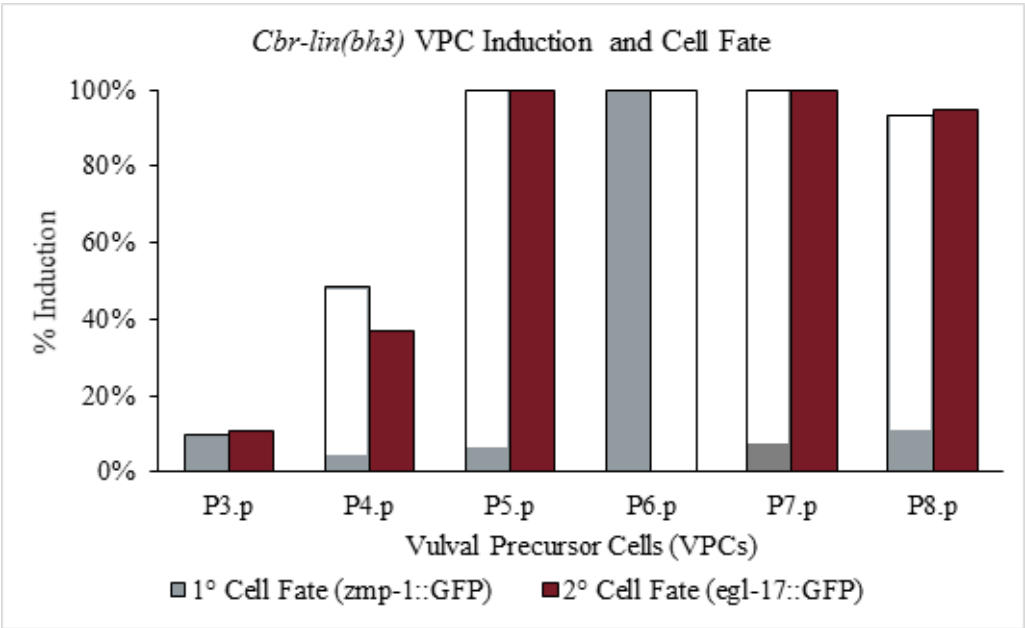

Figure 4.12 Analysis of 1° and 2° cell fate in *Cbr-lin(bh3)* mutants.

Table 4.13 Frequency of VPC induction and cell fate fluorescence in *Cbr-lin(bh3)* mutants

Cbr-lin(bh3)							
mfIs8	P3.p	P4.p	P5.p	P6.p	P7.p	P8.p	N
% Induction	9.0 ± 0.06	51.0 ± 0.2	100.0 ± 0.0	100.0 ± 0.0	100.0 ± 0.0	96.0 ± 0.1	101
% GFP	31.0 ± 0.21	15.0 ± 0.03	5.0 ± 0.43	100.0 ± 0.0	7.0 ± 0.0	21.0 ± 0.11	
mfIs5	P3.p	P4.p	P5.p	P6.p	P7.p	P8.p	N
% Induction	13.0 ± 0.1	47.0 ± 0.12	100.0 ± 0.0	100.0 ± 0.0	100.0 ± 0.0	98.0 ± 0.07	120
% GFP	100.0 ± 0.0	100.0 ± 0.0	100.0 ± 0.0	0.0	100.0 ± 0.0	97.0 ± 0.06	

The undergraduate student Lena So also carried out the cell fate analysis in *Cbr-lin(bh1)* and *Cbr-lin(bh3)* mutants. The results of this experiment were found to be consistent with the data provided by Lena So (Unpublished Data 2017).

4.7 Maternal inheritance effect in *Cbr-lin(bh1)* and *Cbr-lin(bh3)* mutants (By Lena So)

In the presence of maternal effect, genotypically-mutant progenies will be rescued from the mutant phenotype if the mother was heterozygous and carried the wild-type allele (Sharanya et al., 2015). If there is a maternal effect in vulval development, all progenies of *Cbr-lin(bh1)/+* and *Cbr-lin(bh3)/+* will have a wild-type vulva, regardless of their genotype.

If there is no maternal effect in *Cbr-lin(bh1)* strain, 25% of progenies with the genotypes *Cbr-lin(bh1)/Cbr-lin(bh1)*, should display approximately 30% penetrance of the Muv phenotype. As a result, approximately 8% of the total progeny will be Muv. If *Cbr-lin(bh3)* strain does not have maternal effect, 25% of progenies with the genotypes *Cbr-lin(bh3)/Cbr-lin(bh3)*, should display approximately 40% penetrance of the Muv phenotype. Thus, 10% of the total progeny will be Muv if maternal rescue is absent.

Table 4.14 Expected and observed Muv animals derived from heterozygous mothers in *Cbr-lin(bh)* mutants

Strain	Expected % of Muv Progenies	Observed % of Muv Progenies (N)
Cbr-lin(bh1)	8%	6.5% (309)
Cbr-lin(bh3)	10%	9.3% (313)

The percentage of observed Muv progeny from a heterozygous mother is approximately the same as the expected value. Therefore, both *Cbr-lin(bh1)* and *Cbr-lin(bh3)* strains do not demonstrate maternal effect during vulval development as the progenies of heterozygous worm do not receive wild-type mRNA, transcript, or proteins to rescue the mutant phenotype.

This entire experiment was conducted by Undergrad student Lena So (Unpublished Data 2017).

Chapter 5

Discussion, conclusions and future directions

This section summarizes the major findings described in this thesis and highlights the significance of work. The work described in this thesis focuses on the characterization of the *Cbr-ivp* class of genes and the identification of *Cbr-lin(bh)* alleles. These genes involved in vulval development in *C. briggsae*. Research on these genes presents an excellent platform for comparative evo-devo studies to understand the evolution of gene function and developmental mechanisms in *C. elegans*. The results in the thesis supporting the notion that there is an evolutionary functional divergence within the genes in different *Caenorhabditis* species.

5.1 Discussion and Conclusions

This segment briefly discusses the interpretation of results obtained from the experiments. A small part of the literature is presented with each section to further enhance the understanding of the rationale and outcomes of the experiments. The section focuses on the preliminary findings of *Cbr-lin(bh1)* and *Cbr-lin(bh3)* alleles which is followed by a brief discussion on molecular genetic analysis and functional significance of *Cbr-ivp* class of genes and their role in vulva development in *C. briggsae*.

5.1.1 The role of *Cbr-ivp* class of genes in vulval development

Findings of this study suggested that *Cbr-ivp* class of genes function as a negative regulator of vulval differentiation by inhibiting the inappropriate division of vulval precursor cells. In *Cbr-ivp* Muv mutants, additional VPCs undergo more

than one round of division to adopt vulval fates and thus lead to a Multivulva phenotype. Furthermore, it was observed that *Cbr-ivp* class of mutants showed a higher expression of *Cbr-lin-3* transcripts in comparison to wild-type animals, indicating that these genes may act upstream of *Cbr-lin-3* similar to SynMuv family members in *C. elegans*. RNA-Seq data for DE genes also revealed a significantly higher expression of *Cbr-lin-3* in *Cbr-ivp* mutants (log2fold change of 1.796653348 in *Cbr-spr-4(gu163)* and 1.356855843 in *Cbr-htz-1(gu167)*), suggesting that misregulation of *Cbr-lin-3* may contribute to Muv phenotype of *Cbr-ivp* mutant animals. Moreover, RNAi knockdown of *Cbr-lin-3* transcripts resulted in the suppression of multivulva phenotype in mutant animals. Thus, it was concluded that *Cbr-ivp* class of genes function to negatively regulate the *Cbr-lin-3* inductive pathway. The genes that negatively regulate cell division by inhibiting inappropriate signaling, and thus act similar to tumor suppressor genes. Defects in the signaling pathway which results in the high expression of LIN-3/EGF results in the constitutive activation of RAS pathway are commonly associated with cancer (Normanno et al. 2006). Thus, *Cbr-ivp* class of genes in *C. briggsae* may act to inhibit *Cbr-lin-3* transcription in Pn.p cells to promote the specification of wildtype 2-1-2 pattern of vulval cell fates.

5.1.2 *ivph-3* gene in *C. elegans*

ivph-3(gk3691) animals were observed under Nomarski optics for the detailed phenotypic analysis and to understand the defect in vulval morphology. The findings suggested that animals homozygous for the deletion site, which results in a complete loss of function of the *ivph-3* gene, possess a protruding vulva phenotype and are sterile. It is likely that loss of function of *ivph-3* in *C. elegans* prevents the production of fertilized eggs, and that in *C. elegans*, *ivph-3* is an important gene, necessary for growth of a fertile adult.

The penetrance assay revealed that the phenotypic ratio in ivp-3(gk3691) strain does not demonstrate the standard Mendelian Law of segregation. A reduced ratio of Pvl, sterile, homozygous animals in the population may have been resulted from defects that occur prior to the embryo development, such as defects in germline development, oogenesis, spermatogenesis, or fertilization. Thus, *ivph-3(gk3691)* strain needs to be maintained in heterozygous state. *ivph-3(gk3691)/+* have insertion and deletion in single copy of *ivph-3* gene along with a wild-type copy of ivp-3 gene. These animals have wild-type phenotype with myo-2::GFP expression and do not exhibit embryonic and larval lethality.

5.1.3 *ivp-3* genes accounts for functional differences in *C. elegans* and *C. briggsae*

It is possible that *Cbr-ivp-3* functions as a tumor suppressor by restricting the *Cbr-lin-3* over-expression and thus suppressing cell proliferation and possibly cell fate specification. It has been shown previously that Multivulva phenotype of *Cbr-ivp-3(sy5216)* is gonad independent (Sharanya et al., 2015). The characteristics of *Cbr-ivp-3* identified in previous studies and the work carried out in this thesis indicate that *Cbr-ivp-3* has the characteristics of SynMuv family of genes. It has been shown that the Muv phenotype observed in SynMuv mutants are caused by the dysregulation of *lin-3*, indicating that SynMuv genes negatively regulate vulval development by repressing *lin-3* expression. Molecular characterization of SynMuv genes, commonly indicates their involvement in chromatin-level transcriptional regulation. The protein domain information revealed the presence of RNase H-like domain in *Cbr-ivp-3* ORF, furthermore GeneMANIA research revealed 19 genes that have shared protein domain with *ivph-3* and enriched in nucleic acid binding activity (Pabla, 2017). It may be possible that Cbr-IVP-3 may translocate to the nucleus and regulate gene expression, similar to the SynMuv genes. Further work needs to be done to validate the characteristics of Cbr-IVP-3.

The studies on *ivph-3* in *C. elegans* suggested that it is an important gene necessary for the growth of a fertile adult. Although no defect VPCs induction defect has been observed, it is reported that *ivph-3(gk3691)* animals do have morphological defects in vulva development which leads to a protruding vulva phenotype.

Chesney et al., 2006 have demonstrated that *gon-14* in *C. elegans* expressed in the nuclei of many cells in somatic gonad and vulva tissue and found to interact with Class B and Class C Synthetic Multivulva genes (SynMuv). In addition, Dr. Chamberlin lab at Ohio State University, have shown that *htz-1* in *C. elegans* functions as SynMuv gene by interacting with *lin-15A* to negatively regulate the vulva development in *C. elegans* (Chamberlin et al., 2020). Thus, to further understand if *ivph-3* in *C. elegans* works as SynMuv gene to regulate vulva development, experiments were conducted to determine its role in *C. elegans*.

ivph-3(gk3691) mutants were crossed with SynMuv mutants, *lin-15A(n767)*, *lin-8(n111)* and *lin-56(n2728)*, in order to understand the interaction with class A SynMuv genes. The progenies of resultant double did not show Multivulva or any other phenotype (as many SynMuv genes also required for gonadogenesis). Moreover, the penetrance of Pvl phenotype was similar to homozygous *ivph-3(gk3691)* allele. In addition the interaction of the two genes did not augment embryonic and larval lethality, which suggested that *ivph-3* did not interact with class A SynMuv genes. These animals also turned out to be Pvl and Sterile. These results were

found to be parallel to homozygous *ivph-3(gk3691)* mutants. Thus, it was concluded that *ivph-3(gk3691)* double mutants carrying *lin-15A(n767)*, *lin-8(n111)* and *lin-56(n2728)* alleles did not exhibit Muv phenotype. This suggests that although *ivph-3* is required for the normal vulval development similar to *Cbr-ivp-3*, its mechanism of function appears to have diverged in *C. elegans*.

5.1.4 Differentially Expressed genes in *Cbr-spr-4(gu163)* and *Cbr-htz-1(gu167)* mutants

A Gene Ontology (GO) enrichment analysis of DE genes revealed that while there are some differences in gene categories between the two mutants, both the *Cbr-spr-4(gu163)* and *Cbr-htz-1(gu167)* showed enrichment for genes involved in similar processes such as cell cycle and DNA repair. The RNA seq data will be further validated by performing the RT-qPCR on the selected candidate genes.

A comparison of DE genes between the two mutants, revealed a significant overlap between the altered gene expression (197 genes, 181 upregulated and 7 downregulated; Hypergeometric score: 3.790918 e-129) (Figure 3.14). It is interesting to note that while both the *Cbr-spr-4(gu163)* and *Cbr-htz-1(gu167)* showed enrichment for the genes involved in chromosome organization during meiotic cell cycle. *Cbr-spr-4(gu163)* showed enrichment for meiotic nuclear division, mitotic cell cycle and mismatch repair genes categories. *Cbr-htz-1(gu167)* show enrichment for the genes involved in meiosis I, regulation of cell cycle process, DNA repair and posttranscriptional regulation of gene expression. Together, these results suggest that *Cbr-spr-4* and *Cbr-htz-1* may affect similar molecular processes to regulate cell proliferation in the vulva.

5.1.5 Gene mapping in *Cbr-lin(bh1)* and *Cbr-lin(bh3)* strains

The polymorphism mapping was carried out to determine the precise location of mutation on the chromosome. After carrying out PCR, the samples were run on agarose gel to examine band size and intensity. The amplicon sizes of AF16 and HK104 were controls used to compare the frequency of recombination in F2 mutant progeny. Since the mutant strains have an AF16 background, it is expected that amplicons would have higher concentration of AF16 DNA which indicate the mutation is close to the polymorphic site. This is because of the reduced recombination frequency in the region between the indel and mutation when they are located closer together.

The preliminary results demonstrated that the mutant alleles *Cbr-lin(bh1)* and *Cbr-lin(bh3)* are located on chromosome I and chromosome III, respectively. The banding patterns have shown that the mutation in Cbr-lin(bh1) is located on the right arm, thus it is expected that the mutation is located close to cb-m6, cb650, or bhP29. Using cb-m6 (right arm) , it was determined that the mutation is present on the right arm of the chromosome I. Furthermore, fine mapping was performed using indel-based polymorphisms to determine the precise location of the mutation on the respective chromosomes.

In terms of *Cbr-lin(bh3)*, linkage of the mutation to specific region of the chromosome was determined using the selection of indel-based polymorphisms on chromosome III. the results were inconclusive using bdP1, cb-m205, and cb-m46 indels. Thus, additional indels must be used to precisely map the location of the mutation on the chromosome. Mapping of the novel genes will lead to a better understanding and characterization of vulval development.

5.1.6 Complementation assay for *Cbr-lin(bh1)* and *Cbr-spr-4(gu163)*

Complementation experiments are used to determine whether two alleles with recessive mutations are located on the same gene. If two mutations are the alleles of different genes, they should complement each other to restore the wild-type vulval phenotype. Genetic mapping of *Cbr-spr-4(gu163)* revealed that mutation is located on chromosome I and yields a 90% Muv penetrance (Sharanya et al., 2015). The preliminary results of the polymorphism mapping also demonstrated that the mutant allele *Cbr-lin(bh1)* is located on chromosome I.

Thus, complementation assay was carried out between *Cbr-lin(bh1)* and *Cbr-spr-4(gu163)* strains to determine if two alleles are located on different gene loci. If both *Cbr-lin(bh1)* and *Cbr-spr-4(gu163)* are the mutations in the same gene, the resultant F1 cross progenies should have displayed GFP fluorescing worms with Multivulva phenotype, which further indicated that the two genes failed to complement each other. However, the results indicated that the two alleles complemented to restore the wild-type vulval phenotype. Thus, it is evident that these mutations are the alleles of different genes and thus located on different loci. Further, *Cbr-spr-4(gu163)* is not temperature sensitive strain and unlike *Cbr-lin(bh1)* and has high Muv penetrance (90%). Thus, *Cbr-lin(bh1)* can be further characterized to determine novel gene responsible for the Muv phenotype.

5.1.7 Temperature-sensitivity for Muv penetrance

Temperature has been shown to affect vulval development in certain *C. briggsae* strains, such as *Cbr-unc(sy5505)* and *Cbr-unc(5506)* (Sharanya et al., 2012). Specifically, an increase in the temperature reduces the number of P-cells to cause an Egg-laying phenotype (Sharanya et al., 2012). Furthermore, it has been shown that many multivulva mutants when maintain at 25°C showed an increase in Muv penetrance (Ferguson and Horvitz, 1989). Thus, altering the temperature at which the worms are maintained can affect gene expression to yield mutant vulval phenotypes. This may be due to the alteration of signaling pathways or cell division involved in vulval development.

Cbr-lin(bh1) and *Cbr-lin(bh3)*, were studied to determine the effects of temperature on Muv penetrance and expression of the gene responsible for the Muv phenotype. It is evident that a decrease in temperature to 15°C reduces Muv penetrance in *Cbr-lin(bh1)* by 10% in comparison to 20°C. Furthermore, an increase in temperature to 25°C increase Muv penetrance by 15% in comparison to 20°C. Therefore, it can be concluded that *Cbr-lin(bh1)* is a temperature sensitive allele. These results are similar to the previous studies on Muv mutants (Sharanya et al., 2012), indicating that it is possible that the same mechanisms for vulval development are aberrant in *Cbr-lin(bh1)*. Further examination of the VPCs must be performed to determine the mechanisms responsible for forming the pseudovulvae. In *Cbr-lin(bh3)*, the Muv penetrance remained approximately the same (40%) at 15°C, 20°C, and 25°C. Therefore, the gene responsible for the Muv phenotype is not temperature sensitive as varying temperature does not affect the Muv penetrance. This experiment contributes to the overall characterization of the novel genes responsible for vulval development.

5.1.8 Cell fate analysis

Wild-type VPC fate follows the pattern of 3°-3°-2°-1°-2°-3° from P3.p to P8.p (Gupta et al., 2007). In Muv mutants, VPCs adopt atypical cell fates that result in the formation of pseudovulvae. Determination of VPC fate in Muv mutants will provide better indication of signaling pathways and mechanisms that is perturbed to create the abnormality. Shown in Figure 4.7 and 4.8, the pseudovulva in *Cbr-lin(bh1)* and *Cbr-lin(bh3)* express *egl-17::GFP*, indicating the adoption the 2° cell fate. Similarly, in the *Cbr-pry-1(sy5353)* Muv mutant, the VPCs P3.p, P4.p, and P8.p all abnormally adopt the 2° cell fate (Seetharaman et al., 2010). In addition, *Cbr-lin-31(sy5342)* and *C. elegans lin-31(n301)* Muv mutants also

adopt abnormal 2° cell fates (Sharanya et al. 2015). This indicates that the LIN-12/Notch and Wnt signaling pathways may be perturbed to produce the atypical 2° cell fate. Wnt signaling has a role in maintaining VPC competence and cell fate specification (Gleason et al., 2002; Gleason et al., 2006; Myers and Greenwald, 2007). In previous studies of Muv mutants that abnormally adopt the 2° cell fate, it was determined that Wnt signaling orchestrates the expression of genes required to confer a 2° fate (Seetharaman et al., 2010). The study determined that LIN-12/Notch pathway is not responsible for pry-1 mutants (Seetharaman et al., 2010). Thus, it is possible that similar pathways are perturbed to yield the 2° cell fate in *Cbr-lin(bh1)* and *Cbr-lin(bh3)*. However, further experiments must be performed to determine whether LIN-12/Notch and lateral signaling or Wnt signaling is involved in the aberrant adoption of 2° cell fate in the two mutant strains in this study.

Primary cell fate analysis has also been carried out for *Cbr-lin(bh1)* and *Cbr-lin(bh3)*. The use of the marker *zmp-1::GFP* indicate whether the pseudovulva adopt the 1° cell fate. It has been previously determined that the Muv mutants display 1° cell fates in ectopic VPCs other than P6.p (Seetharaman et al., 2010). If VPCs other than P6.p in *Cbr-lin(bh1)* and/or *Cbr-lin(bh3)* adopt the 1° cell fate, it may indicate aberrant signaling or components of the Ras pathway or LIN-12/Notch pathway. Though it was observed that in *Cbr-lin(bh1)* mutants only P6.p adopt 1° cell fate while *Cbr-lin(bh3)* mutant show GFP expression and induction in ectopic VPCs. It maybe possible that *Cbr-lin(bh3)* mutants have a higher level of LIN-3/EGF signals or may have an ineffective lateral signaling system that cause the ectopic induction in VPCs. Further tests must be conducted to determine the specific mechanisms responsible for the Muv phenotype in *Cbr-lin(bh1)* and *Cbr-lin(bh3)*. The examination of pseudovulva cell fates is crucial in understanding abnormalities in VPC induction to generate the Muv phenotype. Furthermore, identifying which VPCs are abnormally induced and frequency of 1° and 2° cell fates will suggest possible signaling pathways that are compromised to produce the Muv phenotype.

5.2 Future directions

The findings of this thesis have contributed to an understanding of a novel class of genes involved in the negative regulation of the vulva development. Although a substantial amount of progress has been made, more work must be carried out in order to determine the significance of *Cbr-ivp* genes during development in both nematode species. Preliminary investigation on *Cbr-lin(bh)* mutants yielded

promising results, extensive research is required to uncover the underlying mechanism involved in vulval development regulation.

5.2.1 Mapping of *Cbr-lin(bh1)* and *Cbr-lin(bh3)* mutations

The work in the thesis concludes that the mutant genes in *Cbr-lin(bh1)* and *Cbr-lin(bh3)* are located on chromosome I and chromosome III, respectively.

5.2.1.1 Determining the precise location of the candidate genes

Fine mapping can be performed using indelbased polymorphisms to determine the linkage of *Cbr-lin(bh1)* and *Cbr-lin(bh3)*, with several phenotypic markers that were assigned to different loci on the chromosomes. The bulk segregant analysis (BSA) method can be used to map the mutation at the precise location on the chromosome. The polymorphisms scheme for the study involved small and medium indels (Koboldt et al., 2010), which has been verified previously on the basis of the genome sequencing. The website www.briggsae.org has the collection of a large number of makers that can be used for various mapping experiments. Single animal-based PCR assay can be carried out to determine map distance which greatly facilitates the search for candidate gene.

5.2.1.2 Determine the candidate genes by Whole Genome Sequencing (WGS) and RNAi knockdown to validate the results

To identify mutations in *Cbr-lin(bh1)* and *Cbr-lin(bh3)*, whole genome sequencing can be targeted. To perform this experiment, genomic DNA from Muv strains can be isolated and sent for sequencing. Once the location of mutation in a region narrowed down (within few mb), the genes that are affected by any mutation should be taken into consideration. The mutations that are causing any change in the reading frame or protein sequence should be prioritize for the further studies. The candidate genes that are pertaining to the vulva development must be examined. RNAi in wild-type background for the final set of predicted of genes helps to narrow down the candidate Muv genes. We rationalized that by narrowing down genetic intervals of the mutations it can be possible to determine potential candidate genes, including *C. elegans* orthologs, and thus, facilitates gene cloning by RNAi and transgene rescue approaches.

5.2.2 Rescuing phenotype by injecting wild-type copy of genes

To further confirm that predicted gene is indeed a Muv gene rescue experiment should be carried out. To carry out the rescue experiment, wild-type copy of the genes can be PCR amplified and injected into the mutant strains *Cbr-lin(bh1)* and *Cbr-lin(bh3)* to check if the wild-type phenotype is restored. Restoring the wild-type phenotype would confirm that the candidate genes are the Muv genes that negatively regulate cell proliferation during vulva development. Transgenic worms can be generated by injecting genes of interest with transformation marker into the syncytial gonad of adult hermaphrodites. The wild-type amplicon with a fluorescent marker, can be injected at in *Cbr-lin(bh1)* and *Cbr-lin(bh3)* animals. The concentration for the injections should be standardized. The wild type F1 worms expressing fluorescence should be cloned and F2 progenies should be observed for stable lines. Transgenic worm should be further analyzed for the Muv phenotype and VPC induction.

5.2.3 Gonad ablation experiments

Laser ablation technique can be used to study the interaction of cells during vulva development. The goal of this study would be whether the ablation of gonad cells (anchor cell) may result in restoring the wild-type phenotype in these mutants. If the multivulva phenotype in these mutants is affected by LIN-3 signaling and/or RAS pathway or if any other mechanism which not linked to RAS pathway results in the multivulva phenotype in *Cbr-lin(bh1)* and *Cbr-lin(bh3)* mutants. Thus, by killing gonad precursors (Z1 to Z4) their role in vulva development can be determined. L1 is the ideal stage for the cell ablation experiment (Kimble 1981). L1 worms be anesthetized by treating with 1 - 10mM sodium azide and ablate using a class IIb laser system (Photonic Instruments Inc.) attached to a Nikon Eclipse 80i Nomarski fluorescence microscope (as described by Sharanya et al., 2015). Animals can be recovered and allowed to grow to mid-L4 stage. The VPC induction would be examined under the Nomarski microscope to check if the ablation results in the suppression of ectopic VPC induction.

5.2.4 Determine whether the genes are conserved in *C. elegans*

To determine whether the genes are conserved and responsible for inhibiting the inappropriate division of Vulva precursor cells in sister species, RNA interference

(RNAi) and CRISPR approaches will be employed in wild-type *C. elegans* strain. If Muv phenotype is observed after RNAi experiment in *C. elegans*, then the genes are conserved between two species and involved in vulva development.

5.2.5 Generating mutations in the candidate genes in wild-type animals

Further mutations will be created in the candidate genes, using CRISPR/Cas 9 endonuclease approaches to generate different alleles for the same genes. CRISPR alleles are important because as mutations in different protein domains provide some insight into the gene function. Different alleles can result in different observable phenotype. Thus, creating different alleles of a gene helps in understanding the important protein domains of the genes.

5.2.6 The phenotypic rescue of *Cbr-ivp-3(sy5216)* mutant through *ivph-3*

Injecting a wild-type copy of *ivph-3* gene into *Cbr-ivp-3(sy5216)* mutant may compensate for the truncated gene product of *Cbr-ivp-3* and rescue the mutant phenotype. Rescuing the wild-type phenotype in the Muv mutants would further confirm that the is gene conserved between the two nematodes and can regulates cell proliferation during vulval development in *C. briggsae*. A 9.7 kb of gene fragment including introns was amplified along with 1899 bp of the 5'UTR and 1227 bp of 3'UTR. An injection mix, containing *myo-2::GFP* and *ivph-3* fragment has been injected into young adult *Cbr-ivp-3(sy5216)* hermaphrodite animals. However, the injection experiment did not result in stable lines. Transgenic rescue lines do not effectively work in nematodes thus, multiple lines need to be generated to determine the efficiency of the *ivph-3* gene to rescue the vulva defect of *Cbr-ivp-3(sy5216)* animals. Rescuing the mutant phenotype of *Cbr-ivp-3(sy5216)* would provide some insight into the functional similarities and/or differences of *ivp-3* gene in both the species.

5.2.7 Generating a transcriptional/translational fusion reporter construct for *Cbr-ivp-3* and *ivph-3*

A transcriptional/translational fusion reporter will be generated to observe the expression pattern of the gene, providing some insight into the function of *Cbr-ivp-3* and *ivph-3*. It is hypothesized that the protein will be observed in VPC's

during the early L3 stage. In order to locate *Cbr-ivp-3* and *ivph-3* throughout development in wild-type animals, a transcriptional/translational reporter plasmid can be constructed. We have generated transcriptional fusion reporter for *Cbr-ivp-3* and *ivph-3* genes. The transcriptional reporter *ivph-3::GFP* showed the GFP expression in vulva, intestine and neurons in F1 but the expression retained only in intestine and neurons in F2. Thus it was decided to use a bigger promotor for *ivph-3::GFP* expression. However, the transcriptional reporter did not show any GFP expression even when the entire promotor was taken into the consideration. A translational *Cbr-ivp-3::GFP* fusion construct incorporate the entire genomic region including introns, which allow to observe the active location of *Cbr-ivp-3* gene expression in live animals. Identifying the active location of *Cbr-ivp-3* in animals through a translational reporter, can help in determining if *Cbr-ivp-3* is acting in a similar way as SynMuv gene and present in the tissues where SynMuv genes are found to restrict *Cbr-lin-3*. If *Cbr-ivp-3* is present in the hypodermis, it infers that *Cbr-ivp-3* functions to regulate the level of *Cbr-lin-3* similar to a SynMuv gene, and thus further indicate that *Cbr-ivp-3* may be a SynMuv gene.

5.2.8 Examine the transcriptional regulation of *Cbr-lin-3* gene by *Cbr-ivp* class of genes

The *Cbr-ivp* mutants show higher levels of *Cbr-lin-3* transcripts, indicating that these genes act upstream of *Cbr-lin-3* similar to SynMuv family members in *C. elegans*. It has been shown that SynMuv genes repress *Cbr-lin-3*/EGF level in hypodermis (hyp7), and thus restrict the multivulva phenotype in nematodes (Cui et al., 2006).

It would be interesting to analyze if *Cbr-ivp* genes regulate *Cbr-lin-3*/EGF level by encoding the protein/ transcription regulator that binds in the 5' UTR and regulate gene expression. To analyze if *Cbr-ivp* genes encodes for a protein/transcription regulator, the encoded protein must be able to bind to the UTR region of target gene and to the other factors needed to alter transcription of a gene. Chromatin Immunoprecipitation (ChIP) can be carried out with the protein of interest (if no antibody is available, a tagged version of the protein overexpressed in the host cells) to pull down upstream sequence of *Cbr-lin-3*. You can evaluate the binding efficiency of your protein to DNA by comparing it to a well-known control that does not bind to DNA (Actin). The pulled down DNA could be amplified by using primers specific to *Cbr-lin-3* 5' UTR region.

It would be possible that the DNA binding through ChIP will not yield any significant consensus in DNA sequence for a binding site, as the *Cbr-ivp* classes of genes might be a repressive transcription factor. In that case a reporter under

an active promoter can be used to evaluate its ability to repress the reporter expression.

5.2.9 Validating genes identified by RNA-Seq data

It has been shown that SynMuv genes prevent the expression of germline specific factor in somatic cells (Lehner et al., 2006; Wang et al., 2005; Unhavaithaya et al., 2002). In *C. elegans* SynMuv mutants, germline P granules were found to be expressed in somatic cells (Wang et al., 2005). Thus, it is possible that *Cbr-ivp* genes might regulate germline specific genes expression in *C. briggsae* and somatic cells might inherit the characteristics of germline in early developmental stages which leads to a mixed cell fate (driven by both somatic and germline factors) and results in multivulva phenotype.

RNAi knockdown of genes that specifically expresses in germline suppresses the SynMuv phenotype in *C. elegans* (Cui et al., 2006). RNA-Seq data for *Cbr-spr-4(gu163)* and *Cbr-htz-1(gu167)* mutants was analyzed extensively for the germline and candidate genes whose expressions were found to be up regulated. It has been observed that many of the genes like *gld-3*, *mes-4* and *pgl-1* is required maternally for the germline development. (Eckmann et al., 2004; Petrella et al., 2011; Cui et al., 2006; Voronina et al., 2012) Thus, checking the expression level of these genes by RT-qPCR and knocking them down along with other candidate genes (expresses exclusively in germline) may be a good approach to examine the interaction of *Cbr-ivp* genes with germline specific genes.

RT-qPCR was carried out to quantify and compare the changes in the expression levels of *Cbr-pgl-1* and *Cbr-mes-4* transcript in wild-type and mutant worms. The RT-qPCR data for both *Cbr-pgl-1* and *Cbr-mes-4* demonstrated a high level of *Cbr-pgl-1* and *Cbr-mes-4* transcript level in *Cbr-spr-4(gu163)*, *Cbr-htz-1(gu167)*, *Cbr-ivp-3(sy5216)* and Cbr-gon14(gu102) animals when compared to wild-type strain. Transcripts were examined at early L1 stage worms. RNA was extracted just few hours after hatching the embryos. Our preliminary result suggested a higher level of *Cbr-pgl-1* and *Cbr-mes-4* transcript. Thus, RNAi plasmid will be generated to knockdown *Cbr-pgl-1* and *Cbr-mes-4* transcript in *Cbr-ivp* class mutants. The RNAi knockdown of *Cbr-mes-4* and *Cbr-pgl-1* transcripts in *Cbr-ivp* strains should result in the suppression of Muv phenotype. Other genes that would be consider under the study will be *Cbr-pie-1* and *Cbr-mex-5*. It will be interesting to see the level of *Cbr-pie-1* and *Cbr-mex-5* transcripts level in *Cbr-ivp* mutants. In addition to the RT-qPCR analysis, RNAi plasmid will be generated to knockdown *Cbr-pie-1* transcript in *Cbr-ivp* class mutants, to see if knocking

down *Cbr-pie-1* and *Cbr-mex-5* transcripts level results in suppression of Muv phenotype.

A comparative analysis of the targeted genes can be carried out by knocking down the orthologous genes in *C. elegans* using RNAi to determine if the mechanism of function of these genes is conserved. The comparative analysis of the targeted genes will further allow us to comprehend the mechanism responsible for the Muv phenotype in *Cbr-ivp* mutants.

5.2.10 Suppressor screen to identify genes that suppresses the Muv phenotype of *Cbr-ivp* mutants

RNAi and EMS based Suppressor screens can be used to identify novel components that function in a cell signaling pathway. EMS (Ethyl Methyl Sulphonate), a muatagen, can used to induce mutations in the gametes of mutant hermaphrodites. Second site mutation that results in the disruption of protein function which either leads to hypo or hyper phenotype are important and screened (Jorgensen and Mango, 2002). Suppressor screens can be used to suppress the multivulva phenotype in *Cbr-ivp* class of mutants. Many components of Ras signaling pathway were screened and identified for mutations that suppress the multivulva phenotype caused by a phosphorylated Ras/LET-60 (Lackner et al., 1994). Suppression of the Muv phenotype of *lin-15* mutations through the second-site mutations resulted in the identification of novel components that acted upstream and downstream of RAS (Han et al., 1990). Suppressing the Muv phenotype of *Cbr-ivp* class of mutants by creating a second-site mutation or knocking down the genes that are the positive regulators of vulva development would make an excellent candidate for the experiment. The second-site mutations, generated by EMS, can help identify the genes that suppress the Muv phenotype. Outcrossing and polymorphism mapping to determine the identity of the second-site mutations can be performed. The second-site mutations can help in the identification of the components associated with the vulval development in *Cbr-ivp-3(sy5216)*.

5.2.11 Further validation of *ivp-3(gk3691)*

The results of *ivp-3(gk3691)* analysis suggested that the reduced ratio of Pvl, sterile, homozygous animals in the population is neither due to the embryonic lethality nor due to larval lethality. A reduced ratio of Pvl, sterile, homozygous animals

in the population may have been resulted from pre-embryonic defects, such as defects in germline development, gametogenesis, ovulation or fertilization. To investigate defects in germline, animals should be analyzed under Nomarski microscope. Oocyte maturation can be observed using markers that specifically expresses in the oocytes. Meiotic division, nuclear envelope dissolution, fertilization, the presence of polar bodies and embryogenesis can be observed when the pronuclei fuse (McCarter et al., 1999). Investigating morphological events in *ivph-3(gk3691)* mutants under Normarki, may help in determining the source of the reduced ratio of Pvl, sterility in homozygous animals. To further determine whether the gene function is conserved between the two species a wild-type copy of *Cbr-ivp-3* gene can be injected into *ivph-3(gk3691)* animals, to determine whether the *C. briggsae* copy of *ivp-3* gene would compensate and rescue the mutant phenotype. The generation of rescue lines would help in understanding the functional conservation of domains during evolution.

5.3 Concluding remarks

The work done in this thesis focuses on using nematodes as an experimental model to identify tumor suppressor genes that impact cell signaling. A forward genetics approach in *C. elegans* and its sister species *C. briggsae*, was carried out to identify and study genes involved in vulva formation. The similarity of the cellular events in vulval development in *C. elegans* and *C. briggsae* has suggested that the underlying genes and genetic networks would be conserved. Comparison of gene function in diverse genetic backgrounds can lead to an understanding of how genetic differences contribute to different responses in development. These findings will demonstrate that although the structure of vulva is similar in nematodes, the fundamental genetic mechanisms include both conserved and divergent functional components and thus will provide evidences about the evolution of genes and their role in development (Cutter 2008).

Bibliography

• Angers, S., and Moon, R. T. (2009). Proximal events in Wnt signal transduction. Nature Reviews Molecular Cell Biology 10, 468-477.

• Aroian, R. V., and Sternberg, P. W. (1991). Multiple functions of let23, a *Caenorhabditis elegans* receptor tyrosine kinase gene required for vulval induction. Genetics 128(2), 251- 67.

• Berset, T., Hoier, E. F., Battu, G., Canevascini, S., and Hajnal, A. (2001). Notch inhibition of RAS signaling through MAP kinase phosphatase LIP-1 during *c. elegans* vulval development. Science 291, 1055–1058.

• Bindra, R. S., Vasselli, J. R., Stearman, R., Linehan, W. M., and Klausner, R. D. (2002). VHL-mediated hypoxia regulation of cyclin D1 in renal carcinoma cells. Cancer Research 62(11): 3014–9.

• Braeckman, B. P., Houthoofd, K., and Vanfleteren, J. R. (2001). Insulin-like signaling, metabolism, stress resistance and aging in *Caenorhabditis elegans*. Mechanisms of Ageing and Development 122, 673–693.

• Brenner, S. (1974). The genetics of *Caenorhabditis elegans*. Genetics 77(1), 71–94.

• Budirahardja, Y., and Gönczy, P. (2009). Coupling the cell cycle to development. Development. 136(17):2861-72.

• Burdine, D. R., Branda, S. C., and Stern, J. M. (1998). EGL-17(FGF) expression coordinates the attraction of the migrating sex myoblasts with vulval induction in *c. elegans*. Development 125, 1083-1093.

• Byerly, L., Cassada, C. R., and Russell, R. L. (1976). The life cycle of the nematode *Caenorhabditis elegans*: I. Wild-type growth and reproduction. Developmental Biology 51, 23-33.

• Chai, Y., Cui, J., Shao, N., Reddy, E. S. P., and Rao, V. N. (1999). The second BRCT domain of BRCA1 proteins interacts with p53 and stimulates transcription from the p21WAF1/CIP1 promoter. Oncogene 18:263–268.

• Chamberlin, M. H., Jain, M. I., Corchado-Sonera, M., Kelley, H. L., Sharanya, D., Jama, A., Pabla, R., Dawes, T. A., Gupta, P. B. (2020). Evolution of transcriptional repressors impacts Caenorhabditis vulval development. Molecular Biology and Evolution 37(5):1350-1361.

• Chen, N., and Greenwald, I. (2004). The lateral signal for LIN-12/Notch in *c. elegans* vulval development comprises redundant secreted and transmembrane DSL proteins. Developmental cell, 6(2), 183-92.

• Chesney, M. A., Kidd III, A. R., and Kimble, J. (2006). *gon-14* functions with class B and class C synthetic multivulva genes to control larval growth in *Caenorhabditis elegans*. Genetics 172, 915-928.

• Church, D., Guan, K. L., and Lambie, E. J. (1995). Three genes of the MAP kinase cascade, *mek-2*, *mpk-1/sur-1* and *let-60* ras, are required for meiotic cell cycle progression in *Caenorhabditis elegans*. Development 121, 2525–2535.

• Clark, S. G., Stern, M. J., and Horvitz, H. R. (1992). *c. elegans* cell-signalling gene *sem-5* encodes a protein with SH2 and SH3 domains. Nature 356, 340-344.

• Corsi, A. K., Wightman, B., and Chalfie, M. (2015). A Transparent window into biology: A primer on *Caenorhabditis elegans*. Genetics 200(2):387-407.

• Cui, M., Chen, J., Myers, T. R., Hwang, B. J., Sternberg, P. W., Greenwald, I., and Han, M. (2006a). SynMuv genes redundantly inhibit *lin-3*/EGF expression to prevent inappropriate vulval induction in *c. elegans*. Developmental Cell 10, 667–672.

• Cui, M., Fay, D. S., and Han, M. (2004). *lin-35*/Rb cooperates with the SWI/SNF complex to control *Caenorhabditis elegans* larval development. Genetics 167, 1177–1185.

• Cui, M., Kim, E. B., and Han, M. (2006b). Diverse chromatin remodeling genes antagonize the Rb-involved SynMuv pathways in *c. elegans*. PLoS Genetics. 2, e74.

• Cutter, A. D. (2008). Divergence times in Caenorhabditis and Drosophila inferred from direct estimates of the neutral mutation rate. Molecular biology and evolution 25(4), 778–786.

• Davidson, E. H. (1990). How embryos work: a comparative view of diverse modes of cell fate specification. Development 1990 108: 365-389.

• de Nooij, J. C., Letendre, M. A., and Hariharan, I. K. (1996). A cyclin-dependent kinase inhibitor, Dacapo, is necessary for timely exit from the cell cycle during Drosophila embryogenesis. Cell 87: 1237–1247.

• Desai, D., Wessling, H. C., Fisher, R. P., and Morgan, D. O. (1995). Molecular and Cellular Biology 15(1):345-50.

• Di Cristofano, A., and Pandolfi, P. P. (2000). The multiple roles of pten in tumor suppression. Cell 100:387–390.

• Duronio, R. J., and Xiong, Y. (2013). Signaling pathways that control cell proliferation. Cold Spring Harbor Perspectives in Biology 5(3):a008904.

• Dyson, N. (1998). The regulation of E2F by pRB-family proteins. Genes and Development 12, 2245–2262.

• Eckmann C. R., Kraemer B., Wickens M., and Kimble J. (2002). GLD-3, a bicaudal-C homolog that inhibits FBF to control germline sex determination in *c. elegans*. Developmental Cell, 3, 697-710.

• Eisenmann, D. M., Maloof, J. N., Simske, J. S., Kenyon, C., and Kim, S. K. (1998). The β-catenin homolog BAR-1 and LET-60 Ras coordinately regulate the Hox gene *lin-39* during *Caenorhabditis elegans* vulval development. Development 125, 3667-3680.

• Eisenmann, D. M., Wnt signaling (June 25, 2005), WormBook, ed. The *c. elegans* Research Community, WormBook.

• Eng, C. (2003). PTEN: one gene, many syndromes. Human Mutation 22: 183–198.

• Fay, D. S., and Yochem, J. (2007). The SynMuv genes of *Caenorhabditis elegans* in vulval development and beyond. Developmental Biology 306(1), 1-9.

• Felix M. A., (2007). Cryptic quantitative evolution of the vulva intercellular signaling network in Caenorhabditis. Current Biology 17: 103–114.

• Ferguson, E. L., and Horvitz, H. R. (1985). Identification and characterization of 22 genes that affect the vulval cell lineages of the nematode *Caenorhabditis elegans*. Genetics, 110(1), 17-72.

• Ferguson, E. L., and Horvitz, H. R. (1989). The multivulva phenotype of certain *Caenorhabditis elegans* mutants results from defects in two functionally redundant pathways. Genetics 123, 109–121.

• Fire, A., Xu, S., Montgomery, K. M., Kostas, A. S., Driver, E. S., and Mello, C. C. (1998). Potent and specific genetic interference by double-stranded RNA in *Caenorhabditis elegans*. Nature 391 pp. 806-811.

• Fodor, A., Riddle, D. L., Nelson, F. K., and Golden, J. W. (1983). Comparison of a new wild-type *Caenorhabditis briggsae* with laboratory strains of *c. briggsae* and *c. elegans*. Nematologica. 29:203–217.

• Gleason, J. E., Korswagen, H. C., and Eisenmann, D. M. (2002). Activation of Wnt signaling bypasses the requirement for RTK/Ras signaling during *c. elegans* vulval induction. Genes and Development. 16, 1281-1290.

• Gleason, J. E., Szyleyko, E. A., and Eisenmann, D. M. (2006). Multiple redundant Wnt signaling components function in two processes during *c. elegans* vulval development. Developmental Biology 298, 442-457.

• Goodsell, S. D. (2009). The Molecular Perspective: p53 Tumor Suppressor. Oncologist 4(2):138-9.

• Greenwald, I. S., Sternberg, P. W., and Horvitz, H. R. (1983). The *lin-12* locus specifies cell fates in *Caenorhabditis elegans*. Cell 34, 435–444.

• Gupta, B. P., Johnsen, R., and Chen, N. (2007). Genomics and biology of the nematode *Caenorhabditis briggsae*. WormBook: the online review of *c. elegans* biology, 1-16.

• Haag, E. S., and True, J. R. (2001). Perspective: From mutants to mechanisms? Assessing the candidate gene paradigm in evolutionary biology. Evolution 55(6), 1077–84.

• Han, M., and Sternberg, P. W. (1990). *let-60*, a gene that specifies cell fates during *c. elegans* vulval induction, encodes a ras protein. Cell 63(5), 921–31.

• Han, M., Golden, A., Han, Y., and Sternberg, P. W. (1993). *c. elegans lin-45* raf gene participates in *let-60* ras-stimulated vulval differentiation. Nature 363(6425), 133-140.

• Hanahan, D., and Weinberg, R. A. (2000). The hallmarks of cancer. Cell 100(1):57-70.

• Harbour, J. W., and Dean, D. C. (2000). Rb function in cell-cycle regulation and apoptosis. Nature Cell Biology 2(4):E65-7.

• Harbour, J. W., and Dean, D. C. (2000). The Rb/E2F pathway: expanding roles and emerging paradigms. Genes and Development 2000. 14: 2393-2409.

• Harper, J. W., Burton, J. L., and Solomon, M. J. (2002). The anaphase-promoting complex: it's not just for mitosis any more. Genes and Development 16(17):2179-206.

• Hartwell, L. H., Culotti, J., Pringle, J. R., and Reid, B. J. (1974). Genetic control of the cell division cycle in yeast. Science 183(4120):46-51.

• He, G., Siddik, Z. H., Huang, Z., Wang, R., Koomen, J., Kobayashi, R., Khokhar, A. R., and Kuang, J. (2005). Induction of p21 by p53 following DNA damage inhibits both Cdk4 and Cdk2 activities. Oncogene 24(18), 2929–2943.

• Hendriks, G. J., Gaidatzis, D., Aeschimann, F., and Großhans, H. (2014). Extensive oscillatory gene expression during *c. elegans* larval development. Molecular Cell 53(3), 380–392.

• Hill, R. J., and Sternberg, P. W. (1992). The gene *lin-3* encodes an inductive signal for vulval development in *c. elegans*. Nature, 358(6386), 470-6.

• Hodgkin, J. (2005). Genetic suppression. WormBook 1.59.1.

• Hoffenberg, R. (2003). Brenner, the worm and the prize. Clinical medicine 3(3):285-6.

• Hong, Y., Roy, R. and Ambros, V. (1998). Developmental regulation of a cyclin-dependent kinase inhibitor controls post-embryonic cell cycle progression in *c. elegans*. Development 125, 3585-97.

• Hopper, N.A., Lee, J., and Sternberg, P.W. (2000). ARK-1 inhibits EGFR signaling in *c. elegans*. Mol. Cell 6, 65–75.

• Hutter, H. (2006). Fluorescent reporter methods. Methods in Molecular Biology 351:155-73.

• Hwang, B., and Sternberg, P.W. (2004). A cell-specific enhancer that specifies *lin-3* expression in the *c. elegans* anchor cell for vulval development. Development, 143-151.

• Inoue, T., Sherwood, D. R., Aspock, G., Butler, J. A., Gupta, B. P., Kirouac, M., Wang, M., Lee, P. Y., Kramer, J. M., Hope, I., Burglin, T. R., and Sternberg, P. W. (2002). Gene expression markers for *Caenorhabditis elegans* vulval cells. Mechanisms of Development 119, S203–S209.

• Jorgensen, E. M. and Mango, S. E. (2002). The art and design of genetic screens: *Caenorhabditis elegans*. Nature Reviews Genetics 3(5), 356–369.

• Kaelin, W. G., and Maher, E. R. (1998) The VHL tumour suppressor gene paradigm. Trends in Genetics 14, 423–426.

• Katz, W. S., Lesa, G. M., Yannoukakos, D., Clandinin, T. R., Schlessinger, J., and Sternberg, P. W. (1996). A point mutation in the extracellular domain

activates LET-23, the *Caenorhabditis elegans* epidermal growth factor receptor homolog. Molecular and cellular biology, 16(2), 529-37.

• Kim, J. and Orkin, S. H. (2011). Embryonic stem cell-specific signatures in cancer: insights into genomic regulatory networks and implications for medicine. Genome medicine 3(11), 75.

• Kimble, J. (1981). Alterations in cell lineage following laser ablation of cells in the somatic gonad of *Caenorhabditis elegans*. Developmental Biology 87, 286-300.

• King, K. L., and Cidlowski, J. A. (1998). Cell cycle regulation and apoptosis. Annual Review of Physiology 60:601-17.

• Kirienko, N. V., Mani, K., and Fay, D. S. (2010). Cancer models in *Caenorhabditis elegans*. Developmental Dynamics 239(5), 1413–48.

• Kirouac, M., and Sternberg, P. W. (2003). cis-Regulatory control of three cell fate-specific genes in vulval organogenesis of *Caenorhabditis elegans* and *c. briggsae*. Developmental Biology 257, 85–103.

• Koboldt, D. C., Staisch, J., Thillainathan, B., Haines, K., Baird, S. E., Chamberlin, H. M., Haag, E. S., Miller, R. D., Gupta, B. P. (2010). A toolkit for rapid gene mapping in the nematode *Caenorhabditis briggsae*. BMC Genomics 11, 236.

• Korswagen, H. C. (2002). Canonical and non-canonical Wnt signaling pathways in *Caenorhabditis elegans*: variations on a common signaling theme. Bioessays 24, 801-810.

• LaBaer, J., Garrett, M. D., Stevenson, L. F., Slingerland, J. M., Sandhu, C., Chou, H. S., Fattaey, A., and Harlow, E. (1997). New functional activities for the p21 family of CDK inhibitors. Genes and Development 11: 847–862.

• Lackner, M. R., Kornfeld, K., Miller, L. M., Horvitz, H. R., and Kim, S. K. (1994). A MAP kinase homolog, *mpk-1*, is involved in ras-mediated induction of vulval cell fates in *Caenorhabditis elegans*. Genes and Development 8, 160–173.

• Lambie, E. J. (2002). Cell proliferation and growth in *c. elegans*. Bioessays 24(1), 38–53.

• Lehner, B., Calixto, A., Crombie, C., Tischler, J., Fortunato, A., Chalfie, M., and Fraser, A.G. (2006). Loss of LIN-35, the *Caenorhabditis elegans* ortholog of the tumor suppressor p105Rb, results in enhanced RNA interference. Genome Biology 7, R4.

• Levine, A. J. (1997). p53, the cellular gatekeeper for growth and division. Cell 88: 323–331.

• Levine, A. J., and Puzio-Kuter, A. (2010). The control of the metabolic switch in cancer by oncogenes and tumor suppressor genes. Science 330, 1340–1344.

• Levine, E. M., (2004). Cell cycling through development. Development 131: 2241-2246.

• • Lisztwan J., Imbert G., Wirbelauer, C., Gstaiger, M., and Krek, W. (1999). The von Hippel-Lindau tumor suppressor protein is a component of an E3 ubiquitin-protein ligase activity. Genes and Development 13:1822–33.

• Maher, E. R., and Kaelin, W. G. (1997). Von Hippel-Lindau disease. Medicine 76 pp. 381-391.

• Mahon, P. C., Hirota, K., and Semenza, G. L. (2001). FIH-1: a novel protein that interacts with HIF-1α and VHL to mediate repression of HIF-1 transcriptional activity. Genes and Development 15: 2675–2686.

• Malumbres, M., and Barbacid, M. (2005). Mammalian cyclin-dependent kinases. Trends in Biochemical Sciences 30(11):630-41.

• Malumbres, M., and Barbacid, M. (2009). Cell cycle, CDKs and cancer: a changing paradigm. Nature Reviews Cancer 9(3):153-66.

• Mautner, B., and Huang, D. (2003). Molecular biology and immunology. Seminar in Oncology Nursing 19(3): p. 154-61.

• McCarter, J., Bartlett, B., Dang, T., and Schedl, T. (1999). On the Control of Oocyte Meiotic Maturation and Ovulation in *Caenorhabditis elegans*. Developmental biology 205(1), 111–128.

• Mello, C.C., Draper, B.W., and Priess, J.R. (1994). The maternal genes *apx-1* and *glp-1* and establishment of dorsal-ventral polarity in the early *c. elegans* embryo. Cell 77, 95–106.

• Mendenhall, M. D. (1993). An inhibitor of p34CDC28 protein kinase activity from *Saccharomyces cerevisiae*. Science 259(5092):216-9.

• Millar, J. B., and Russell, P. (1992). The cdc25 M-phase inducer: an unconventional protein phosphatase. Cell 68(3):407-10.

• Montagut, C., and Settleman, J., (2009). Targeting the RAF-MEK-ERK pathway in cancer therapy. Cancer Letters 283:125–134.

• Morrison, S. J., Shah, N. M., and Anderson, D. J. (1997). Regulatory mechanisms in stem cell biology. Cell 88(3):287-98.

• Myers, T. R., and Greenwald, I. (2007). Wnt signal from multiple tissues and *lin-3*/EGF signal from the gonad maintain vulval precursor cell competence

in *Caenorhabditis elegans*. Proceedings of the National Academy of Sciences 104, 20368-20373.

• Neidich, J. A. (2005). Inborn Errors of Development: The Molecular Basis of Clinical Disorders of Morphogenesis. American journal of human genetics 76(2), 368.

• Nevins, J. R. (1998). Toward an understanding of the functional complexity of the E2F and retinoblastoma families. Cell Growth and Differentiation 9:585–593.

• Normanno, N., De Luca, A., Bianco, C., Strizzi, L., Mancino, M., Maiello, M. R., Carotenuto, A., De Feo, G., Caponigro, F., and Salomon, D. S. (2006). Epidermal growth factor receptor (EGFR) signaling in cancer. Gene 366(1), 2-16.

• Nurse, P., Thuriaux P., and Nasmyth, K. (1976). Genetic control of the cell division cycle in the fission yeast *Schizosaccharomyces pombe*. Molecular and General Genetics 146, pages 167–178(1976).

• Ortmann, B., Druker, J., and Rocha, S. (2014). Cell cycle progression in response to oxygen levels. Cellular and Molecular Life Sciences 71: 3569-3582.

• Pabla, R. (2017). The genetic and functional characterization the tumour suppressor *ivp-3* in *Caenorhabditis briggsae*. M. Sc. Thesis, McMaster University.

• Petrella, L. N., Wang, W., Spike, C. A., Rechtsteiner, A., Reinke, V., and Strome, S. (2011). SynMuv B proteins antagonize germline fate in the intestine and ensure *c. elegans* survival. Development 138:1069–1079.

• Pines, J. (1999). Four-dimensional control of the cell cycle. Nature Cell Biology 1(3):E73-9.

• Pucci, B., Kasten, M., and Giordano, A. (2000). Cell cycle and apoptosis. Neoplasia 2(4):291-9.

• Ranawade, A. (2017). PRY-1/Axin regulate aging, lipid metabolism and seam-cell asymmetric cell division in *Caenorhabditis elegans*. Ph. D. Thesis, McMaster University.

• Reinke V., Smith H. E., Nance J., Wang J., Van Doren C., Begley R., Jones S. J., Davis E. B., Scherer S., Ward S., Kim, S.K. (2000). A global profile of germline gene expression in *c. elegans*. Molecular Cell 6, 605-616.

• Riddle, D. L., Blumenthal, T. E., Meyer, B. J., and Priess, J. R. (1997). Introduction to *C. elegans*- *C. elegans* II - NCBI Bookshelf.

• Schafer, A. K. (1998). The cell cycle: A review. Veterinary Pathology 35:461-478.

• Schumacher, B., Hofmann, K., Boulton, S., and Gartner, A. (2001). The *c. elegans* homolog of the p53 tumor suppressor is required for DNA damage-induced apoptosis. Current biology 11(21), 1722–1727.

• Sears, R. C., and Nevins, J. R. (2002). Signaling networks that link cell proliferation and cell fate. The Journal of Biological Chemistry 277(14):11617-20.

• Seetharaman, A., Cumbo, P., Bojanala, N., and Gupta, B. P. (2010). Conserved mechanism of Wnt signaling function in the specification of vulval precursor fates in *c. elegans* and *c. briggsae*. Developmental Biology. 346 (1): 128–13.

• Seyfried, T. N., and Huysentruyt, L. C. (2013). On the origin of cancer metastasis. critical reviews in oncogenesis 18(1-2):43-73.

• Sharanya, D., Fillis, C. J., Kim, J., Zitnik, E. M., Ward, K. A., Gallagher, M. E., Chamberlin, H. M., Gupta, B. P. (2015). Mutations in *Caenorhabditis briggsae* identify new genes important for limiting the response to EGF signaling during vulval development. Evolution and development, 17(1), 34 - 48.

• Sharanya, D., Thillainathan, B., Marri, S., Bojanala, N., Taylor, J., Flibotte, S., Moerman, D. G., Waterston, R. H., Gupta, B. P., (2012). Genetic Control of Vulval Development in *Caenorhabditis briggsae*. G3 (Bethesda) 2(12): 1625-1641.

• Sharma-Kishore, R., White, J. G., Southgate, E. and Podbilewicz, B. (1999). Formation of the vulva in *Caenorhabditis elegans*: a paradigm for organogenesis. Development 126, 691 -699.

• Shaye, D. D., and Greenwald, I. (2002). Endocytosis-mediated down regulation of LIN-12/Notch upon Ras activation in *Caenorhabditis elegans*. Nature, 420(6916), 686–90.

• Sherr, C. J. (1996). Cancer cell cycles. Science 274(5293):1672-7.

• Sherr, C. J. and Roberts, J. M. (2004). Living with or without cyclins and cyclin-dependent kinases. Genes Dev 18(22):2699-711.

• Sigal, A., and Rotter, V. (2000). Oncogenic mutations of the p53 tumor suppressor: The demons of the guardian of the genome. Cancer Research 60: 6788–6793.

• Simske, J. S., and Kim, S. K. (1995). Sequential signaling during *Caenorhabditis elegans* vulval induction. Nature 375(6527), 142-6.

• Spruck, C. H., and Strohmaier, H. M. (2002). Seek and destroy: SCF ubiquitin ligases in mammalian cell cycle control. Cell Cycle 1(4):250-4.

• Stein, L. D., Bao, Z., Blasiar, D., Blumenthal, T., Brent, M. R., Chen, N., Chinwalla, A., Clarke, L., Clee, C., Coghlan, A., et al. (2003). The genome sequence of *Caenorhabditis briggsae*: a platform for comparative genomics. PLoS Biol 1(2), e45.

• Sternberg, P. W. (2005). Vulval development. WormBook : the online review of *c. elegans* biology, 1-28.

• Sternberg, P. W. and Horvitz, H. R. (1989). The combined action of two intercellular signaling pathways specifies three cell fates during vulval induction in *c. elegans*. Cell 58, 679-693.

• Stevaux, O., and Dyson, N. J. (2002). A revised picture of the E2F transcriptional network and RB function. Current Opinion in Cell Biology 14: 684-691.

• Stiernagle, T. (2006). Maintenance of *c. elegans*. WormBook : the online review of *c. elegans* biology, 1-11.

• Sulston, J. E., and Horvitz, H. R. (1977) Post-embryonic cell lineages of the nematode, *Caenorhabditis elegans*. Developmental Biology 56 (1): 110-156.

• Sundaram, M. V. (2004). Vulval development: the battle between Ras and Notch. Current Biology 14, R311-R313.

• Sundaram M. V. (2013). Canonical RTK-Ras-ERK signaling and related alternative pathways. WormBook ed. The *c. elegans* Research Community, Wormbook.

• Sundaram, M. V. (February 11, 2006). RTK/Ras/MAPK signaling WormBook, ed. The *c. elegans* Research Community, WormBook.

• Unhavaithaya, Y., Shin, T. H., Miliaras, N., Lee, J., Oyama, T., and Mello, C. C. (2002). MEP-1 and a homolog of the NURD complex component Mi-2 act together to maintain germline-soma distinctions in *c. elegans*. Cell 111, 991–1002.

• Voronina E., Paix A., and Seydoux G. (2012). The P granule component PGL-1 promotes the localization and silencing activity of the PUF protein FBF-2 in germline stem cells. Development, 139, 3732-40.

• Wang, D., Kennedy, S., Conte Jr., D., Kim, J. K., Gabel, H. W., Kamath, R. S., Mello, C. C., Ruvkun, G. (2005). Somatic misexpression of germline P granules and enhanced RNA interference in retinoblastoma pathway mutants. Nature 436, 593–597.

• Wang, M. and Sternberg, P. W. (2000). Patterning of the *c. elegans* 1° vulval lineage by RAS and Wnt pathways. Development 127,5047 -5058.

• Wang, X., Zhao, Y., Wong, K., Ehlers, P., Kohara, Y., Jones, S.J., Marra, M.A., Holt, R.A., Moerman, D.G., Hansen D. (2009) Identification of genes expressed in the hermaphrodite germ line of *c. elegans* using SAGE. BMC Genomics 10:213

• Wicks, S. R., Yeh, R. T., Gish, W. R., Waterston, R. H., and Plasterk, R. H. (2001). Rapid gene mapping in *Caenorhabditis elegans* using a high density polymorphism map. Nature Genetics 28, 160–164.

• Winston, W. M., Sutherlin, M., Wright, A. J., Feinberg, E. H., and Hunter, C. P. (2007). *Caenorhabditis elegans* SID-2 is required for environmental RNA interference. Proceedings of the National Academy of Sciences 104:10565–10570.

• Wood, W. B. (1988) Introduction to *c. elegans* biology. In the Nematode *Caenorhabditis elegans*. W.B. Wood (ed). Cold Spring Harbor, NY: Cold Spring Harbor Laboratory, pp. 1–16.

• Wormbase WS255 [Internet]. 2016. CBG03376 [cited 2016 Oct 21]. Available from www.wormbase.org/species/*c. briggsae*/gene/WBGene00026246

• Wormbase WS255 [Internet]. 2016. *Y67D8C.3* [cited 2016 Oct 21]. Available from http://www.wormbase.org/species/*c. elegans*/gene/WBGene00022067

• Yang, L., Kuang, L. G., Zheng, H. C., Li, J. Y., Wu, D. Y., Zhang, S. M., Xin, Y., Chen, Y., and Yang, S. (2003). PTEN encoding product: a marker for tumorigenesis and progression of gastric carcinoma. World Journal of Gastroenterology 9(1), 35–39.

• Yoo, A. S., Bais, C., and Greenwald, I. (2004). Crosstalk between the EGFR and LIN-12/Notch pathways in *c. elegans* vulval development. Science 303, 663–666.